Südöstlicher Atlantik und südwestlicher Indik: Rekonstruktion der sedimentären und tektonischen Entwicklung seit der Kreide
AISTEK-II: Mosambik Rücken und Mosambik Becken

Southeastern Atlantic and southwestern Indian Ocean: reconstruction of the sedimentary and tectonic development since the Cretaceous
AISTEK-II: Mozambique Ridge and Mozambique Basin

Report of the RV "SONNE" cruise SO-183, Project AISTEK-II
20 May to 7 July 2005

Edited by Wilfried Jokat
with contributions from the Scientific Party of SO-183

Berichte zur Polar- und Meeresforschung 521 (2006)
ISSN 1618-3193

BMBF Förderkennzeichen 03G0183A

Wilfried Jokat

Alfred-Wegener-Institut für Polar- und Meeresforschung

FB Geosystem

Am Alten Hafen 26

D-27568 Bremerhaven

Germany

wjokat@awi-bremerhaven.de

Index

Zusammenfassung

Das Forschungsschiff Sonne verließ Kapstadt am 20. Mai um 9:00 UTC in Richtung des Untersuchungsgebietes. Zu Beginn der Expedition SO-183 wurden zwei Drehkreise zur Kalibrierung des Vektor-Magnetometers in der Umgebung des südafrikanischen Observatoriums Hermanus durchgeführt. Nach drei Tagen Transit bei schlechten Wetterbedingungen wurde ein weiterer Drehkreis im Norden des Messgebietes, zusammen mit dem geschleppten Magnetometersystem durchgeführt.
Die magnetische und bathymetritsche Messfahrt begann am 23. Mai während schlechten Wetters. Entlang dem ganzen ersten Profil konnte das Schiff nur eine Geschwindigkeit von 5-8 kn beibehalten, was zu einem massiven Zeitverlust führte. In den nächsten Tagen konnte das Schiff jedoch trotz des schlechten Wetters größtenteils mit der geplanten Geschwindigkeit von 10 kn fahren.

Am 29. Mai (19:00 UTC) wurden alle Sensoren wegen eines heftigen Sturmes mit Windstärken von 9-10 bf abgeschaltet. Während des ganzen Tages kam das Schiff nur mit 5-8 kn voran. Die Messungen wurden ein weiteres Mal wegen starker Dünung unterbrochen. Ab dem Morgen des 31. Mai konnte der normale Messbetrieb wieder aufgenommen werden. Vorteilhaftes Wetter begünstigte den geophysikalischen Messbetrieb. Während der ersten Juniwoche wurde der zentrale und nördliche Mosambikrücken untersucht. Da die gemessenen Potentialfelddaten die Existenz kontinentaler Kruste nicht belegen konnten, wurde das magnetische Messnetz weiter nach Norden verlegt. Entgegen der Erwartungen wurden systematische Magnetfeldumkehrungen entlang der 3-4 Linien innerhalb des gewählten Korridors gefunden. Dies legt den Schluss nahe, dass der untersuchte Teil des Mosambikrückens ozeanischen Ursprungs ist. Diese Interpretation wurde durch zusätzliche Daten weiter bekräftigt. Aus diesem Grund wurde der Korridor so weit nach Norden ausgedehnt, wie dies im Rahmen der vorgegebenen Schiffszeit möglich war. Fast jeden dritten Tag wurde die Messfahrt unterbrochen um Steilhänge entlang des Mosambikrückens zu beproben. An den 5 ausgewählten Positionen wurden überwiegend Basalte erprobt.
Am 8. Juni war die Messfahrt über dem Mosambikrücken beendet. Die Expedition wurde im nächsten Messgebiet, dem Mosamikbecken fortgesetzt. Die Profilfahrt im Mosambikbecken begann bei 20°S 38°E. Für den Rest der Woche begünstigte ruhige See das Vorankommen der Messfahrt. Im zentralen Teil des Mozambikbeckens wurden zwei Linien bis 20°30´S verlängert um auch die ältesten mesozoischen Sequenzen zu vermessen. Die Messungen wurden am 16. Juni unterbrochen um den Jaguar Seamount zu beproben. Beide Dredgen waren erfolgreich und enthielten voraussichtlich Basalte. Die magnetische Messfahrt wurde am Abend des 16. Juni fortgesetzt. Am späten Vormittag des 19. Juni wurde das kleine französische Atoll Bassas da Inida passiert und am 23. Juni die Insel L´Europe. Die Messungen im östlichen Teil des Mosambikbeckens waren am 30. Juni beendet. Auf dem Weg zum Zielhafen Durban wurden Verbindungslinien für die während der Datenbearbeitung durchzuführende Tagesgangkorrektur und Kreuzungspunktanalyse gefahren und um Lücken im Messraster bei etwa 39°E zu schließen. Diese Linien wurden bei 21°42´E beendet. Anschließend wurde

eine weitere E-W Linie vermessen, um alle N-S Linien zu verbinden. Entlang der westlichen Begrenzung des Messgebietes wurde eine weitere Linie bis 28°S vermessen. Die Messungen wurden am 4. Juli um 19:00 UTC beendet. Auf dem Weg nach Durban wurde der Mosambikrücken bei 30°36´S 37°09´E erfolgreich beprobt. Die Expedition endete am 7. Juli 09:00 lokale Zeit in Durban.

Summary

The ship left Cape Town on schedule at May 20th 9:00 UTC and headed towards the research area. In the beginning two calibration circles for the Vector-Magnetometer were performed off the South African observatory Hermanus. After three days of transit (bad weather) another calibration circle in the north of our research area was conducted in combination with a towed magnetometer.
The magnetic and bathymetric profiling started at May 23rd during bad weather conditions. The ship could only maintain a speed ranging between 5 and 8 knts for the entire first profile, which led to a massive loss in survey time. During most of the profiles in the next days we had unfavourable weather conditions. However, most of the time the ship could cruise with the planned survey speed of 10 knts.

At May 29th all sensors of the ship were shut down (19:00 UTC) due to a heavy storm with sea state 9-10 bf. During the entire day the ship could only maintain a speed of 5-8 knts. The measurements were again interrupted due to a strong swell. During the morning of May 31st regularly measurements could be continued. Favourable weather conditions allowed excellent progress for the geophysical profiling. During the first week of June the central and northern Mozambique Ridge was surveyed. The magnetic network was shifted northwards, since no potential field anomalies could be found, which indicate the presence of continental crust. In contrast, systematic magnetic reversals were visible on the 3-4 tracks, within the chosen corridor. This strongly suggests that the investigated part of the Mozambique Ridge is of oceanic origin. This interpretation was more and more supported by the data. Thus, the corridor was extended northwards as much as the ship time allowed. Almost every third day the survey was interrupted to dredge escarpments along the Mozambique Ridge. Mostly basalts were recovered at 5 sites.
On June 8th the survey along the Mozambique Ridge was finished, and the ship moved into the new research area, the Mozambique Basin. The survey in the Mozambique Basin started at 26°00'S 38°00'E. For the rest of the week a constantly calm sea favoured the survey progress. In the centre of the Mozambique Basin we extended two lines to 20°30'S to map the oldest Mesozoic sequences. The survey was interrupted at June 16th to dredge the Jaguar seamount. Both dredges were successful and recovered most likely basalts. The magnetic survey was continued in the evening of June 16th. At the late morning of June 19th we passed one of the little French atoll called Bassas da India and at 23rd of June the island L'Europe. The survey pattern in the Mozambique Basin in the east was finished at June 30th. On the way to our destination port, Durban, we acquired connection lines for the future diurnal and mistie corrections, and filled the missing lines in the middle of the survey area around 39°E. These lines were terminated at 21°42'E. Then, another E-W line was acquired to connect all the N-S track lines. At the westernmost boundary of our box we collected another N-S line down to 28°S. The magnetic survey was finished at July, 4th 19:00 UTC. On our way back to Durban the Mozambique Ridge was dredged at 30°36'S 37°09'E. The expedition was finished on July, 7th 09:00 local time in Durban.

1. Marine Geophysics

(W. Jokat, M. Watkeys, C. Kopsch, M. Brayshaw, K. Kitada, M. Tauchnitz, R. Krocker, A. Labrenz, R. Niebling, S. Riedel, Z. Thackeray)

1.1 General objectives

During the last 180 Myr the distribution of the continents especially on the southern hemisphere changed significantly. The movements of the continents in time and space had fundamental consequences for the paleoceanography, the distribution of spreading systems, the basin evolution, the global water mass circulation pattern, the terrestical environment and finally, the long term climate history of the earth. Especially, to better understand the transition from the “Green house” earth of the Mesozoic to the Cenozoic “Cold House” earth with continental wide glaciations is a topic within various research programmes (e.g. IODP).

Continental break-up is in general connected with extensive onshore volcanism before, during and also after the plates split. The relationship between pre-break-up magmatism and the onset of the formation of true oceanic crust is a matter of debate. More and more data, however, indicate that between both events there is a time span of 20-30 Myr. This is also true for the volcanism prior to the separation of Africa from Antarctica. Massive volcanism occurred around 183 Myr onshore on both continents, but the drift of the plates did not start before 155 Myr. Several geological structures like the Astrid, Gunnerus, Mozambique and Madagascar ridge as well the Agulhas Plateau might have been affected by volcanism during or after the break-up of Gondwana. In order to better understand the distribution, relative timing and age of the plate separation and the associated volcanism, the nature of the different features must be known to be incorporated into a sound geodynamic model. For this, both extensive marine magnetic investigations as well as seismic refraction and reflection data in critical areas are needed to provide this information.
One of these critical areas along the Antarctic coast is the Riiser-Larsen Sea and the Lazarev Sea. While in the latter no sea floor spreading anomalies were found so far, the Riiser-Larsen Sea could be dated to have started to form around 155 Ma. However, to constrain this model only a few high quality magnetic lines are available. Most of the information was gathered in the conjugate sea off the coast of SE-Africa, namely the Mozambique and Natal basins. However, the data are more than 20 years old and its distribution is quite uneven to use it as a base for a detailed geodynamic model. Furthermore, the Mozambique Ridge remained a problem for all reconstructions in this region. From geophysical investigations and dredge samples gathered at the flanks of the ridge in the late 80’s, the ridge was considered to be of continental origin. This interpretation caused a significant overlap of this ridge with the Antarctic continent, if a tied fit of both continents was applied. The latest published models for the Lazarev and Riiser-Larsen seas locate the Mozambique Ridge in the Lazarev Sea, where no spreading anomalies have been found. To solve some of these problems of the Gondwana reconstruction, the FS Sonne operated in May-July 2005 off the coast of SE-Africa. The major objectives of the cruise were:

- Acquire new magnetic data south of the southernmost tip of the Mozambique Ridge to better describe the drift history of this continental fragment.
- Retrieve dredge samples at critical locations to better describe the nature of the basement in order to relate it to the onshore geology of SE-Africa.
- Acquire new marine magnetic data in the Mozambique Basin to allow a more detailed description of the opening history. Several models predict that the eastern part of the Mozambique Basin is older and/or that the western Mozambique Basin might have a different opening history. Did the basin opened step wise? If yes, how?

Parallel to the magnetic data swath bathymetry, high resolution echosounder and gravity data were acquired to supplement to magnetic data sets, and to provide information for the selection of the dredge sites. Finally, the swath data, although they have not a complete coverage of the area, will be used for a new bathymetric map for the region between Madagascar and Mozambique.

For this research project the research vessel Sonne was made available from 20th May to 7th July 2005. In this report technical information on the equipment, the measurements, and the first results will be presented.

1.2 Marine Magnetics

To perform this experiment a SeaSpy sensor was leased for this cruise. It was originally intended to tow a SeaSpy gradiometer to compensate for the daily variations. For several reasons, the second sensor did not arrive in time in the port. Thus, we had to perform the experiment with one sensor only. As a backup system a fixed ship mounted fluxgate magnetometer was used, which could be borrowed on short notice from the National Institute of Polar Research, Tokyo.
The SeaSpy sensor was towed 200 m behind the vessel, and the general cruising speed was between 10-11 ktns. The sensor worked fine during most of the time. It hang up only 2-3 times during the entire cruise. The data acquisition was performed with a Laptop, which received the necessary position information from the shipboard system (Fig. 1). In general, the data acquisition system was set up as follows (Fig. 1):

- Every sensor had its own Laptop for recording the data independently
- As a backup system the “Main PC” monitored all three sensors and stored again the different types of data (Gravimeter, towed magnetometer, fluxgate).

These magnetic data were loaded in a commercial software package (LCT) to perform some basic quality checks. This included the IGRF correction. Without this correction the data were difficult to read since the Earth’s magnetic field is quite variable in the investigated area (Fig. 2). With this setup in total 24121 km of new magnetic data were acquired in the Mozambique Basin (15338 km) and along the Mozambique Ridge (8783 km). The data are of excellent quality. They will be corrected for diurnal variations after the cruise with data from the magnetic observatories in the vicinity of our survey areas.

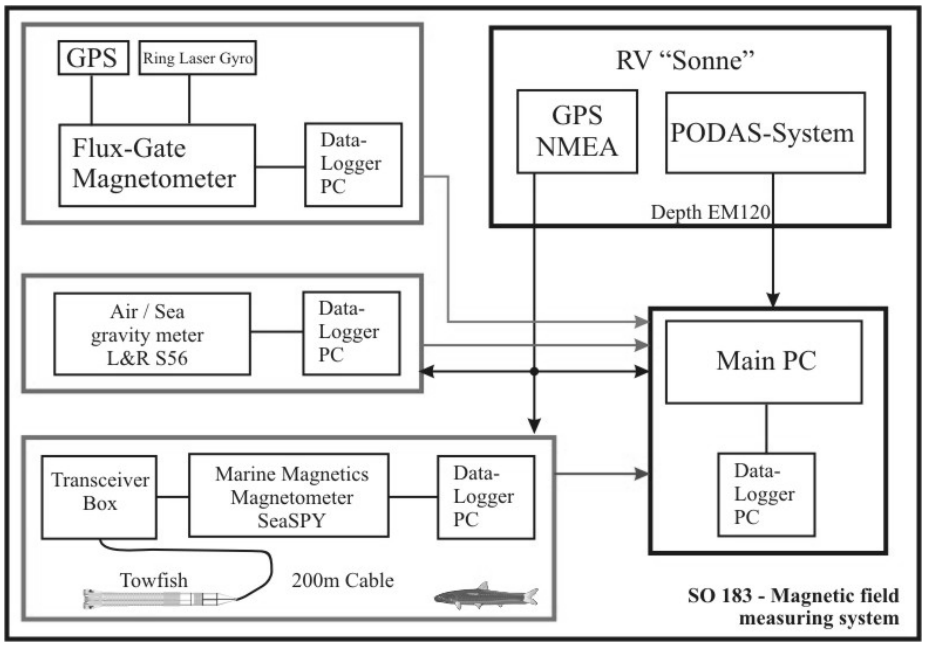

Fig. 1: Set up of data acquisition system.

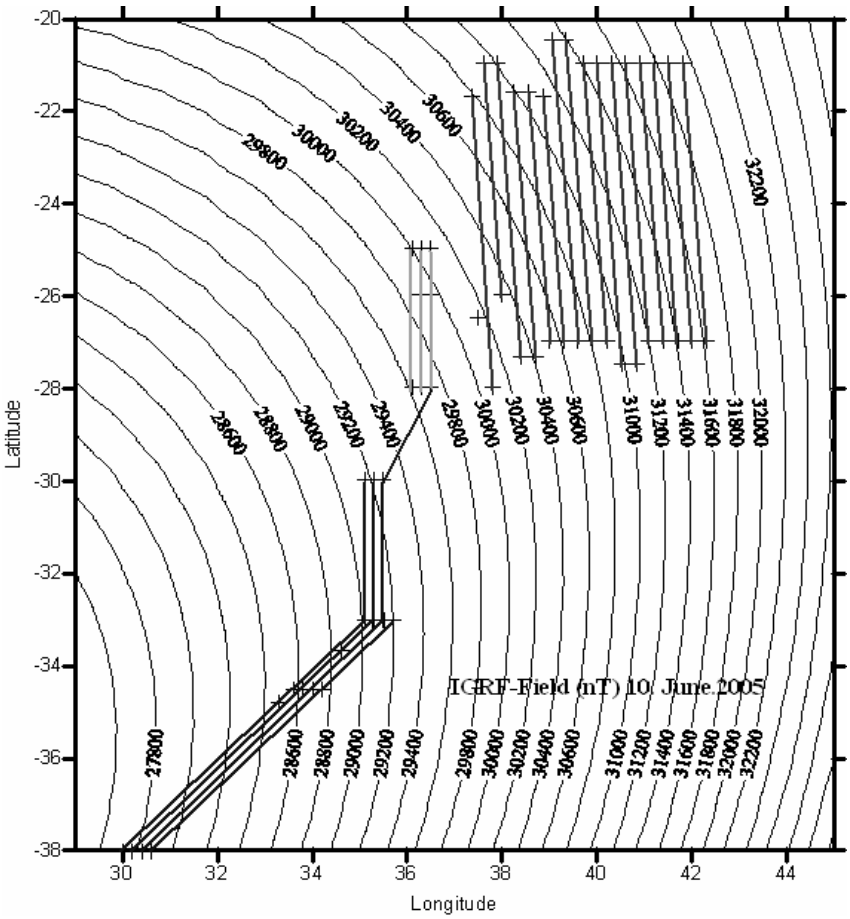

Fig. 2: International Geomagnetic Reference Field (IGRF) in the survey area, calculated for the 10th of June 2005.

1.3 First Results

The main objective of this project was to gather new marine magnetic data in order to better constrain the nature and evolution of geological features, which formed a common boundary between Antarctica and southern Africa. The present geodynamic models for the Mozambique Ridge, Mozambique Basin and on the conjugate side the Lazarev and Riiser-Larsen seas have only few constraints on the detail of the opening history. While in the Lazarev Sea no sea floor spreading anomalies were found, in the Riiser Larsen Sea only one 40 km wide high resolution magnetic survey exists to constrain the movements between Africa and Antarctica. This is not sufficient for a detailed model, since especially the continental Mozambique Ridge could not be fit in the pre-break up models without severe overlaps of the ridge with the Antarctic continent. Since no spreading anomalies could be identified in the Lazarev Sea south of Maud Rise, this problem could not be solved from the Antarctic side.
Thus, the first survey was concentrated at the southern part of the Mozambique Ridge towards the Agulhas Plateau to identify any spreading anomalies, which could document portions of the ridge's spreading history. In total 9 lines were planned in order to safely identify also weak anomalies. The actual results were surprising. From the beginning of the survey we found strong systematic magnetic reversal in the abyssal plains southwest of the Mozambique Ridge. The Mesozoic chron M4 could be identified close to the Agulhas Plateau on every line we acquired. Thus, the first aim of this survey was reached. We needed a clear M4 anomaly to safely date the more northern Mesozoic reversal. After having acquired four tracks in the southwest, we changed our strategy since the reversals were very clear and showed an excellent correlation between the tracks. In the next step we wanted to document the continent-ocean boundary with magnetics and gravity between the continental Mozambique Ridge and the ocean basin. Thus, the corridor consisting of the four tracks centred on the crest of the ridge was extended northwards by approximately 100 km. To our surprise still sea floor spreading anomalies showed up at the southern part of the ridge. Although the corridor was extended three times northward, Mesozoic magnetic reversal were found instead of a more continental-like magnetic pattern. Finally, the survey ended close to the coast of Mozambique showing some evidence that we have entered some kind of transition zone. These results within a 40 km wide corridor were so surprising that we did not have enough time for some more lines in the middle part. However, the magnetic data show that the Mozambique Ridge is not a continental fragment, but an oceanic feature. It was formed during the separation of Africa and Antarctica. With some confidence the Mesozoic chrons M21-24 could be identified in the very north of the ridge.
Our current interpretation is that ongoing massive magmatic activity from M24 to M10 time created the ridge, while the separation of Antarctica and Africa continuously opened the Lazarev Sea. The conjugate feature, though less elongated, in Antarctica is the Astrid Ridge. Both features indicate that for almost 40 million years this area was the focus of volcanic activity accompanying the dispersal of Gondwana. The Mozambique Ridge might also be the evidence for the ongoing activity and presence of a thermal anomaly ("hot spot"?) in the mantle. Currently we cannot state, if the Mozambique Ridge

filled immediately step by step the open space in the Lazarev Sea, which was created by the movements of Africa, or if the volcanism was concentrated in the area of the Astrid Ridge during the Early-Middle Cretaceous. In any case, it is very likely that from the current water depths, the ridge erupted sub-aerial. Therefore, it might have prevented any water exchange between the young Mozambique Basin and the Lazarev Sea for more than 25 Myr after the separation of Africa and Antarctica. Finally, with the oceanic origin of the Mozambique Ridge the overlapping problem for tied fit reconstructions no longer exists.

The larger part of the magnetic survey was concentrated in the Mozambique Basin. Here, it was of outmost interest to test the different hypotheses on differential opening of the basin and the pre-break up position of Madagascar. Here, the area east of 40°E was of special interest, since almost no magnetic data existed here to constrain any geodynamic model. In total 17 lines, each 360 km long, with a spacing of 30 km were acquired across the entire basin.
In the west we observed strong magnetic reversal with an excellent correlation between the lines. The reason for the strong anomalies might be that the oceanic basement is rather close to the sea floor. The bathymetric data indicate that the sea floor topography might be highly influenced by the topography of the underlying oceanic crust. Some 100 km south of the small atolls Bassas da India and L'Europe the magnetic field becomes very flat. This might be an indication that the seamounts did not erupt at the spreading centre, but that they are younger than the surrounding oceanic crust. Their lavas might have floored the older oceanic crust, and thus attenuated their magnetic signals. East of 40°E the magnetic reversal are difficult to correlate between the lines and they show very low amplitudes. A good interpretation on the age of these anomalies cannot be given at the writing of this report. Most likely they indicate the presence of fracture zones, which offset the spreading system quite rapidly. This cannot be resolved by the wide spacing of our survey. A thicker sediment cover towards Madagascar might also strongly attenuate the magnetic signals and broaden their wavelength. However, in summary the general model as introduced by French researchers (Segoufin, 1978; Segoufin & Patriat, 1980) seems to be correct. However, the new data prove that the eastern Mozambique Basin is younger than the western one. Towards Madagascar we found again stronger magnetic anomalies, but they are difficult to interpret at the current state of their processing. Details on the dating have still to be done.

The data are not shown here in the cruise report, because a final processing of the lines was not possible, since we had no online access to the diurnal data of the magnetic observatories. The waypoints of the magnetic survey are summarized in table 1.

Table 1: Waypoints during SO183 cruise.

Event	Place	Date of start	Lat_{Begin}	Lon_{Begin}	Lat_{End}	Lon_{End}	Distance	Total distance	Speed	Time
			[°]	[°]	[°]	[°]	[nm]	[nm]	knots	[h]
WP-1	CapeTown	20.05-09:00	-34	18	-34.5	33.6	774	774	12	64.5
WP-2	Line-1	24.05-02:00	-34.5	33.6	-38	30	273	273	10	27.3
WP-3		24.05-03:00	-38	30	-38	30.2	9	282	10	0.9

WP-4	Line-2	25.05-04:00	-38	30.2	-34.5	33.8	273	555	10	27.3
WP-5		26.05-05:00	-34.5	33.8	-34.8	33.3	31	586	10	3.1
26.05 05:00-15:00 Dredges #1+2 at Mozambique Ridge: 1xrocks; 1xempty; Position 34°47'S, 33°19'E; Sum:10 h										
	Transit	26.05-15:00	-34.5	33.3	-34.5	34	35	808	10	3.5
WP-6	Line-3	26.05-19:00	-34.5	34	-38	30.4	273	858	10	27.3
WP-7		27.05-21:00	-38	30.4	-38	30.6	9	868	10	0.9
WP-8	Linie-4	28.05-22:00	-38	30.6	-33	35.7	390	1258	10	39.0
plus10h	Dredge	28.05.-18:00	-38	30.6	-35.15	33.5				
28.05 19:00-07:00 Dredges #3+4 at the southern Mozambique Ridge (3h CTD, 4h Transit) 7 h dredging ==> Sum: 11 h										
29.05 08:00 Magnetic calibration circles 2h Dredges at 35°16,5!S 33°13,6'E										
29+30.05 ship could not make progress due to a strong storm. Linie 4 was interrupted in the night of 29.05!!!										
WP-09	Line-1+	31.05-06:30	-34.5	33.6	-33	35.1	117	1375	10	11.7
WP-10		31.05-19:00	-33	35.1	-33	35.3	10	1385	10	1.0
WP-11	Line-2+	31.05-20:00	-33	35.3	-34.5	33.8	117	1502	10	11.7
WP-12		01.06-06:00	-34.5	33.8	-34.5	34	10	1512	10	1.0
WP-13	Line-3+	01.06-07:00	-34.5	34	-33	35.5	117	1629	10	11.7
WP-14		01.06-18:00	-33	35.5	-33	35.7	10	1639	10	1.0
WP-15	Line-4+	01.06-19:00	-33	35.7	-34.5	34.2	117	1756	10	11.7
	Transit	02.06-05:00	-34.4	34.3	-33.67	34.6	46	820	10	4.6
02.06 09:00-12:00 Dredge #5 at the southern Mozambique Ridge (4h Transit) 3 h dredging ==> Sum: 7 h										
		02.06-12:00	-33.67	34.6	-33	35.1	47	1803	10	4.7
WP-16	Line-1++	02.06-16:00	-33	35.1	-30	35.1	180	1983	10	18.0
WP-17		03.06-08:00	-30	35.1	-30	35.3	10	1994	10	1.0
WP-18	Line-2++	03.06-09:00	-30	35.3	-33.01	35.28	181	2174	10	18.1
WP-19		04.06-03:00	-33	35.28	-33	35.52	12	2186	10	1.2
WP-20	Line-3++	04.06-05:00	-33	35.52	-30	35.5	180	2366	10	18.0
04.06. 16:00- 01:00 Dredges #6+7 in the central part of MOZ Ridge (1 h Transit. 2 h CTD) 5 h dredging +2h calibration circles Sum: 9h										
WP-21	Line-3+++	05.06-06:00	-30	35.5	-28	36.5	131	2497	10	13.1
WP-22		05.06-19:00	-28	36.5	-26	36.5	120	2617	10	12.0
WP-23		06.06-06:00	-26	36.5	-26	36.3	11	2628	10	1.1
WP-24	Line-2+++	06.06-07:00	-26	36.3	-28	36.3	120	2748	10	12.0
WP-25		06.06-18:00	-28	36.3	-28	36.1	11	2759	10	1.1
WP-26	Line-1+++	06.06-19:00	-28	36.1	-25	36.1	180	2939	10	18.0
WP-27		07.06-13:00	-25	36.1	-25	36.3	11	2950	10	1.1
WP-28	Line-2+++	07.06-14:00	-25	36.3	-26	36.28	60	3010	10	6.0
WP-29		07.06-20:00	-26	36.28	-26	36.52	13	3023	10	1.3
WP-30	Line-3+++	07.06-21:00	-26	36.52	-25	36.5	60	3083	10	6.0
WP-31		08.06-02:30	-25	36.5	-26.5	37.5	105	3188	10	10.5
08.06. 08:00- 10:00 Search for a dredge location without success, therefore only survey time--no dredging (5 h Transit) 2.5 h CTD Sum: 5h										
WP-32	Transit	08.06-12:00	-26.5	37.5	-26	38	40	3228	10	4.0
-----	**Line 5**	**not acquired**	**-27**	**37.5**	**-21**	**37**	**361**	**none**	**none**	**none**
------	**Line 6**	**not acquired**	**-27**	**37.8**	**-21**	**37.3**	**361**	**none**	**none**	**none**
WP-35	Line-7	08.06-15:00	-26	38	-21	37.6	301	3529	10	30.1
WP-36		09.06-19:00	-21	37.6	-21	37.9	17	3545	10	1.7
WP-37	Line-8	09.06-21:00	-21	37.9	-27.33	38.4	381	3926	10	38.1
WP-38		11.06-10:00	-27.33	38.4	-27.33	38.7	16	3942	10	1.6
WP-39	Line-9	11.06-11:30	-27.33	38.7	-21.62	38.25	343	4286	10	34.3
WP-40		12.06-20:00	-21.62	38.25	-21.6	38.55	17	4303	10	1.7

WP-41	Line-10	12.06-21:30	-21.6	38.55	-27	39	325	4627	10	32.5
-----	**Line-11**	**not acquired**	**-27**	**39.3**	**-21**	**38.8**	**361**	**none**	**none**	**none**
WP-42		14.06-04:00	-27	39	-27	39.6	32	4660	10	3.2
WP-43	Line-12	14.06-07:00	-27	39.6	-20.5	39.05	391	5051	10	39.1
WP-44		15.06-20:00	-20.5	39.05	-20.5	39.35	17	5068	10	1.7
WP-45	Line-13	15.06-22:00	-20.5	39.35	-27	39.9	391	5442	10	39.1
16.06. 07:00-08:00 2xmagnetic calibration circles										
16.06 08:00-18:00 Dredges #8+9 ---> Jaguar Seamount (3h Survey) Sum: 10 h										
16.06. 20:00-22:00 CTD										
WP-46		18.06-02:00	-27	39.9	-27	40.2	16	5458	10	1.6
WP-47	Line-14	18.06-04:00	-27	40.2	-21	39.7	361	5803	10	36.1
WP-48		19.06-14:30	-21	39.7	-21	40	17	5820	10	1.7
WP-49	Line-15	19.06-16:00	-21	40	-27.5	40.53	391	6194	10	39.1
WP-50		21.06-05:00	-27.5	40.53	-27.5	40.83	16	6210	10	1.6
WP-51	Line-16	21.06-06:00	-27.5	40.83	-21	40.3	391	6601	10	39.1
WP-52		22.06-19:00	-21	40.3	-21	40.6	17	6618	10	1.7
WP-53	Line-17	22.06-21:00	-21	40.6	-27	41.1	361	6979	10	36.1
WP-54		24.06-10:00	-27	41.1	-27	41.4	16	6995	10	1.6
WP-55	Line-18	24.06-11:00	-27	41.4	-21	40.9	361	7356	10	36.1
WP-56		25.06-22:30	-21	40.9	-21	41.2	17	7373	10	1.7
WP-57	Line-19	25.06-24:00	-21	41.2	-27	41.7	361	7734	10	36.1
WP-58		27.06-12:00	-27	41.7	-27	42	16	7750	10	1.6
WP-59	Line-20	27.06-13:30	-27	42	-21	41.5	361	8111	10	36.1
WP-60		29.06-01:00	-21	41.5	-21	41.8	17	8128	10	1.7
WP-61	Line-21	29.06-02:30	-21	41.8	-27	42.3	361	8489	10	36.1
30.06. 18:00-19:00 2x calibration circles										
WP-62		30.06-19:00	-27	42.3	-26.98	39.3	160	8649	10	16.0
WP-63	Line-11	01.07-11:00	-26.98	39.3	-21.7	38.85	318	8967	10	31.8
WP-64		02.07-18:00	-21.7	38.85	-21.7	37.35	84	9051	10	8.4
WP-65	Line-6	03.07-03:00	-21.7	37.35	-28	37.8	379	9430	10	37.9
WP-66	Transit	04.07-19:30	-28	37.8	-30.6	37.15	160	9589	11	14.5
WP-67 05.07. 05.07-09:30-18:00 Dredge #10+11 at 30°36'S 37°09'E Sum: 8.5 h										
WP-68	Tranist	05.07-18:00	-30.6	37.15	-29.82	30.933	326	1146	10	32.6
	Durban	**07.07-08:00**								

All dates are board time (UTC+2).

References

Segoufin, J. (1978). Anomalies magnetique mesozoique dans le bassin de Mozambique, C.R. Sceances, *Acad. Sci. Ser.* 2, 287D, 109-112.

Segoufin, J. and P. Patriat (1980). Existence d'anomalies mesoziques dans le bassin de Somali; Implications pour les relations Afrique-Antarctique-Madagascar, C.R. Sceances, Acad. *Sci. Ser.*, 291B (2), 85-88.

1.4 Fluxgate magnetometer

(K. Kitada)

1.4.1 Introduction

The vector geomagnetic anomaly consists of three magnetic anomaly components, namely North, East, and vertical components. Measuring these components, we can immediately quantify the strike of a boundary of a magnetic anomaly, in addition to its polarity, in a single geophysical track. Consequently, the vector geomagnetic anomaly field is useful for marine geoscientists in terms of revealing seafloor tectonics, because anomaly amplitudes from the total intensity magnetometer data are often much reduced, depending on the orientation of the ambient geomagnetic field and magnetic lineations. These orientations however, have no effect on vector anomalies, hence the advantage of using the vector magnetometer.

1.4.2 General experimental setup

Vector magnetic field data are collected by a shipboard three-component magnetometer (STCM), using a deck-mounted magnetometer, gyro and GPS antenna. The STCM system which was supplied by the National Institute of Polar Research (NIPR) in Japan, consists of a fluxgate magnetometer sensor, ring laser gyro, GPS antenna, data logger and data acquisition system (PC). These instruments are connected as shown in Figure 3. All the data were recorded at 5 Hz sampling rate by a data logger and data acquisition system, which monitors the status of the STCM system.

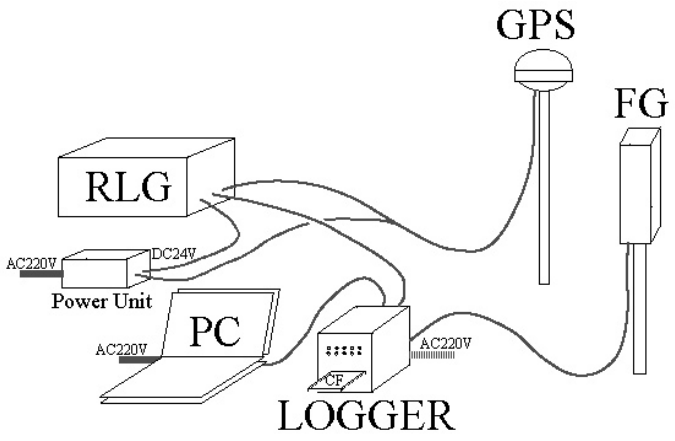

Figure 3: Overview of the STCM system illustrating the connection setup of the various components.

Specifications

Fluxgate magnetometer sensor [FG]

Range:	± 70,000 nT
Resolution:	0.01 nT.
Accuracy:	0.4 nT
Sampling rate:	8 Hz
Serial output:	RS-232C
Range of thermometer:	-55-125℃
Accuracy of thermometer:	0.5℃

Data logger [SFG-2005]
The data logger records acquired data to a Compact Flash Card medium. This logger also sends data to the PC for data backup and monitoring.

Data volume: ~50 MB per day
Sampling rate: 5 Hz

Ring laser gyro [RLG]
The attitude sensor is composed of three ring laser gyros, and three single-axis accelerometers.

Roll and Pitch angles
- Resolution: less than 0.005 degrees
- Accuracy: less than 0.1 degrees
- Sampling rate: 5Hz

Heading angle
- Resolution: less than 0.005 degrees
- Accuracy: 0.20 degrees with 0.01 degree/hour rms drift rate
- Sampling rate: 5Hz

Data format
The file name is in the format "DTFG-YYMMDD-hhmmss.dat".
YY=year, MM=month, DD=day, hh=hour, mm=minute, ss=second.
This file is named according to the start time of recording, according to the time of the PC (not UTC time).

The data format is as follows (asterisk denoted parameters explained below):
HH:MM:SS.SS(UTC),GyroMode*,0,Lat.(Deg.),Long.(Deg.),Heading(Deg.),Roll(Deg.),Pitch(Deg.),Hx(nT),Hy(nT),Hz(nT),Temp.(degree)**,depth,N-S Speed(kt),E-W speed(kt).
An example of this format is presented in Table 2.

*GyroMode: 0 N/A
1 alignment mode on land
2 alignment mode on ship
3 GPS hybrid mode
4 inertia mode

**Temp. is the temperature recorded by the thermometer inside the magnetometer sensor.

Table 2: Example of data format

HH:MM:SS.SS	Lat.	Long.	Heading	Roll	Pitch	Hx	Hy	Hz	Temp	depth	N-S	E-W.
07:12:44.00	3,0,-34.19218,	33.90967,	40.792,	-0.753,	3.593,	8741.22nT,	-12202.27nT,	-24192.26nT,	23.8,	-1.0,	7.697,	8.003
07:12:44.00	3,0,-34.19217,	33.90968,	40.792,	-0.472,	3.818,	8816.00nT,	-12260.74nT,	-24133.56nT,	23.8,	-1.0,	7.704,	7.984
07:12:44.00	3,0,-34.19217,	33.90969,	40.798,	-0.187,	4.026,	8969.24nT,	-12367.17nT,	-24017.62nT,	23.8,	-1.2,	7.724,	7.952

1.4.3 Circle calibration

The STCM data contains the effects of the magnetic field of the ship, which must be corrected in order to derive the real geomagnetic field. The coefficients of the B and H matrix related to the permanent and induced magnetic field of the ship are estimated by the circle calibrations. The circle calibrations are made by steering the ship in a tight circle, both clockwise and counter-clockwise to perform a figure-of-eight (Figure 4). During this cruise, circle calibrations were conducted six times, and these are documented in Table 3, and illustrated

in Figure 5. The coefficients of the B and H matrix derived from circle calibrations during this cruise are also listed in Table 4.

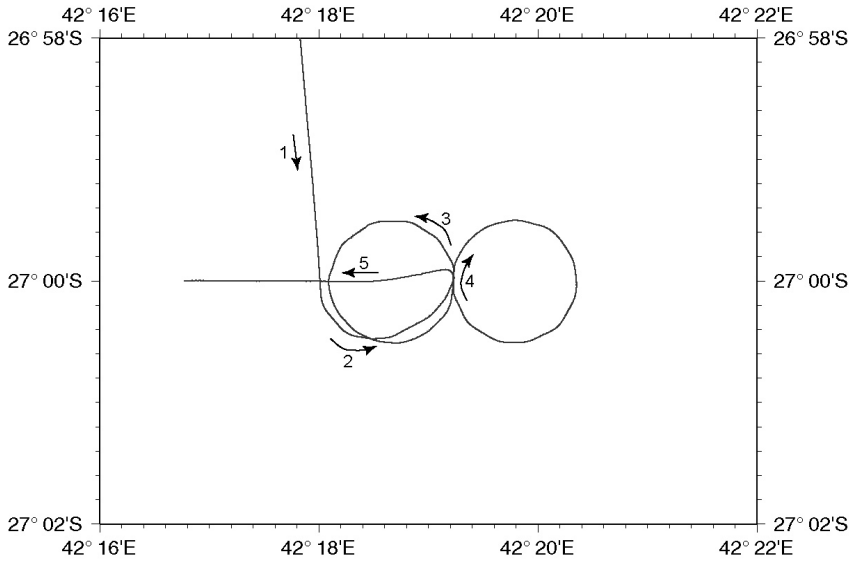

Figure 4: An example of a circle calibration.

Table 3: List and locations of circle calibrations conducted

No.	Date	Time(UTC)	Latitude	Longitude
1	20.05.2005	15:08-16:22	34°44.25′S	19°00.00′E
2	23.05.2005	14:26-15:26	34°30.00′S	33°37.25′E
3	29.05.2005	06:30-07:50	35°12.75′S	35°28.95′E
4	04.06.2005	22:19-23:29	30°50.00′S	35°30.00′E
5	16.06.2005	05:19-06:32	22°10.00′S	39°40.00′E
6	30.06.2005	15:50-16:45	27°00.00′S	42°19.23′E

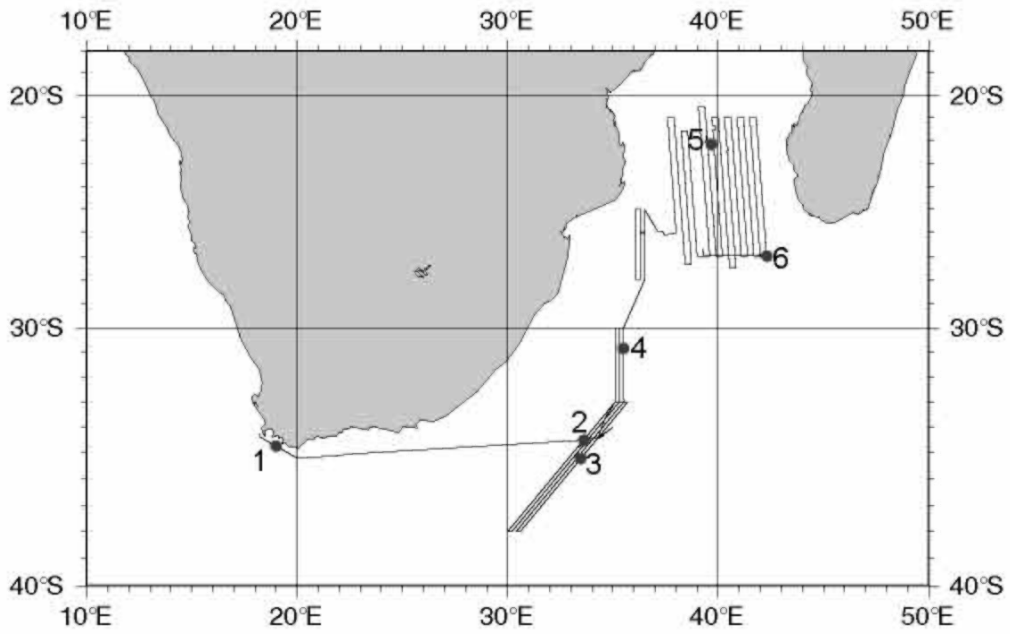

Figure 5: Locations of circle calibrations during SO-183

Table 4: Coordinates of **B** and **H** matrix calculated.

B(1,1)	**B(1,2)**	**B(1,3)**	**H(1,1)**
1.05435	-0.07085	-0.22000	-11949.5
B(2,1)	**B(2,2)**	**B(2,3)**	**H(2,1)**
0.04713	1.21166	-0.29741	-7059.9
B(3,1)	**B(3,2)**	**B(3,3)**	**H(3,1)**
-0.02828	0.00382	0.72552	-7133.6

1.5 Gravity

(S. Riedel)

All geophysical methods are based on contrasts between the physical properties of different rock material, e.g. density, magnetization, electrical properties, elasticity, etc.. It should also be borne in mind that geophysical results have to be combined with geological information to provide geologically realistic and useful information.

Anomalous behaviour in the vertical component of the gravitational attraction, commonly called gravity anomalies result from local variations in density in the crust. The success with which the gravity method can be applied depends on the density contrast between the different rock types that have to be differentiated and the size to depth ratio of the anomalous bodies. Gravity meters can not do direct measurements of the gravitational attraction because they can only measure the difference in gravity between two stations namely **g**. Before the results of the survey can be compared and interpreted in geological

terms, the raw gravity measurements have to be corrected and converted to what is commonly known as a Free-air or Bouguer anomaly value.

1.5.1 Reductions and Corrections

The following reductions have to be applied to gravity observations:

Instrumental drift and corrections for Earth tides:

Gravity meter readings change ('drift') with time as a result of elastic creep in the spring mechanism, thus produces an apparent change in gravity at a given station. Earth tides may cause a change in gravity of up to $0.3\,mGal$ with a minimum period of about 12 hours (This may be neglected during marine gravity surveys). The instrumental drift can be determined by repeating measurements at a base station. The observed values are a function of time, the so-called drift curve. By subtracting the amount of drift (and tidal effect) from the observed gravity values, corrections for the stations may be carried out.

Due to the fact that no base station is available at sea, a well known absolute value from a landsite station must be transferred to the vessels gravimeter. This procedure has to be done before and after the cruise. Therefore the values obtained during the survey may be compared to the world wide base values i.e. the international gravity network (IGSN).

Latitude reduction:

Both the variation in centrifugal force due to the Earth's radius and the variation due to polar flattening produce an increase of gravity with latitude. The Geodetic Reference System 1967 (GRS67) gives the theoretical value of the gravity g at a given latitude Φ:

$$g_{th} = 978031.846(1 + 0.005278895\sin^2\phi + 0.000023462\sin^4\phi) \qquad [mGal]$$

The latitude correction δg_L is obtained by differentiating the equation above (the $\sin^4\phi$ term is neglected):

$$\delta g_L = \frac{\partial g_{th}}{\partial s} = \frac{1}{R_e}\frac{\partial g_{th}}{\partial \phi} = -0.811\sin^2\phi \qquad [mGal/km]$$

Where s is the horizontal N-S distance and ($R_e\phi$) is the radius of the Earth. The correction is negative with distance northward in the northern hemisphere or positive with distance southwards in the southern hemisphere. This is to compensate for the increase in the gravitational field from the equator towards the poles.

Free-air reduction:

Since gravity varies inversely with the square of distance, it is necessary to correct for changes in elevation between stations to reduce field readings to a datum plane. The free air reduction is the difference between gravity

measured at sea level and at an elevation of h metres with no rock in between, and is positive at elevations above sea level, and negative below. The acceleration of gravity g is given by:

$$g = (\frac{\gamma M_e}{R_e^2}) r_1$$

Where γ is the universal gravity constant, M_e the mass of the Earth, R_e the radius of the Earth and r_1 extends downwards to the centre of the Earth. Differentiating with respect to the radial distance gives the gradient of the gravity acceleration due to the variations in the distance from the Earth's centre:

$$\delta g_{FA} = \frac{\partial g_{FA}}{\partial R_e} = -\frac{2\gamma M_e}{R_e^3} = -\frac{2g}{R_e} = -0.3086 \quad [mGal/m]$$

Due to the fact that the measuring profile is on sea-level, only the height of the gravity meter above sea level, the influence of Earth tides and the sea conditions needs to be taken into account. But the estimation of these “values” is complicated and will not alter the accuracy of the measured by more than 1 $mGal$, therefore they are excluded.

Eotvoes-correction:

When gravity is being measured from a moving platform it is subjected to an acceleration due to the rotation of the earth. This is the vertical component of the coriolis acceleration. This effect is at its maximum at the equator where the centrifugal force due to the earth spinning is greatest. This acceleration is named after Baron von Eotvoes (1919)

$$\delta g_{eot} = 7.487 v \cos\phi \sin a + 0.00415 v^2 \quad [mGal]$$

Where v is the ships speed in knots, ϕ the latitude in degrees and a the ships heading in relation to geographic north.

The term v represents the centrifugal acceleration moving over a curved surface of the earth and for normal ship operations, this value is very small, therefore it is usually discarded in quick calculations:

$$\delta g_{eot} = 7.487 v \cos\phi \sin a \quad [mGal]$$

For example a ship is sailing at the equator westward at 10 knots the gravity would be increase by 75 $mGal$ (correction would be –75 $mGal$)

The Eotvoes effect is greatest at the equator, course change is critical in northern and southern directions and velocity change is important in eastern and western directions.

Bouguer reduction:

The gravity effect of the material between sea-level and the gravimeter station is taken into account in the Bouguer reduction (~1/3 of free air reduction) which is derived by assuming an infinite horizontal slab of thickness $h[m]$ equal to the station elevation in the vicinity of the stations and given by:

$$\delta g_B = 2\pi\gamma\rho h = 0.0419\rho \qquad [mGal/m]$$

Compared to normal land based surveys, marine gravity surveys are the reverse case: the reference field is the sea surface and the water depth over ground will be replaced with a constant density. That means that the applied reduction is a terrain-correlated Bouguer reduction and the used density will be the middle-value of the firsts layer of the ocean floor.

When all of the proceeding reductions and corrections have been applied to the observed gravity reading, one obtains the value of the Bouguer anomaly g_B for the station:

$$g_B = g_{obs} - g_{th} + (\delta g_L + \delta g_{FA} - \delta g_B + \delta g_{eot})$$

Where g_{obs} is the station reading, g_{th} the theoretical gravity, δg_L the latitude reduction, δg_{FA} the free-air reduction, δg_B the Bouguer reduction and δg_{eot} as Eotvoes correction.

The Bouguer anomaly value is the difference between the theoretical gravitational attraction of the earth and the measured attraction at sea-level for a crust with a uniform thickness and density of 2670 km/m^3. Thus the gravity values may be compared to world wide base values.

1.5.2 The Sensor

The LaCoste & Romberg S56 sensor is a high-dampened and astasized version of the normal L&R-land gravity meter, which is mounted on a stabilising platform (Fig. 6a,b). This platform holds the sensor unit in the horizontal plane, thus compensating for the roll and pitch of the vessel.
On the top of the vertical sensor is a pair of gyros and accelerometers, these instruments control torque motors which stabilise the long and short axes of the gravity meter. A special algorithm between these three units keeps the platform stable like a dampened pendulum. The period of the platform can be set, depending on the movement of the vessel, i.e. in case of ocean waves the platform period would be long enough to compensate for this movement.

The system provides all the equipment necessary for filtering, logging and pre-processing gravity measurements. It also provides the electronic control for the platform, the power system and platform and monitor registration facilities.

a 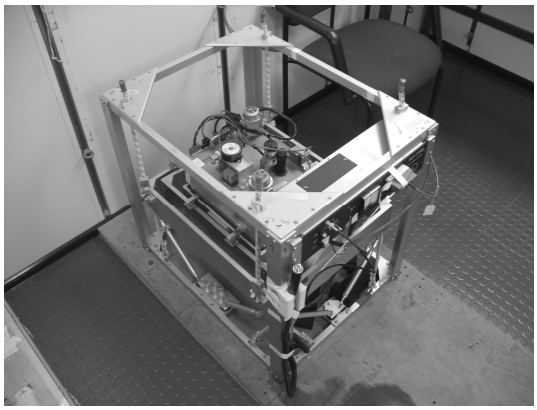 b 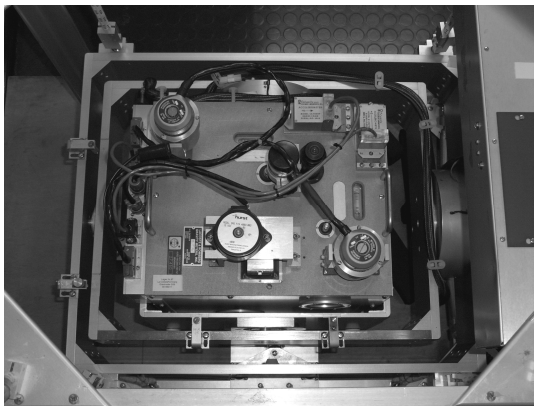

Figures 6a,b: Fotographs of the LaCoste & Romberg S56 sensor as mounted on the stabilising platform.

The sensor itself may be imagined as a mass, attached to a movable beam, which is free to rotate about (Figures 7 and 8). The beam is supported by a zero-length-spring. The spring/mass system is monitored every 10th second and is connected to a feedback loop and nulled. With respect to operating on a moving platform, the mechanical system needs dampeners. The density of the dampers is chosen in a way that any attracting force (acceleration) is converted into a constant velocity in the beam. The measured position of the beam, the spring tension and a mathematical model of the mechanic of the sensor allows the determination of the relative value of g.

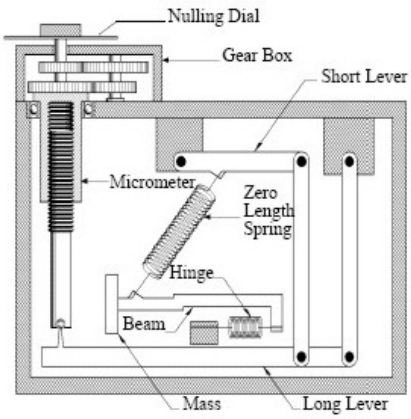

Figure 7: Principle drawing of the sensor system.

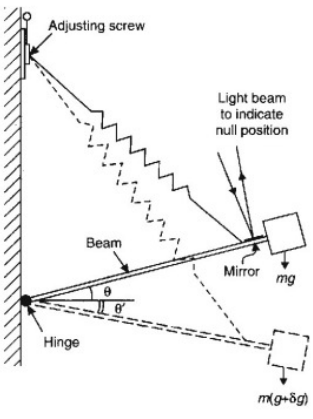

Figure 8: The movable beam, supported by a zero-length-spring..

Due to the construction of the instrument the sensor can be described as a 1-dimensional harmonic oscillator.

$$g_{sen} + \ddot{\ddot{B}} + b\ddot{B} + f\dot{B} + kB - cST + CC = 0$$

Where CC is the Cross Coupling (the mathematical description of the horizontal dynamic system of the beam in a vertical movement), ST is the spring tension (the upward force excerted by the zero-length-spring to balance the downward pull of gravity on the mass), B is the beam (position of the mass, which will have a range of motion of about 1mm, measured with an capacitance position indicator in $[V]$), $\ddot{\ddot{B}}$ is the vertical acceleration (determined from beam position, mostly proportional to instantaneous imbalance between the spring tension and gravity) and f, k, b, c are scale factors.

Due to the massive damping of the movable beam $(\ddot{B} = 0)$ the equation can be reduced to.

$$g_{sen} = ST + K\dot{B} + CC + \ddot{\ddot{B}}$$

This means that a gravity value may be calculated with a linear sensor model. K is a constant which will convert the measured arm velocity to gravity (depending on the beam sensitivity and dampening).

1.5.3 Output format

ID	*time*			*g*	*ST*	*CC*	*rBeam*	V_{cc}	A_l	A_x	V_e	A_x^2	X_{acc_2}	L_{acc_l}	X_{acc_2}	L_{acc_2}	*PPD*	*PP*
2005157	**10**	**0**	**0**	**9115.48**	**9119.47**	**1.28**	**-2369.1**	**-461.0**	**-701.0**	**-564.0**	**681.0**	**311.0**	**235.0**	**465.0**	**-585.0**	**-810**	**00FFFFFF**	**75**
2005157	**10**	**0**	**1**	9115.48	9119.47	**-40.48**	**-4192.3**	**-1265.0**	**-425.0**	**-283.0**	**83.0**	**219.4**	**388.0**	**1014.0**	**-757.0**	**-1227**	**00FFFFFF**	**75**

Field	**Symbol**	**Units**	**Filter**
LineID	*ID*	-	
Time	*time*		
Gravity	*g*	[mGal]	60 point digital,
Spring tension	*ST*	[CU]	3x20s,
Cross coupling	*CC*	[CU]	3x20s,
Beam	*rBeam*	[mV]	3x20s,

The cross coupling term and his parameter:

$$CC = X^2_{acc}\ddot{\ddot{B}} + L^2_{acc}\dddot{B} + V_e\ddot{\ddot{B}} + V_{cc}\dddot{B} + A_x\ddot{\ddot{B}} + A_l\dddot{B} + A_x^2\ddot{\ddot{B}}$$

V_{cc}	[mV]	3x20s
A_l	[mV]	3x20s
A_x	[mV]	3x20s

	V_e	[mV]	3x20s
	A_x^2	[mV]	3x20s
	X_{acc}^2	[mV2]	3x20s
	L_{acc}^2	[mV2]	3x20s
	X_{acc}	[mV]	3x20s
	L_{acc}	[mV]	3x20s
parallel port data	PPD	hex word	
platform period	PP	number	

1.5.4 Installation and Operation

During operation the gravity meter may be described as a black box system. This means that during the survey the equipment is virtually autonomous. Nevertheless, a daily check interval is required to control:

- the internal pressure,
- the spring tension syncronisation,
- the heater cycling phase

More care is required during the installation the system. The initial setup will determine whether a survey is successful or not. Due to the different system a brief description is provided in the appendix.

1.5.5 Gravity Base Station Readings

A gravity meter can only measure the difference in gravity between two stations, therefore there is a need to transfer the vessel-measured “raw data” to a well known landsite base station.
With a normal land gravity meter we may measure a value of g at a given time at a known base station then again next to the ship. With a transfer function we compare these values with the sea-gravity meter. This must also be completed after the cruise to compare and check the data for drifting processes and abnormal behaviour. The calibration process ensures that all measurements at sea level become useful for global research.

The Council of Geoscience in Pretoria provided the following base station information:

Cape Town:
Station “UCT NEW”, in the Menzies building (University of Cape Town), western side of the entrance foyer on the second level.

Latitude [°]	Longitude [°]	Height [m]	Gravity [mGal]
-33.5730	18.2739	109.76	979616.80 (± 0.1)

Durban:
Station “DURM” at the Durmarine Building, Port Captain’s Office

Latitude [°]	Longitude [°]	Height [m]	Gravity [mGal]
-29.6875	31.0355	5.00	979348.66 (± 0.02)

The dockside measurements were performed at the beginning and end of the expedition in Cape Town and Durban with a LaCoste & Romberg land gravity meter (Type G-744). The corresponding readings with the land gravity meter and the respective absolute gravity value are listed below.

Station	Reading [mGal]	Absolute gravity [mGal]
Cape Town “UCT NEW”	3090.35	979616.80
Cape Town Harbour	3111.68	979638.13
Durban “DURM”	2818.58	979348.66
Durban Harbour	2822.62	979352.70

The corresponding readings of the S56 air-sea gravity meter at the dockside were:

Station	Reading [mgal]
Cape Town Harbour	9669.88
Durban Harbour	9376.72

Using the above given values for the absolute gravity at the dockside and the measurements made onboard the ship a drift of 7.71 mgal can be calculated for the S56 gravity meter for the duration of the expedition.

2. Geology – Dredge report

(M. Watkeys, M. Brayshaw, Z. Thackeray)

2.1 Introduction

The break-up of Gondwana was the single most important geological event to have affected the southern hemisphere in the past 500 million years. The Mozambique Ridge and Mozambique Channel are features central to this break-up because, to the east lay the future boundaries between Madagascar, India, Australia and Antarctica while to the west, the boundaries between Africa, South America and Antarctica.

The Mozambique Channel of undoubted oceanic origin, having formed during the initial separation between Africa and Antarctica in the late Jurassic and early Cretaceous. The Mozambique Ridge, on the other hand, is of less clear origin. The ridge separates the Mozambique Channel to the east from the Natal Valley to the west. It rises up to 3 km above the flanking oceanic crust, extending northwards from 35 degrees S to the coast of central Mozambique. Dredging has produced not only basalt from the ridge but also metamorphic rocks. These have been interpreted as indicating the presence of a continental basement to the ridge that is similar to the *ca*. 1.0 Ga basement found in SE Africa and western Dronning Maud Land, Antarctica. This conclusion has proved to be an obstacle to any tight refit between Africa and Antarctica that is suggested from the matching geology. It is not possible to juxtapose the proposed conjugate margins without eliminating the Mozambique Ridge and that is impossible if the ridge is continental.

One of the aims of the cruise was to establish where the position of the continent-ocean boundary was along the Mozambique Ridge through the use of magnetic characterisation of the crust. Dredging could then take place on either side of this boundary to ascertain the nature of the basement. However the magnetic survey very quickly revealed that there was no continent-ocean boundary because the whole ridge was unequivocally oceanic in origin. Consequently the dredging strategy changed and was aimed at obtaining samples of the ridge at various localities along its length to examine its evolution. The cruise also gave the opportunity to sample the volcanic rocks of the Mozambique Channel at Jaguar Seamount close to the atoll of Bassa da India.

2.2 Dredging

2.2.1 Methodology

It was clear from previous work that one of the problems with dredging would be that the basement was very rarely exposed and could be covered by up to 2.5 km of sediment. Dredge sites were chosen by close examination of the Parasound profiles in conjunction with the bathymetry maps produced en route by the Kongsberg Simrad EM120 multibeam echo sounder. Where possible steep sections were chosen that might represent fractures zones that would expose the basement.

The ship was stationed at a position above the base of the chosen slope and the chain-bag dredge lowered onto the ocean floor. Some further line was then laid out, 200 m or more depending on the depth, and the ship then allowed to drift upslope. Tension on the winch was then monitored to establish whether the dredge was biting or whether it was jammed against a rock and needed releasing. Once the ship had drifted to the final position above the top of the slope, the chain-bag dredge was winched in, again monitoring the tension carefully. A problem encountered on some of the dredges was that the chain-bag had become caught up in the teeth of the dredge. This not only considerably reduced the volume of rock that could be sampled but may actually have resulted in some samples being tipped out of the dredge.

2.2.2 Dredge locations

Five of the dredge localities were on the Mozambique Ridge and one was on the Jaguar seamount in the Mozambique Channel (Figure 9 and Table 5). One of the dredge sites on the Mozambique Ridge yielded no samples (DL0) and two of them (DL1 and DL2) required two dredges in order to collect the rocks. DL4 yielded samples DL-80 and Dl-81 on the first dredge and the remaining samples on the second dredge. The first dredge on the Jaguar seamount (DL4) brought up one rock sample (DL4-79) with all the other samples from this site collected by the second dredge. All the samples collected at the dredge sites are listed in Appendix 3.1.

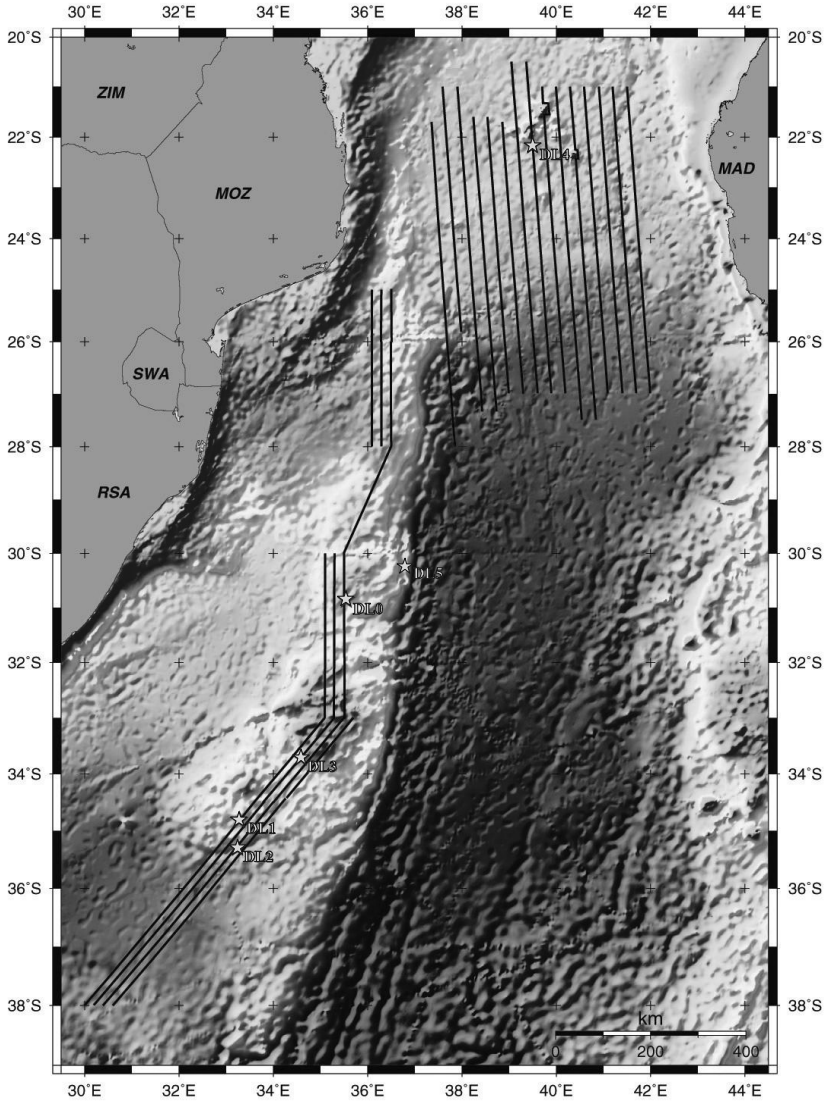

Figure 9: Map showing the dredge locations on the Mozambique Ridge (DL0, DL1, DL2 and DL3) and in the Mozambique Channel (DL4)

Table 5: Summary of dredge localities

Station	Date	Dredge	Time (UTC)	Latitude	Longitude	Depth
DL1	26/05/2005	On bottom	07:26	34° 48' 52 S	33° 17' 27 E	2699 m
		Off bottom	08:20	34° 48' 15 S	33° 17' 62 E	2461 m

		On bottom	10:02	34° 48' 58 S	33 ° 17' 21 E	2725 m
		Off bottom	12:00	34° 48' 04 S	33 ° 17' 78 E	2440 m
DL2	28/05/2005	On bottom	22:27	35° 18' 53 S	33° 14' 45 E	4077 m
		Off bottom	23:28	35° 17' 53 S	33° 14'16 E	3526 m
	29/05/2005	On bottom	01:39	35° 18' 37 S	33° 14' 23 E	3932 m
		Off bottom	03:37	35° 17' 06 S	33° 13' 62 E	3508 m
DL3	02/06/2005	On bottom	08:05	33° 41' 16 S	34° 36' 14 E	1898 m
		Off bottom	09:13	33° 40' 52 S	34° 36' 51 E	1804 m
DL0	04/06/2005	On bottom	18:12	30° 53' 04 S	35 ° 33' 26 E	2264 m
		Off bottom	18:49	30° 52' 47 S	35 ° 33' 27 E	1920 m
		On bottom	20:07	30° 53' 32 S	35° 33' 43 E	2346 m
		Off bottom	21:15	30° 52' 16 S	35° 33' 45 E	1889 m
DL4	16/06/05	On bottom	11:22	21° 56' 48 S	39° 28' 71 E	1111 m
		Off bottom	13:03	21° 56' 46 S	39° 28' 57 E	984 m
		On bottom	14:05	21° 56' 47 S	39° 28' 67 E	1097 m
		Off bottom	15:52	21° 56' 23 S	39° 28' 32 E	756 m
DL5	05/07/05	On bottom	10:53	30° 33' 43 S	36° 52' 26 E	2945 m
		Off bottom	11:46	30° 32' 67 S	36° 51' 84 E	2621 m
		On bottom	13:19	30° 33' 63 S	36° 52' 31 E	2925 m
		Off bottom	15:01	30° 32' 91 S	36° 51' 90 E	2660 m

2.3 Brief description of the dredged rocks

2.3.1 Dredge Site 1 (DL1)

This site, which is towards the southern end of the Mozambique Ridge (Figure 9 and Table 5), yielded 23 samples, ranging in size from 35 cm x 26 cm x 12 cm to 12 cm x 6 cm x 4 cm. Of these, five samples comprised breccia overlain by shale, while the remaining samples were shale.

The breccia consists of poorly sorted, angular clasts, up to 10 cm x 5 cm in size, consisting of variably weathered and altered basaltic fragments. In one sample a clast of amygdaloidal basalt appears to be part of a columnar joint. The breccia is overlain by very fine grained, finely laminated black shale. In three of the samples, the laminations are crosscut by straight burrows that are about 5 mm in diameter and up to 7 cm deep. In the two other samples, the burrows are confined to the breccia. This demonstrates that the breccia was exposed, weathered and burrowed, before the shale was deposited so there may have been a significant time-break between formation of the basalt breccia and

deposition of the shale. In two cases, the burrows terminate in a bivalve cast that maybe *Pholas* sp.

The shale overlying the breccia appears to be the same rock type that comprises the remaining 18 samples. All are very fine grained, black shales and most have well developed laminations with even the suggestion of 1 cm to 2 cm thick bedding in some samples. Close examination reveals possible low angle cross-laminations within one bed while others may contain very subtle fining, upwards, graded bedding. The surfaces of some samples are covered in small black nodules, approximately 1 mm in diameter. This feature, together with the dull, metallic lustre of some samples, is taken as indicating that manganese has precipitated on the surface. It will not be possible to establish whether all the shales are manganifereous until thin-sections are examined and geochemical analyses undertaken, but the suspicion is that this may be the case.

The shale laminations in some samples are gently folded. In some cases, this may be due to the draping effect when manganese precipitates on a curved surface laminations. In other cases, however, it appears to involve soft-sediment deformation. In one instance, folding seems to have commenced as box-folds, with limbs of 2.5 cm long and crests 4 cm long, and then the bedding begins to become overfolded and the upper limb thrust out.

2.3.2 Dredge Site 2 (DL2)

This site was at the southernmost extremity of the Mozambique Ridge (Figure 9 and Table 5). Seven samples were dredged from this site. They range in size from 30 cm x 20 cm x 5 cm to 11 cm x 10 cm x 2 cm.

Three of the samples consist of basalts enclosed in black shale. The basalt is fine to medium grained with a subophitic texture. Two of the specimens are amygdaloidal and are cut by some thin veins, up to 1 mm thick. There is evidence of alteration with the plagioclase appearing have partially altered to epidote while pyroxene may have partially altered chlorite. In the other specimen, the basalt is medium grained and does not appear to have been badly altered, except within 3 mm of the edge of the clast where it is weathered.

The black shale enclosing the basalt has the same appearance as the shale at dredge site 1. It is black, very fine grained and laminated. In this case, however, it can be seen that the laminations are parallel to the edges of the basalt fragments, and therefore wrap around the clasts. This would suggest that the shale is a chemical precipitate rather than a detrital sedimentary rock and has a bearing on the interpretation of the shales from that previous dredge site. However, there is no evidence of the bedding or any of the folding observed at the previous site. Three of the other samples all consist of this shale, each with a thin rind attached that may be the outer weathered portion of a basalt clast.

The remaining specimen is of particular interest. It is a pinkish weathered sedimentary rock that is medium grained and moderately sorted. It contains

subangular clasts of felsic rock fragments and quartz as well as round light green clasts that could be amygdales from basalt. It also contains subangular to angular clasts of dark, fine grained rock fragments which might be basalt. The fine grained, pinkish groundmass appears now to be a clay mineral. The initial appearance of the rock suggests that it is a feldspathic arkose. However the texture is reminiscent of a volcaniclastic rock, so an origin involving explosive felsic volcanism cannot be ruled out until this rock is examined in thin-section.

2.3.3 Dredge Site 3 (DL3)

This site dredge the south-west flank and top of a small hill towards the centre of the southern section of the Mozambique Ridge (Figure 9 and Table 5). A total of 33 rocks samples were collected at this dredge site, ranging in size from 40 cm x 28 cm x 10 cm to 7 cm x 7 cm x 5 cm. In addition, 10 manganese nodules were dredged, ranging from 5 cm to 10 cm diameter.

All of the rocks recovered were either encrusted in manganese or were the products of manganese precipitation. At least 19 of the samples appeared to have been originally shales, silty shales, siltstones or sandstones. Three samples were burrowed and bioturbated, two contained bivalve remains or their imprints while two others contained bone fragments. A further two had contorted laminations. When the nodules were sectioned, calcium carbonate was commonly found in the core. The core of the larger samples was porous and comprised decomposed calcareous or ferruginous material.

2.3.4 Dredge Site 4 (DL4)

This site, on the Jaguar seamount, yielded a total of 16 rock samples, the largest being 72 cm x 36 cm x 18 cm and the smallest 12 cm x 11 cm x 10 cm. All of the samples were volcanic rocks, enclosed in the inevitable drape of black shale. They can be broadly subdivided into three groups: olivine basalts, pyroxene-phenocryst basalts and altered basalts.

Three of the samples consisted of grey-green coloured olivine basalt. They are characterised by being spotted with olivine up to 3 mm in diameter. The olivine is altered to colours varying from light grey to reddish-brown, probably due to serpentinisation. In one of the samples, the basalt is overlain by a clastic rock, with subrounded to rounded medium grain size clasts set in a more angular matrix. Some of the rounded clasts have concentric laminations and the whole layer appears to be a lapilli tuff. This is, in turn, overlain by the shale drape.

Five of the samples are basalts containing distinctive euhedral pyroxene phenocrysts of which are aligned in some specimens. The phenocrysts may be up to 20 mm long by 5 mm wide and, when smaller, seem to make up about 30% of the rocks. The pyroxenes, which are recognisable by their shape, have altered to a fine grained intergrowth of a white and a black mineral. Fragments of these occur in the lapilli tuff overlying one of the olivine basalt samples. In places, the basalt is intruded by white veins, generally varying between 1 mm to

2 mm thick. The injection of these veins is associated with brecciation of the basalt, so it has been affected by a hydrothermal event.

The remaining samples, bar one, are basalts altered to varying degrees, probably by this hydrothermal event. In some samples there is pervasive alteration through the whole rock, resulting in pinkish-grey to yellow brown colours, while in others the alteration is associated with veining. In one case, the altered rock may not have originally been basaltic but felsic in composition as it appears to be a dyke that intruded brecciated pyroxene basalt that is relatively unaltered.

Evidence of the presence of a more felsic magma is preserved in one sample. This comprises basalt containing parallel felsic layers up to 1 cm thick and with a similar spacing (Figure 10). In between the layers, the felsic material forms rounded blebs up to 3 mm in diameter that seem to be immiscible droplets.

2.3.5 Dredge Site 5 (DL 5)

This site was on the eastern side of the Mozambique Ridge where the basement was indicated as being exposed by Raillard (1990). The eastern flank of a N-S trending ridge was dredged and six samples obtained. All were of manganese shales, some of which contained angular to subangular grit to pebble-sized clasts of quartz and a metamorphic rock. In hand specimen, these rocks appear to be fine-grained actinolite schist, but this needs to be confirmed by examination in thin-section. The largest sample (DL5-85) contains a quartz breccia that also contains small angular clasts of a fine-grained metamorphic rock that appears to be a diorite gneiss. Again, thin-section work will be needed to confirm this.

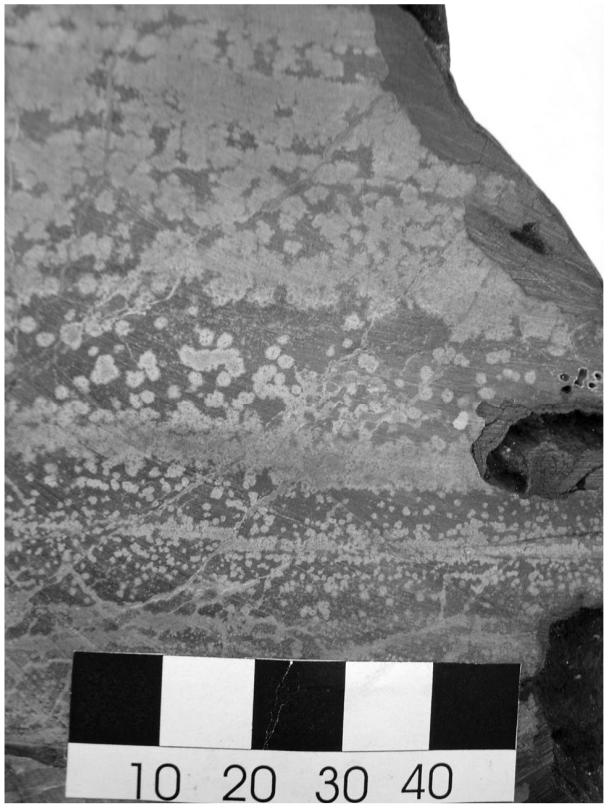

Figure 10: Immiscibility droplets in a basalt from the Jaguar seamount (DR4-65) (scale bar in mm)

2.4 Modelling the depth of formation of the oceanic crust

2.4.1 Background equations

An important point of interest is the depth below sea-level or height above it at which the igneous rocks of the basement formed. As the Mozambique Channel is oceanic crust, its development can be modelled by well-established depth equations, allowing these depths or heights to be calculated. Aseismic ridges on oceanic crust, can also be modelled in the same way (Detrick *et al*., 1977), so it is also possible to undertake these calculations for the Mozambique Ridge.

Parsons and Slater (1977) demonstrated that the depth (D) of the oceanic crust is proportional to the square root of its age (T) according the equation:

$$D = 2500 + (350\sqrt{T}) \quad (1)$$

It was recognized by Parsons and McKenzie (1978) that the above equation was applicable only to oceanic crust younger than 80 Ma. For older crust the following equation applies:

$$D = 6400 - 3200 \exp(-T/62.8) \quad (2)$$

The original depth (positive value) or height (negative value) at which oceanic crust younger than 80 Ma formed ($D_{o<80}$) can be calculated by modifying equation 1:

$$D_{o<80} = D_c - (C\sqrt{T}) \quad (3)$$

where D_c is the depth corrected for sediment loading and C is an empirical value. Hayes (1988) showed that for the Indian Ocean a figure of 280 was best for C rather than 350 as in equation 1.

For oceanic crust older than 80 Ma, assuming that the average depth of a mid-ocean ridge is 2500 m (which is the reason for 2500 in equation 1), equation 2 can be rearranged to give the original depth ($D_{o>80}$) as:

$$D_{o>80} = D_c + 3200 \exp(-T/62.8) - 3900 \quad (4)$$

The depth correction for sediment loading (D_c) is obtained from Crough's (1983) equation:

$$D_c = d_w + t_s (\rho_s - \rho_m / \rho_w - \rho_m) \quad (5)$$

where d_w is the water depth, t_s is the sediment thickness, ρ_s is the density of the sediments, ρ_m is the density of the mantle and ρ_w is the density of sea-water. This equation gives the present corrected depth to the top of the oceanic crust when the sediment loading effect is removed.

2.4.2 Application of the depth models

These equations were applied to data obtained along all the ship tracks in both the Mozambique Channel and the Mozambique Ridge using the parameters in table 6. Sediment thicknesses were obtained from Raillard (1990) who has a figure indicating two-way time in seconds (twt) to the basement. By assuming a seismic velocity of 1.5 km s^{-1} in water and 2.0 km s^{-1} in sediment, these two-way times were converted to sediment thickness in metres using the following equation:

$$t_s = (twt * 1000) - [(2\ d_w)/1.5] \quad (6)$$

The original depths and heights were calculated using both the equation for crust younger than 80 Ma ($D_{o<80}$)(equation 3) and the equation for crust older than 80 Ma ($D_{o>80}$)(equation 4) in order to compare the range of results. The latter equation, which is the correct one to use in this case, yields shallower depths and greater heights by over 300 m. An example of these results for one line are presented in table 7 and the overall results for all the lines in the Mozambique Channel and Mozambique Ridge are shown graphically in Figure 11.

Table 6: Parameters used in the equations

d_w	From bathymetry obtained by the Kongsberg Simrad EM120 system (m)
t_s	Estimated from two-way time (m) (equation 6)
ρ_s	1.9 kg m^{-3}
ρ_m	3.22 kg m^{-3}
ρ_w	1.03 kg m^{-3}
C	280
T	Obtained from interpretation of magnetic anomalies (Ma)

Table 7: Example of the results of the depth calculations for one line.

Locality		**Measured depths and thicknesses**			**Age**		**Calculated depths**		
Line 3		Line 3					Line 3		
Latitude	Longitude	To basement	Water	Sediment			Dc	Do>80	Do<80
decimals	*decimals*	twt (s)	d_w (m)	t_s (m)	anomaly	(Ma)	(m)	(m)	(m)
26.5	38.35	7.4	4514	1381	M2	124	5347	1891	2229
26.5	38.35	7.2	4569	1108	M4	126	5237	1767	2094
25.7	38.3	7.1	3759	2088	M10	130	5018	1521	1825
25.4	38.25	6.75	3568	1993	*M12*	135	4769	1242	1516
24.1	38.5	6.3	3128	2129	*M16*	140	4411	856	1098
22.7	38.05	6.75	3288	2366	M21	147	4714	1122	1319
21.9	38	6.75	3211	2469	M24	153	4699	1079	1236

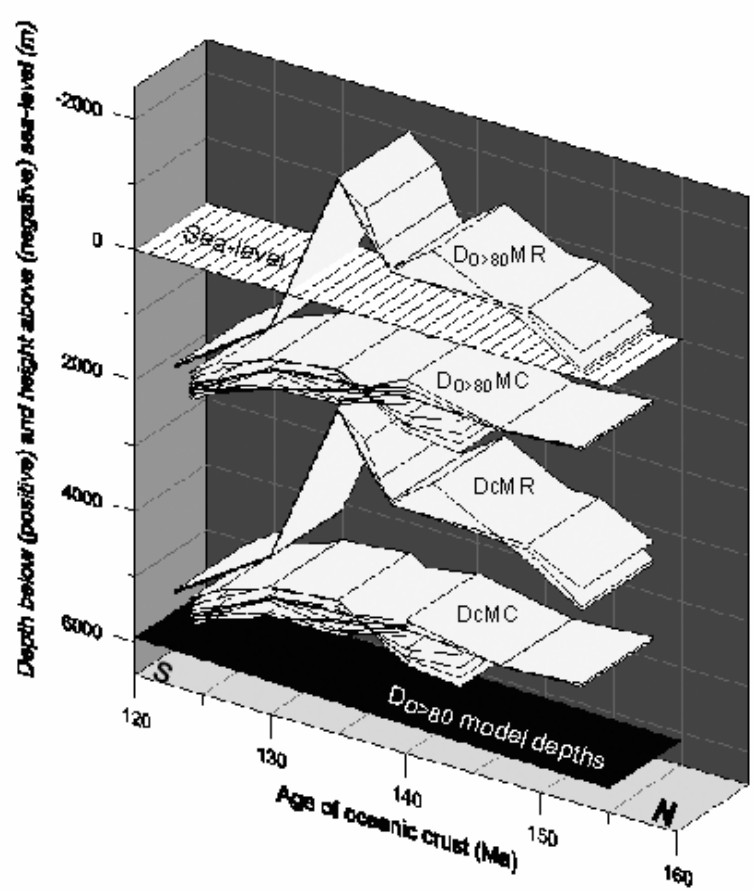

Figure 11: Corrected present depths from equation 3.5 (D_c), and original depths or heights of the oceanic crust at the time of formation from equation 3.4($D_{o>80}$), in the Mozambique Channel (MC) and on the Mozambique Ridge (MR). The section of the Mozambique Channel analysed here extends from 22°S to 27°S while the Mozambique Ridge extends from 26.5°S to 37 °S.

2.4.3 Discussion of the depth model results

One of the concerns with these calculations was the potential source of error due to the regional nature of Raillard's (1990) map, together with the simplified estimate of thickness from the two-way time (equation 6). However, the shallowest portion of the Mozambique Ridge has an insignificant amount of sedimentary cover, with basement exposed in places, so the results from that locality (135 Ma on Figure 11) are unaffected by this conversion. Also, the ship tracks crossed the same magnetic anomaly on the Mozambique Ridge that not only had different depths but also different two-way times. In these cases the corrected depths yielded very similar results for the same anomaly. This also occurred in the Mozambique Channel and consequently the calculated values are considered valid.

Three aspects are immediately clear from these results:

- The corrected depths for the Mozambique Channel and the Mozambique Ridge are approaching the model depths at 125 Ma.
- The corrected depths for the Mozambique Channel are shallower than usual for oceanic crust (on average 77.5% of the model depths) and

show a trend of decreasing depth with increasing age, in contrast to the model depths.
- The calculations for the original depths and height of formation of the Mozambique Ridge reveal that, prior to about 132 Ma, the present top of the ridge formed above sea-level.

The fact that the depths at 125 Ma are converging on the model depths gives some confidence that the deviations seen from the expected behaviour of oceanic crust in the older ages are real. Any explanation needs to take note of the fact that the southernmost part of the Mozambique Channel on Figure 11 is just north of the northernmost part of the Mozambique Ridge. This is due to an offset in the segments of mid-ocean ridge that produced the crust in these two regions.

In the case of the Mozambique Ridge, the most probable explanation for its original elevation is that it represents a zone of voluminous volcanism, the cause of which may have been a hot-spot. The slightly elevated depths of the Mozambique Channel might be due its proximity to the hot-spot trace or be due to increasing depth of the mid-ocean ridge from 155 Ma to 125 Ma. These two effects may indeed be related. Alternatively they may be due to uplift caused by later igneous activity that gave rise to the Bassa da India group of volcanoes. In this case, the corrected depths close to these volcanoes would be expected to be more elevated, but this is not the case. In Fact the opposite may be the case as there is a suggestion in the data that the volcanoes may be flexing the oceanic crust downwards. Thus the former hot-spot explanation is preferred.

All of the dredge sites on the Mozambique Ridge, with one exception, are calculated to have originally formed above sea-level, as was the site on the Jaguar seamount (Table 8). The results of Figure 11 give the impression that from about 155 Ma to 125 Ma the whole of the Mozambique Ridge was a promontory above sea-level, extending southwards from the Mozambique mainland from 26.5°S to 33°S. This is misleading because the depths and heights shown are the values when each part of the ridge formed; they do take into account the subsidence that took place after emplacement. To illustrate this, Figure 12 shows the ridge at 135 Ma, at the time of the highest emplacement of the oceanic crust. The values of heights and depths of the older portions of the ridge were calculated both according to the subsidence rates typical of oceanic crust younger than 80 Ma (equation 1) and according to the subsidence rate indicated in the Mozambique Channel.

Based on this premise and the current level of erosion, the Mozambique Ridge would have been a volcanic archipelago at 135 Ma rather than a continuous plateau above sea-level. At the very least, it would have been an impediment to the circulation of ocean water below 1000 m. However, these values are calculated for the present surface of the Mozambique Ridge and do not take into account any crust that may have been eroded away since 135 Ma. In addition, the original depths of formation of the crust in the Mozambique Channel are not only elevated above the model depths but are virtually the same between 135 to 155 Ma. This indicates that the rate of subsidence is not only lower than the expected rate, but that it probably only began in this region after 135 Ma. There is no reason to suppose that it would have been any

different on the adjacent Mozambique Ridge. Taking all of this into consideration, it seems likely that the Mozambique Ridge was indeed a subaerial volcanic plateau building out into a widening ocean.

Table 8: Corrected present depth (D_c) and original depth of formation below (positive) or above (negative) present sea-level ($D_{o>80}$) of the oceanic crust at the dredge localities, using average depths (dw) at each locality , the parameters in Table 6 and equations 3.4, 3.5 and 3.6

Locality	twt (s)	dw (m)	ts (m)	Age (Ma)	Dc (m)	Do>80 (m)
DL0	3.3	2105	493	139	2402	-1448
DL1	3.5	2581	59	133	2617	- 899
DL2	5.1	3761	85	130	3812	316
DL3	3.0	1851	532	135	2172	-1355
DL4	0	982	0	144	982	-2595
DL5	0	2793	0	139	2793	-757

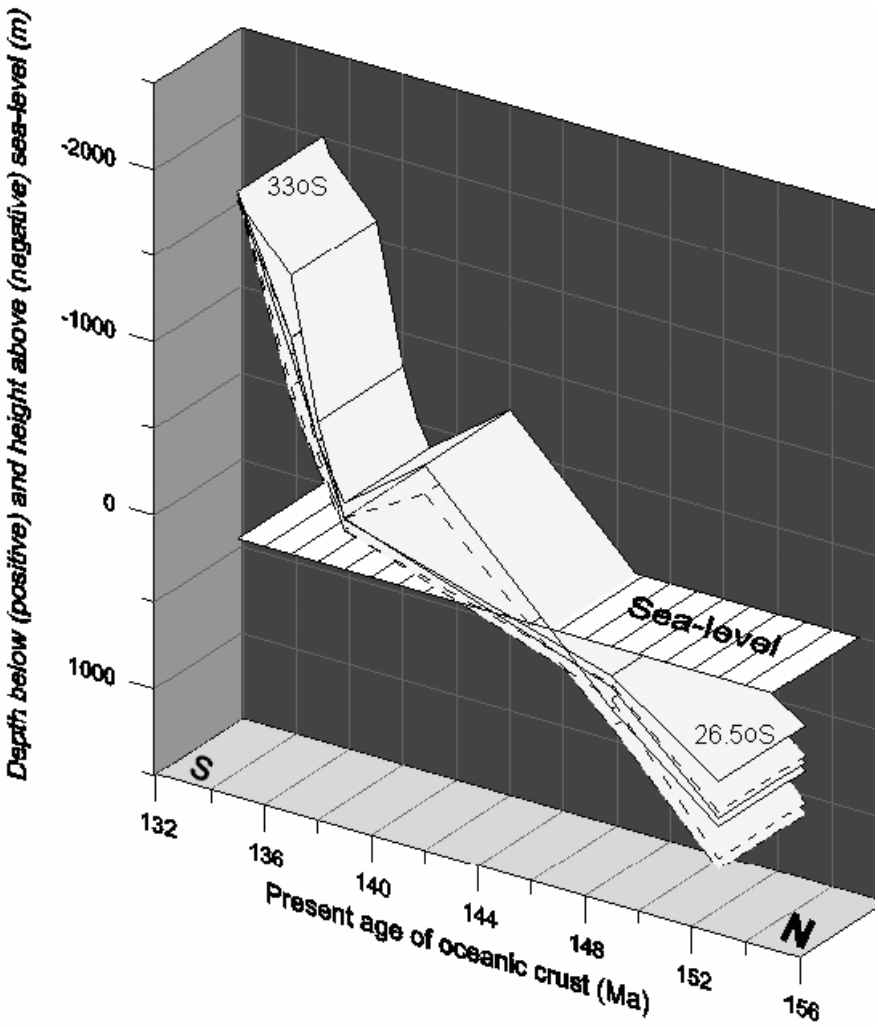

Figure 12: Modelled depths and heights along the Mozambique Ridge at 135 Ma. Dashed lines were calculated by subjecting the original depths and heights of formation to subsidence rates typical of oceanic crust younger than 80 million years old (equation 3.1). Solid lines were obtained by setting the subsidence rate at 77.5% of this value, based on the subsidence in the Mozambique Channel. The degrees shown are the present latitudes.

References

Crough, S.T. 1983. The correction for sediment loading on the seafloor. *Journal of Geophysical Research*, 88, 6449-6454.

Detrick, R.S., Sclater, J.G. and Thiede, J. 1977. The subsidence of aseismic ridges. *Earth and Planetary Science Letters*, 34, 185-196.

Hayes, D.E. 1988. Age-depth relationships and depth anomalies in the South Indian Ocean and South Atlantic Ocean. *Journal of Geophysical Research*, 93, 2937-2954.

Parsons, B. and McKenzie, D. 1978. *Journal of Geophysical Research*

Parsons, B. and Sclater, J.G. 1977. An analysis of the variation of ocean floor bathymetry and heat flow with age. *Journal of Geophysical Research*, 82, 803-827.

Raillard, S. 1990. Les Marges de l'Afrique de l'Est et les Zones de Fracture associées: Chaine Davie et Ride du Mozambique, These de Doctorat de l'Université Paris 6, 272 pp..

3. Bathymetric group

(R. Krocker, A. Labrenz, R. Niebling)

3.1 SIMRAD Multibeam Echo Sounder EM 120 System Description

The Simrad EM120 Multibeam Echo Sounder is an acoustic system to do extensive mapping of the ocean floor. A swath of multiple beams is generated which makes it possible to map a corridor below the ships track up to 5 or 6 times that of the water depth.

It consists of the following units:

- Transmit transducer array
- Receive transducer array
- Transceiver and Preamplifier Unit
- Operator Station

The EM120 transducers are linear arrays with separate units for transmit and receive.
The operating frequency of the EM 120 multibeam echo sounder is 12 kHz. This frequency is standard for deep ocean echo sounding, and gives a good balance between reasonably small dimensions, narrow beams, and good range capability.

The system has 191 beams per ping as narrow as 1° and an angular coverage sector of up to 150°. The beam spacing is normally equidistant, corresponding to 1% of depth at 90° angular coverage, 2% at 120° and 3% at 140°. Equiangle beam spacing is as well possible.

The ping rate is only limited by the round trip travel time in the water up to a ping rate of 5 Hz. The transmit fan is split into several individual sectors which are frequency coded (from 11.25 to 12.60 kHz). They are transmitted sequentially at each ping, with independent electronic steering according to the vessel attitude (roll, pitch and yaw) and with respect to the survey line heading. The swath can then be stabilized to fall on a line perpendicular to the survey line.
Pulse length and range sampling rate are variable with depth for best resolution.

3.2 SO183 Cruise Track

The cruise is separated into five sections as can be seen on figure 13. The first section is the transfer from Cape Town to the first survey area. The length of the transfer amounts to 1459 km. The second section comprises the first systematic survey; it consists of four parallel profiles between -34.5° and -38.0° latitude with a length of 2498 km. Due to bad weather conditions the following four planned profiles were not completed, but the existing profiles were lengthened to the north, to -33° latitude. The expansion to the north amounts 932 km. The third section forms the connection between the first and the second systematic survey areas, including additional profiles with a length of 2639 km. The fourth section is largest and occupied the half cruise duration. The measured tracks of the second systematic survey have a length of 11743 km. The fifth and final section is the transfer to Durban harbour with a length of 932 km. The directly bathymetric sampled area amounts to 215617 km². For comparison: The area of Germany amounts to 356910 square kilometres.

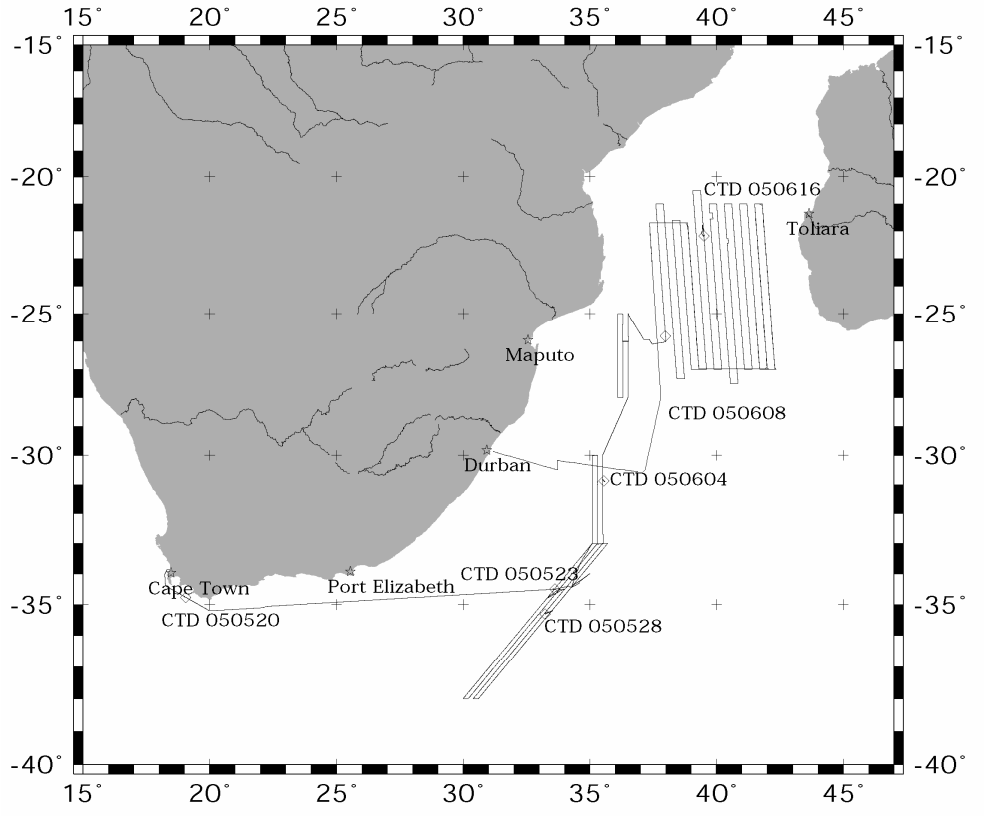

Figure 13: Tracks and CTD locations of SO183 cruise.

Table 9: Overview of sailed track length and bathymetric sampled area.

Section	Length [km]	Area [km²]
Transfer 1	1459	8662
Survey 1	2498	25610
Expansion of Survey 1	932	7379
Transfer2	2639	20936
Survey 2	11743	144565
Transfer 3	932	8465
total	**20203**	**215617**

3.3 Data acquisition and editing

The data acquisition is performed and controlled by the SIMRAD system, requiring set parameters. The data are stored in the SIMRAD internal binary format and are organized by survey and line number. In accordance with the various parts of the cruise as mentioned above, corresponding survey names were created. The line files are found within the corresponding survey directory. The storage interval of the system is set to thirty minutes, therefore, in the event of data loss, the cost is restricted. 48 files are built per day and 2267 files during the entire cruise with a complete size of 11.3 gigabyte.
On several occasions during file saving an error occurred, as not every half an hour a new file was created. Instead, the measured data were added to one single file. The cause of the error could not be determined. Therefore the operator must always ensure that the correct file size and number are present during data acquisition. In one case the erroneous large file could not be opened with Caris HIPS. An interface to the SIMRAD file format was written, as well as a program splitting the large file into half hour files was created to combat the error. During cruise time of 48 days, we continuously collected data with a data lack of only a view minutes.

To achieve a good coverage of the seafloor, the swath angle may be set to a high value, but the size of the angle also influences the data quality. A higher angle causes a degraded signal to noise ratio that will worsen with bad weather conditions. If the signal to noise ratio decreases and contact with the sea floor is lost, the swath angle will be decreased by system automatically. But in this case the edges of the profiles may still include many outliers, therefore the swath angle should be decreased further manually. In the case of a lost horizon, a constraint for the depth may be forced. If the signal to noise ration reaches the maximum operating limit, the system will often register the horizon at double depth. To suppress these multiples the depth constraint must be forced again. During bad weather conditions and in shallow waters, where multiples are difficult to detect, the sonar operator needs to pay attention continuously to the incoming data. In this situation the variation and optimization of swath angle is an important task of the watch keeper.
Figure 14 shows the consequence of bad weather conditions to data acquisition. During the upper profile in figure 14, the wind of 9 Bft came directly from the front, the ship was heaving and pitching and air was passing under the

transducers. During the lower profile the same wind conditions occurred, but the ship was sailing with the wind, reducing pitch, roll and heave. The EM120 sonar system installed on RV Sonne seems to be very susceptible to weather conditions.

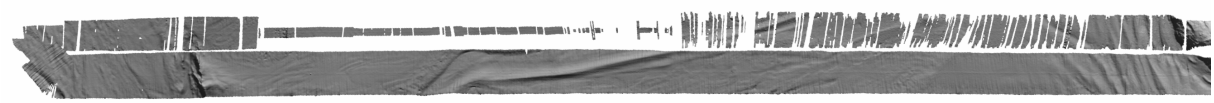

Figure 14: Degraded signal during bad weather conditions.

Caris HIPS software was used to process the bathymetry data, instead of the software package produced by SIMRAD. This decision was taken, because HIPS is the usual software at AWI, where the data has to be edited further after the cruise. The software was installed on a PC, which was placed by the system administrator at the bathymetric systems exclusive disposal.
The SIMRAD raw data could be imported by a conversion wizard without any problems. The data cleaning was done by flagging the rough errors. The careful cleaning of data and elimination of systematic errors will be completed after the cruise. Figure 15 shows the systematic error in the range of the centerbeam and its consequence to the gridded data (figure 16.).

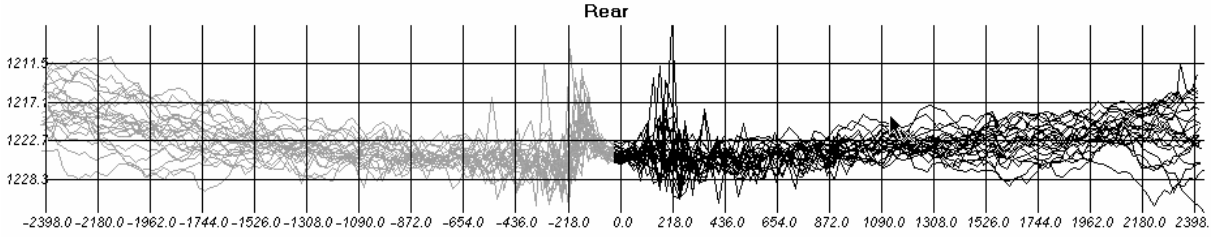

Figure 15: Systematic error in the range of the centerbeam.

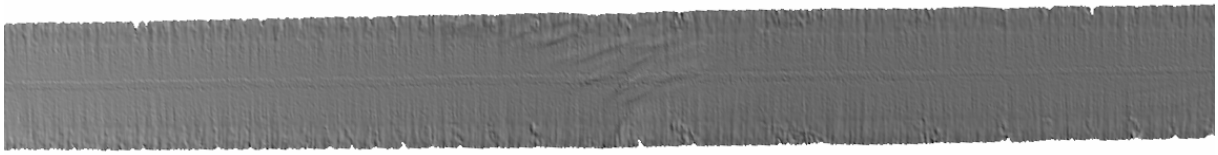

Figure 16: Consequence of systematic errors in the gridded data. Smooth appearance in the middle of the beam and errors at its flanks.

Furthermore, figure 15 demonstrates the roughness of the edges, which is caused by the larger uncertainty of edge beams. The vertical (across track) structures are due to small errors in roll correction. All these effects have to be minimized or eliminated in the future.

The cleaned data were exported to three column xyz ASCII files, for use in external gridding and plotting applications.

Calculating the irregular distributed depths into a regular grid, the software products Caris HIPS and GMT (Generic Mapping Tool) have been used. The

faster and more practical solution is the HIPS tool, where the requested gridding area needs to be defined as a Fieldsheet. Within it a grid can be calculated with variable scale, and plotted with various colour schemes and sun illuminations. The figures at the end of this contribution have been created this way. The disadvantage of this method is that hardcopies of the grids do not include frames or borders representing geographic references.
Another possibility of creating grids is to use GMT software, which runs in the UNIX environment. During the cruise, scripts have been written and improved to grid and plot bathymetric data using GMT commands nearly automatically.
The visualized bathymetry was fundamental in finding dredge locations.

3.4 CTD measurements

During the cruise six CTD measurements have been made to determine water conditions. Salinity, temperature and pressure are the main factors affecting the speed of sound in water. Therefore these parameters were sampled every meter of waterdepth, with this information the sound velocity may be calculated by the Del Crosso formula (see below).

$$C = 1448.6 + 4.618\,T - 0.0523\,T^2 + 1.15\,(S-35) + 0.018\,D$$

with T: Temperature of seawater [° C]
S: Salinity of seawater [‰]
D: Waterdepth [m]

Table 10: Statistics of the CTD measurements

Name	Date Time	Longitude	Latitude	Depth [m]
SO183_01_20050520.asvp	20.05.2005 16:58	19°0’	-34°44’	122
SO183_02_20050523.asvp	23.05.2005 16:06	33°36’	-34°30’	1982
SO183_03_20050528.asvp	28.05.2005 22:36	33°14’	-35°17’	3365
SO183_04_20050604.asvp	04.06.2005 19:12	35°35’	-30°53’	2233
SO183_05_20050608.asvp	08.06.2005 14:09	38°00’	-26°01’	1865
SO183_06_20050616.asvp	16.06.2005 21:36	39°30’	-22°09’	2794

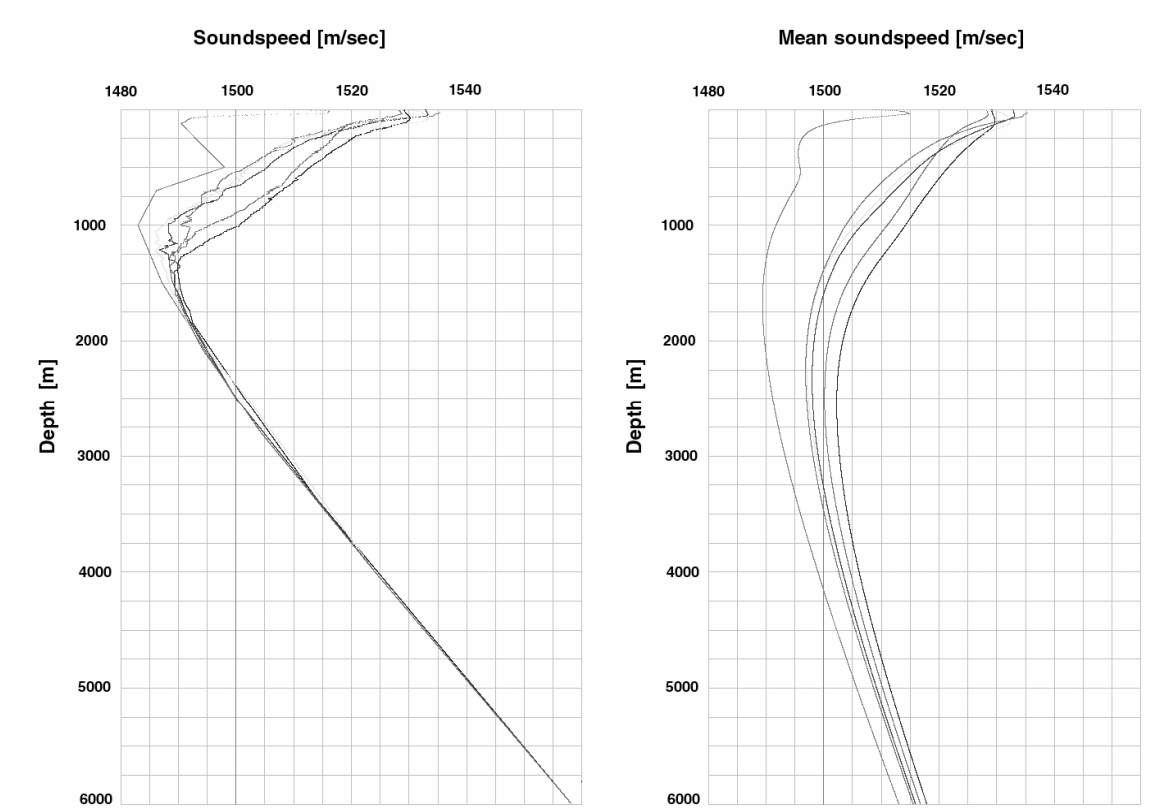

Figure 17: Sound velocity as a function of water depth.

3.5 Bathymetric products and interpretation of topography

Figures 18 to 21 give examples of different seafloor features, as detected by the sonar system. Each figure illustrates a single profile demonstrating the excellent resolution of the echo sounder Simrad EM120.
Figure 18 gives an example of the seafloor sprinkled with little volcanoes, with an exaggeration of 200 to 600 meters. The swathwidth amounts to 6 km. Figure 19 shows a volcano of 1400 m height at a base of 3000 meter. You can clearly see the typical features of an undersea volcano. Figure 20 gives an example of rough seafloor topography. Figure 21 shows the well defined seafloor channel with a width of 7 km and a depth of 400 meters.

Figure 18: Mud volcanoes

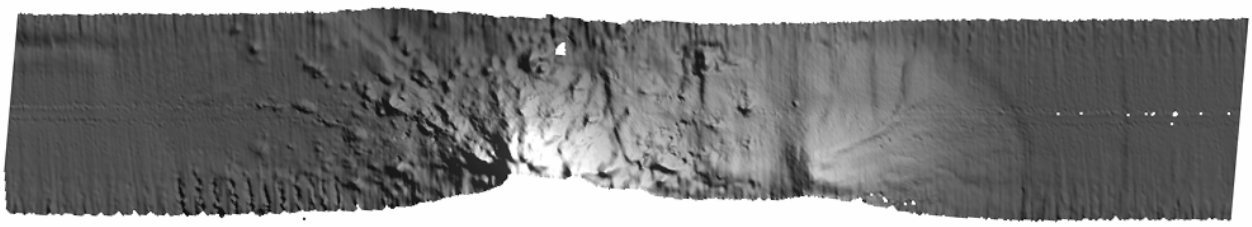

Figure 19: Sea mount

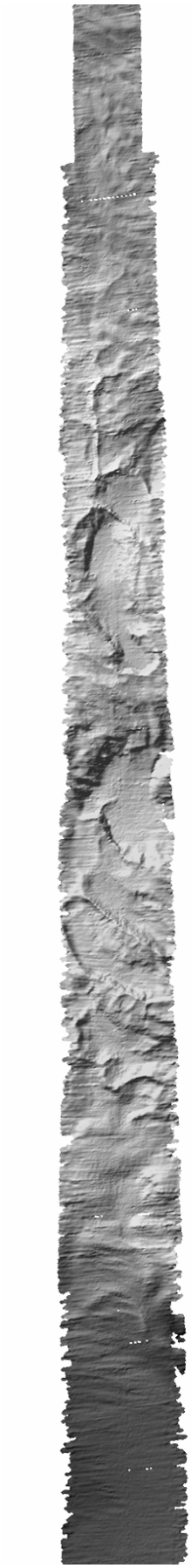

Figure 20: Rough seafloor

Figure 21: Seafloor channel

4. Parasound

M. Watkeys, C. Kopsch, M. Brayshaw, K. Kitada, M. Tauchnitz, R. Krocker, A. Labrenz, R. Niebling, Z. Thackeray)

The Parasound sub-bottom profiler is a seismic system, which may detect the internal structures of sedimentary cover along the ships track.

To penetrate the sedimentary layers at the sea floor with acoustic signals, a low frequency signal is required.
The Parasound sub-bottom profiler combines a reasonably small transmitter with a very narrow beam by generating the low frequency in the water column.

This method of operation is based on the so-called “parametric effect”, which results from the non-linearity of the motion-equation of acoustic waves in a fluid medium.
The transmitter produces signals of two different frequencies. Due to the parametric effect in the water column another signal will be generated, whose main frequency is the difference between the two original frequencies.

For the current cruise, one frequency is always 18 kHz. The second can be adjusted between 20.5 kHz and 23.5 kHz, in most cases it is set to 22 kHz. The resulting parametric signal used for sub-bottom profiling will then be 4 kHz.

The main advantage of parametric signals is that they are emitted within a very narrow beam. Using the before mentioned frequencies, an opening angle of 4° is created. According to this angle, the detected area on the seafloor will have a diameter of approximately 7% of the total water depth which allows a high lateral resolution.

The data are digitized and stored in the ParaDigMa-System.

Appendix

Appendix 1 Data files from magnetic profiling with the ship towed system

date	julday	time	name	space	Notes
050523	143	15.26 - 22.24	050523-mag	3,259	
	143/144	22.24 - 05.44	050523-mag-1	3,425	Date
050524	144	07.25 - 09.05	050524-mag	1,257	
	144	09.05 - 16.06	050524-mag-1	3,912	
	144	16.40 - 22.28	050524-mag-2	1,584	
050525	145	00.08 - 06.16	050525-mag	1,541	
	145	06.28 - 23.59	050525-mag-1	4,498	
050526	146	00.00 - 03.01	050526-mag	0.776	DP1:(-34.496991;33.802962)
	146	16.18 - 23.59	050526-mag-1	1,993	system-crash
050527	147	00.00 - 21.31	050527-mag	5,658	
	147	21.31 - 23.59	050527-mag-1	0.619	
050528	148	00.00 - 16.53	050528-mag	4,332	DP2: (-35.19180;33.50446)
050529	149	07.53 - 18.18	050529-mag	2,657	
050530	150	10.04 - 21.56	050530-mag	2,924	
050531	151	04.42 - 23.59	050531-mag	4,788	
050601	152	00.00 - 23.59	050601-mag	5,967	
050602	153	00.00 - 03.03	050602-mag	0.762	DP3: (-33°41'16";34°36'14")
	153	14.00 - 23.59	050602-mag-1	2,482	
050603	154	00.00 - 21.35	050603-mag	5,403	
	154	21.35 - 23.59	050603-mag-1	0.601	
050604	155	00.00 - 14.38	050604-mag	3,653	DP0: (-30°53'04"; 35°33'26")
	155	22.17 - 00.05	050604-mag-1	452	
050605	156	00.05 - 23.59	050605-mag	5,990	
050606	157	00.00 - 23.59	050606-mag	6,073	
050607	158	00.00 - 23.59	050607-mag	6,086	
050608	159	13.12 - 23.59	050608-mag	2,580	
050609	160	00.00 - 19.22	050609-mag	4,645	
	160	19.22 - 23.59	050609-mag-1	1,100	
050610	161	00.00 - 13.35	050610-mag	3,099	
	161	13.36 - 13.46	050610-mag-1	0.009	
	161	13.46 - 23.59	050610-mag-2	2,369	
050611	162	00.00 - 23.59	050611-mag	5,752	
050612	163	00.00 - 23.59	050612-mag	5,768	
050613	164	00.00 - 19.53	050613-mag	9,616	merged data currupted (00.00 - 20.08 (050614))
050613	164	19.53 - 23.59	050613-mag-1	0.967	
050614	165	00.00 - 20.08	050613-mag		merged data currupted (see above)
050614	165	20.08 - 23.59	050613-mag-2	0.923	
050615	166	00.00 - 23.59	050615-mag	5,780	
050616	167	00.00 - 06.31	050616-mag	1,576	DK (05.00 UTC) und DP4:(-21°56'48"; 39°28'71")
	167	19.49 - 23.59	050616-mag-1	1,015	
050617	168	00.00 - 23.59	050617-mag	5,851	
050618	169	00.00 - 23.59	050618-mag	5,841	
050619	170	00.00 - 23.59	050619-mag	5,895	
050620	171	00.00 - 23.59	050620-mag	5,808	
050621	172	00.00 - 23.59	050621-mag	5,674	
050622	173	00.00 - 23.59	050622-mag	5,715	
050623	174	00.00 - 23.59	050623-mag	5,715	
050624	175	00.00 - 01.00	050624-mag	5,943	date, 25/06/05: 00-01Uhr
050625	176	01.00 - 23.59	050625-mag	5,485	

050626	177	00.00 - 23.59	050626-mag	5,732	
050627	178	00.00 - 23.59	050627-mag	5,668	
050628	179	00.00 - 01.18	050628-mag	6,000	date, 29/06/05:00-01.18
050629	180	01.18 - 23.59	050629-mag	5,347	date, 29/06/05; 01.18-23.59
050630	181	00.00 - 23.59	050630-mag	5,625	DK
050701	182	00.00 - 23.59	050701-mag	5,640	
050702	183	00.00 - 23.59	050702-mag	5,636	
050703	184	00.00 - 23.59	050703-mag	5,620	
050704	185	00.00 - 17.29	050704-mag	3,998	

Appendix 2 An example of the fluxgate magnetometer data

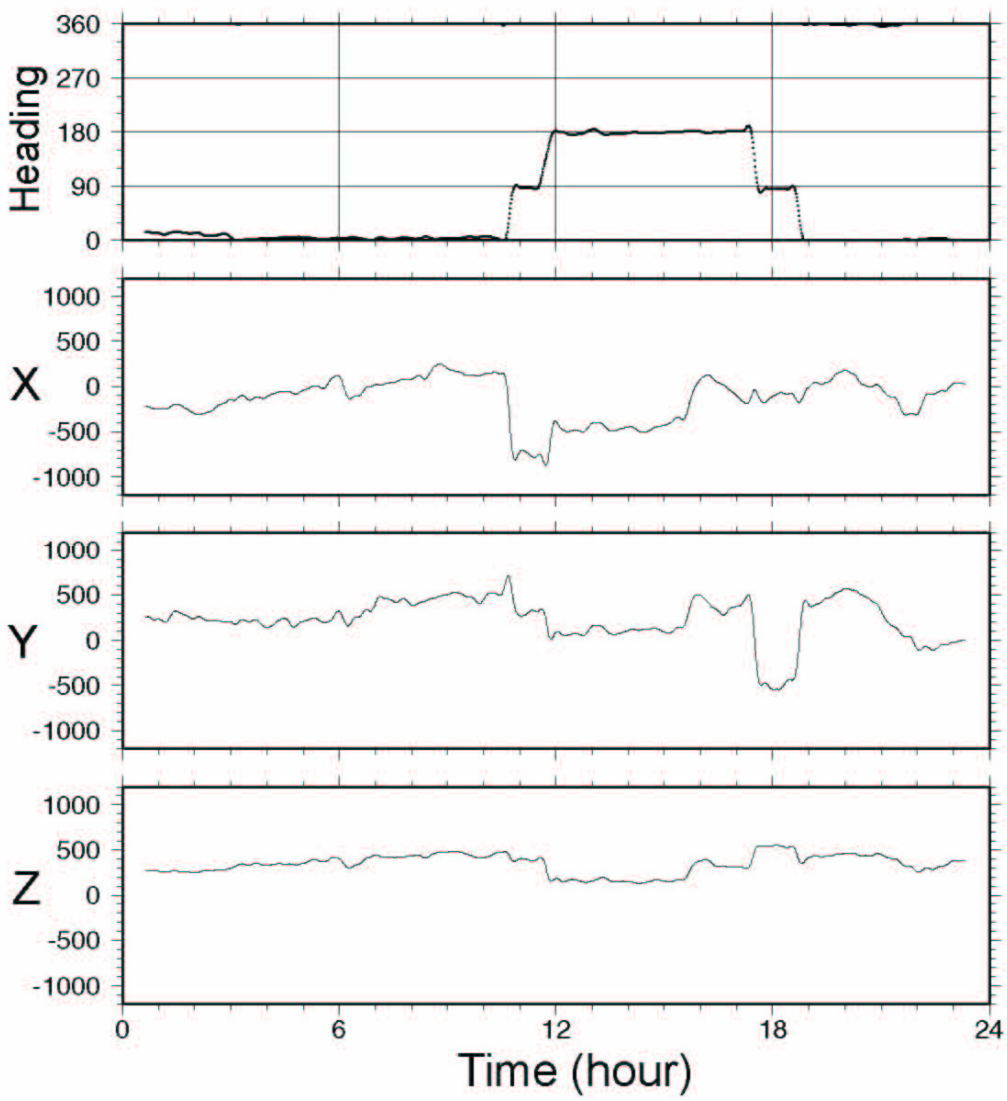

X, Y and Z are the North, East, and vertical component anomalies referred to IGRF-2000, respectively.

Appendix 3 File list of fluxgate magnetometer data

File name	File size	Start time (UTC)	End time (UTC)	Comments
DTFG-050519-174138.dat	14,387 KB	2005/05/19/ 17:41:38	2005/05/19/ 23:59:57	
DTFG-050520-000000.dat	54,639 KB	2005/05/19/ 23:59:57	2005/05/20/ 23:59:57	
DTFG-050521-000000.dat	30,247 KB	2005/05/20/ 23:59:57	2005/05/21/ 13:18:45	
DTFG-050521-131854.dat	24,340 KB	2005/05/21/ 13:18:54	2005/05/21/ 23:59:57	
DTFG-050522-000000.dat	28,285 KB	2005/05/21/ 23:59:58	2005/05/22/ 12:27:48	
DTFG-050522-133355.dat	189 KB	2005/05/22/ 13:34:54	2005/05/22/ 13:38:55	
DTFG-050522-135333.dat	23,007 KB	2005/05/22/ 13:54:21	2005/05/22/ 23:59:58	
DTFG-050523-000000.dat	23,015 KB	2005/05/22/ 23:59:58	2005/05/23/ 10:08:02	
DTFG-050523-101224.dat	10 KB	2005/05/23/ 10:10:23	2005/05/23/ 10:12:38	
DTFG-050523-101318.dat	1,321 KB	2005/05/23/ 10:13:18	2005/05/23/ 10:48:18	
DTFG-050523-104824.dat	3,882 KB	2005/05/23/ 10:48:24	2005/05/23/ 12:30:36	
DTFG-050523-123829.dat	25,876 KB	2005/05/23/ 12:38:37	2005/05/23/ 23:59:58	
DTFG-050524-000000.dat	30,702 KB	2005/05/23/ 23:59:58	2005/05/24/ 13:31:52	
DTFG-050524-133515.dat	103 KB	2005/05/24/ 13:35:15	2005/05/24/ 13:37:57	GPS TEST
DTFG-050524-133803.dat	86 KB	2005/05/24/ 13:38:04	2005/05/24/ 13:40:02	GPS TEST
DTFG-050524-134021.dat	322 KB	NO RECORD	NO RECORD	
DTFG-050524-134853.dat	731 KB	2005/05/24/ 13:48:52	2005/05/24/ 14:08:19	(NO RECORD BECAUSE OF GYRO RESTART)
DTFG-050524-141846.dat	0 KB	NO RECORD	NO RECORD	GPS TEST
DTFG-050524-141935.dat	323 KB	2005/05/24/ 14:22:07	2005/05/24/ 14:30:35	GPS TEST
DTFG-050524-143619.dat	35 KB	NO RECORD	NO RECORD	GPS TEST
DTFG-050524-145629.dat	0 KB	NO RECORD	NO RECORD	GPS TEST
DTFG-050524-151046.dat	58 KB	NO RECORD	NO RECORD	GPS TEST
DTFG-050524-151432.dat	19,963 KB	2005/05/24/ 15:14:04	2005/05/24/ 23:59:53	
DTFG-050525-000001.dat	54,583 KB	2005/05/24/ 23:59:54	2005/05/25/ 23:59:58	
DTFG-050526-000000.dat	23,427 KB	2005/05/25/ 23:59:58	2005/05/26/ 10:20:19	
DTFG-050526-130235.dat	0 KB	NO RECORD	NO RECORD	SYSTEM CHECK
DTFG-050526-130506.dat	24,861 KB	2005/05/26/ 13:05:17	2005/05/26/ 23:59:58	
DTFG-050527-000000.dat	54,554 KB	2005/05/26/ 23:59:58	2005/05/27/ 23:59:56	
DTFG-050528-000002.dat	54,526 KB	2005/05/27/ 23:59:56	2005/05/28/ 23:59:58	
DTFG-050529-000000.dat	54,524 KB	2005/05/28/ 23:59:58	2005/05/29/ 23:59:58	
DTFG-050530-000000.dat	17,815 KB	2005/05/29/ 23:59:58	2005/05/30/ 07:51:33	
DTFG-050530-081155.dat	416 KB	2005/05/30/ 08:12:24	2005/05/30/ 08:22:52	
DTFG-050530-082851.dat	5,261 KB	2005/05/30/ 08:28:51	2005/05/30/ 10:47:06	
DTFG-050530-114609.dat	24,413 KB	2005/05/30/ 11:46:09	2005/05/30/ 22:29:06	GPS PROBLEM IS FIXED at 30/05 11:56
PC RECORDING MISS		2005/05/30/ 22:29:07	2005/05/31/ 07:03:12	This data is in next file.
DTFG-050530-222000L.dat	19,100 KB	2005/05/30/ 22:20:00	2005/05/31/ 07:10:00	This is converted from binary data (logger).
DTFG-050531-000000.dat	0 KB	NO RECORD	NO RECORD	SYSTEM CHECK
DTFG-050531-070313.dat	62 KB	2005/05/31/ 07:03:13	2005/05/31/ 07:04:52	SYSTEM CHECK
DTFG-050531-070511.dat	38 KB	2005/05/31/ 07:05:11	2005/05/31/ 07:06:11	SYSTEM CHECK
DTFG-050531-070626.dat	11 KB	2005/05/31/ 07:06:27	2005/05/31/ 07:06:44	SYSTEM CHECK
DTFG-050531-071035.dat	38 KB	2005/05/31/ 07:10:35	2005/05/31/ 07:11:34	SYSTEM CHECK
DTFG-050531-071244.dat	38,198 KB	2005/05/31/ 07:12:44	2005/05/31/ 23:59:58	
DTFG-050601-000000.dat	54,560 KB	2005/05/31/ 23:59:58	2005/06/01/ 23:59:58	
DTFG-050602-000000.dat	54,527 KB	2005/06/01/ 23:59:58	2005/06/02/ 23:59:58	
DTFG-050603-000000.dat	54,528 KB	2005/06/02/ 23:59:58	2005/06/03/ 23:59:58	

DTFG-050604-000000.dat	54,530 KB	2005/06/03/ 23:59:58	2005/06/04/ 23:59:57	
DTFG-050605-000000.dat	54,530 KB	2005/06/04/ 23:59:58	2005/06/05/ 23:59:58	
DTFG-050606-000000.dat	54,497 KB	2005/06/05/ 23:59:58	2005/06/06/ 23:59:57	
DTFG-050607-000000.dat	54,449 KB	2005/06/06/ 23:59:58	2005/06/07/ 23:59:56	
DTFG-050608-000000.dat	54,448 KB	2005/06/07/ 23:59:57	2005/06/08/ 23:59:57	
DTFG-050609-000000.dat	54,444 KB	2005/06/08/ 23:59:57	2005/06/09/ 23:59:57	
DTFG-050610-000000.dat	54,449 KB	2005/06/09/ 23:59:57	2005/06/10/ 23:59:57	
DTFG-050611-000000.dat	54,447 KB	2005/06/10/ 23:59:57	2005/06/11/ 23:59:57	
DTFG-050612-000000.dat	54,448 KB	2005/06/11/ 23:59:57	2005/06/12/ 23:59:57	
DTFG-050613-000000.dat	54,447 KB	2005/06/12/ 23:59:57	2005/06/13/ 23:59:57	
DTFG-050614-000000.dat	54,444 KB	2005/06/13/ 23:59:57	2005/06/14/ 23:59:57	
DTFG-050615-000000.dat	54,442 KB	2005/06/14/ 23:59:57	2005/06/15/ 23:59:57	
DTFG-050616-000000.dat	54,471 KB	2005/06/15/ 23:59:57	2005/06/16/ 23:59:57	
DTFG-050617-000000.dat	54,535 KB	2005/06/16/ 23:59:57	2005/06/17/ 23:59:57	
DTFG-050618-000000.dat	48,533 KB	2005/06/17/ 23:59:57	2005/06/18/ 21:21:38	
PC RECORDING MISS		2005/06/18/ 21:21:38	2005/06/19/ 07:15:21	This data is in next file.
DTFG-050618-212100L.dat	21,983 KB	2005/06/18/ 21:10:00	2005/06/19/ 07:20:00	This is converted from binary data (logger).
DTFG-050619-000000.dat	0 KB	NO RECORD	NO RECORD	
DTFG-050619-070912.dat	0 KB	NO RECORD	NO RECORD	
DTFG-050619-071502.dat	38,079 KB	2005/06/19/ 07:15:21	2005/06/19/ 23:59:57	
DTFG-050620-000000.dat	54,524 KB	2005/06/19/ 23:59:57	2005/06/20/ 23:59:57	
DTFG-050621-000000.dat	54,444 KB	2005/06/20/ 23:59:57	2005/06/21/ 23:59:57	
DTFG-050622-000000.dat	54,533 KB	2005/06/21/ 23:59:57	2005/06/22/ 23:59:57	
DTFG-050623-000000.dat	54,485 KB	2005/06/22/ 23:59:57	2005/06/23/ 23:59:53	
DTFG-050624-000000.dat	54,454 KB	2005/06/23/ 23:59:53	2005/06/24/ 23:59:56	
DTFG-050625-000000.dat	54,459 KB	2005/06/24/ 23:59:57	2005/06/25/ 23:59:56	
DTFG-050626-000000.dat	54,452 KB	2005/06/25/ 23:59:56	2005/06/26/ 23:59:56	
DTFG-050627-000001.dat	54,457 KB	2005/06/26/ 23:59:57	2005/06/27/ 23:59:56	
DTFG-050628-000000.dat	54,449 KB	2005/06/27/ 23:59:56	2005/06/28/ 23:59:56	
DTFG-050629-000000.dat	54,458 KB	2005/06/28/ 23:59:57	2005/06/29/ 23:59:56	
DTFG-050630-000000.dat	54,491 KB	2005/06/29/ 23:59:56	2005/06/30/ 23:59:56	
DTFG-050701-000000.dat	54,634 KB	2005/06/30/ 23:59:56	2005/07/01/ 23:59:55	
DTFG-050702-000000.dat	54,525 KB	2005/07/01/ 23:59:55	2005/07/02/ 23:59:56	
DTFG-050703-000000.dat	38,913 KB	2005/07/02/ 23:59:56	2005/07/03/ 23:59:56	
DTFG-050704-000000.dat				

*GPS had not worked well before 30/05 11:56, but GPS problem was FIXED at 30/05 11:56

Appendix 4 Date and time of persons at the „Peildeck”

Date	Time	Remarks
31.05.2005	14:35 - 14:44	1 Mann im Mast
01.06.2005	16:32 - 16:35	1PD
02.06.2005	06:39 - 06:56	1PD
03.06.2005	06:19 - 06:29	1PD
05.06.2005	12:05 - 12:10	1PD
05.06.2005	13:10 - 13:12	1PD
05.06.2005	13:21 - 13:26	1PD
06.06.2005	12:05 - 12:10	1PD
07.06.2005	09:20 - 09:22	1PD
08.06.2005	15:28 - 15:30	1PD
08.06.2005	15:36 - 15:39	1PD
08.06.2005	15:42 - 15:48	1PD
09.06.2005	16:45 - 16:46	1PD
11.06.2005	15:30 - 15:31	1PD
13.06.2005	12:08 - 12:12	1PD
16.06.2005	06:44 - 07:06	1PD/ oder am 18.06.??
18.06.2005	08:18 - 09:14	4PD
18.06.2005	16:07 - 16:09	1PD
19.06.2005	08:27	1PD
24.06.2005	08:04 - 08:10	2PD
25.06.2005	15:28 - 15:29	1PD
25.06.2005	15:41 - 15:46	1PD
26.06.2005	06:50 - 06:55	1PD
30.06.2005	09:48 - 09:52	1PD
01.07.2005	13:40 - 13:45	1PD
02.07.2005	12:03 - 12:10	1PD
02.07.2005	15:20 - 15:25	1PD

Appendix 5 Gravity Units

The unit of gravitational measurement is Gal named after Gallileo and is $1\,cm/s^2$.
This unit is too large for geophysical prospecting so one uses either Milligals $[mGal]$ or Microgals $[\mu Gal]$. Occasionally one may come across the gravity unit $[gu]$.

The relationships are:
$1\,Gal = 1\,cm/s^2$ the earth field is approximately $981\,Gal$,
$1\,mGal = 0.001\ Gal$ or $10\,Gal$,
$1\,\mu Gal = 0.000001\,Gal$ or $10\ Gal = 0.001\,mGal$ or $10\,mGal$,
$1\ gu = 0.0001\,Gal$ or $10\,Gal$

The unit most used in marine gravity surveys is $mGal$:
$1\,mGal\,1 = 10\ gu = 1000\,\mu Gal = 0.001\ Gal$

The earth's gravity field varies from $978\,Gal$ at the equator (0° latitutde) to $983\,Gal$ at the poles (90° latitude).

Appendix 6 Installation and testing the L&R S56 air/sea gravity meter system

INSTALLATION OF SENSOR IN FRAME

- remove lid of gravity box cage
- before moving the sensor box:
  ensure that the sensor is clamped □
- cable connections
  - 230 VAC power on host computer (laptop) □
  - 230 VAC power on UPS (check if loaded) □
  - host computer – board computer (serial) □
  - host computer – grav. Platform control box (serial) □
  - pulse stretcher – board computer (or GPS PPS) □
    (if GPS PPS is not available use manual switch)
- check if gimbal leveling screws are secured □
- balance sensor in gimbal frame □
- fix 3 screws in bottom of sensor box □
- connect cable to sensor □
- (check shockmount airpressure, airborne) □

POWER ON SENSOR

- switch on UPS □
- press two breakers on ZLS power supply unit □
- check if heater lamps are burning □
- check main power in host computer □
- start host computer program:
  - switch on host computer □
  - choose "no cardworks" □
  - type "ultra" □
    ULTRASYS will start
- symbols for heat up procedure on screen?
- check pressure gauge value [expected values: 27.4 to 28.5] 29,13
- wait for:
  thermostating

spin up of gyros
answer question: to unclamp the beam with: N □
program starts displaying numerical values
- equalize on/off intervalls of meter heater (lowest) lamp (pot) □
- check ST is off (Ultrasys: S, [3,] –9) □
- check alarm off (Ultrasys: S, [4,] –9) □
- check sync of ST on S56 with PC value
  if out of sync set ST to counter value (Ultrasys: P, 4, xx, -9) 9670 ------- 9671
- replace MYLINE by new line name, YYMMDDFFFF (Ultrasys: P, 1, xx, –9) SO183AIS_2
- check serial output
  1 or 10 sec, long format (Ultrasys: C, 2, -8, -9, -9) 10
  HighRes (Ultrasys: P, -9) □

GRAVITY: PRE SENSOR CHECKS

LEVELLING PLATFORM

- check platform levelling □
- adjust if required

BEAM CHECK

- check ST off (Ultrasys: S, [3,] –9) □
- check beam zero
  clamp beam twice
  if abs(raw beam) > 10 adjust zero screw 2
  until abs(raw beam) < 10
- check beam gain
  unclamp beam □
  press CRTL-U on host computer to slew beam up
  if raw beam .ne. 9000 +/- 20 adjust gain screw 9015
  press CRTL-U on host computer to stop slewing
  check beam position
  press CRTL-D on host computer to slew beam to 0 □
  press CRTL-D on host computer to stop slewing □
- check beam zero once more and adjust again if necessary 1
- slew ST abs to base reading xx if available (Ultrasys: P, 8, 1, xx, -9)
  (AD-LAB: 11273.6, Neumayer2002: 12771.0, St. Nord: 13092.1, LYR: 12985.6, OP-LUNE 2002: 11390,4, EBASE 2002 12741.0)

BASE READING

- check platform levelling
  adjust if required
- unclamp beam (wait until TC moves down) □
- check synch of ST 9675
- turn ST on (Ultrasys: S, 3, -9) □
- wait until TC < 1.0, abs(raw beam) < 2, DG ≈ base reading ST
- carry out 5 readings every 30 seconds, (note in log pages) □
- Result:

Time: 10:04:00	DG: 9670,2	ST: 9671,1	RB: 2	TC: 1,7
Time: 10:04:30	DG: 9670,2	ST: 9670,8	RB: 0	TC: -2,7
Time: 10:05:00	DG: 9670,2	ST: 9670,4	RB: -3	TC: -2,0
Time: 10:05:30	DG: 9670,2	ST: 9670,3	RB: 1	TC: 0,5
Time: 10:06:00	DG: 9670,3	ST: 9670,6	RB: -13	TC: 0

K-CHECK

Time: 18:30:30 ST: 9669,9 TC: -0,2
Turn ST off (Utrasys: S, 3, -9) □

Slew ST relative by +30 (Ultrasys: P, 8, 2, 30, -9) □
Wait until TC is stable (~ 15 min)
Time: 18:42:00 ST: 9670,7 TC: -28,8
Slew ST relative by -60 (Ultrasys: P, 8, 2,-60, -9) □
Wait until TC is stable (~ 15 min)
Time: 18:55:00 ST: 9669,0 TC: 30.2
Slew ST relative by +30 (Ultrasys: P, 8, 2, 30, -9) □
Wait until TC is stable (~ 15 min)
Time: 19:06:00 ST: 9669,9 TC: 0,5
If TC values are within 5% of the slewed values, then k-factor ok

- Check ST off (Ultrasys: S, [3,] –9) □
- Clamp beam □
- Set alarm on (Ultrasys: S, 4, -9) □

GENERAL CHECKS

- Check for platform tilts
- Check synch of ST

BASE READING (after survey)

- Check air temperature
- Check temperature of ZLS control unit
- Check platform levelling
  Adjust if required
- Unclamp beam (wait until TC moves down) □
- Check synch of ST counter 9377, ST 9376.6
- Turn ST on (Ultrasys: S, 3, -9) □
- Wait until TC < 1.0, abs(raw beam) < 2, DG ≈ base reading ST
- carry out 5 readings every 30 seconds, (note in log pages) □
- Result:

Time: 09:30:00	DG: 9376.6	ST: 9377.0	RB: 0	TC: 1.9	
Time: 09:30:30	DG: 9376.7	ST: 9377.0	RB: -4	TC: -1.3	
Time: 09:31:00	DG: 9376.7	ST: 9376.9	RB: -3	TC: 0.3	
Time: 09:31:30	DG: 9376.8	ST: 9376.9	RB: 4	TC: -0.3	
Time: 09:32:00	DG: 9376.8	ST: 9376.8	RB: 2	TC: 0.1	

- Turn ST off (Ultrasys: S, [3,] –9) □
- Clamp Beam □
- Set torque motors off (Ultrasys: S, 2,-9) □
- Secure Plattform of gravitymeter with PU-Dampers □

GRAVITY AFTER SURVEY PROCEDURES

- Slew ST to parking position □
- Switch off gravity system (Ultrasys: P, 9, y) □
  Switch off host computer
  Press two breakers on ZLS power supply unit
  Switch off UPS
- Switch off 220V-Inverters □
- Install auxiliary heating system on gravity meter or ship it □

Appendix 7 Data storage and file notation information

There are hourly data files, named with year, julday and hour of recording [YYYY_hh.julday].
For example:

2005_15.183
2005_16.183
2005_17.183

Appendix 8 Summary of dredge locations and samples

	Date	Dredge	Time (UTC)	Latitude	Longitude	Depth
DL1	26/05/2005	On bottom	07:26	34° 48' 52 S	33° 17' 27 E	2699 m
		Off bottom	08:20	34° 48' 15 S	33° 17' 62 E	2461 m
		On bottom	10:02	34° 48' 58 S	33 ° 17' 21 E	2725 m
		Off bottom	12:00	34° 48' 04 S	33 ° 17' 78 E	2440 m
Sample	**Size**	**Description**				
01	20 x 26 x 12cm	20 cm diameter fragment part of a amygdaloidal basaltic flow top breccia, overlain by 6cm burrowed shale				
02	25 x 22 x 13cm	Flow top breccia consisting of weathered angular fragments of basalt and amygdaloidal basalt (up to 10 x 5 cm angular fragment, forming 6 cm thick uppermost part of a flow top breccia); overlain by 5cm thick burrowed shale				
03	33 x 22x 9cm	Weathered angular basaltic fragments forming uppermost 6 cm of a flow top breccia; overlain by 5cm shale				
04	15 x 16 x 6cm	Burrowed shale with a lower bedded zone truncated by upper zone				
05	15 x 8 x 4cm	Shale: soft-sediment folded, bivalve trace fossil imprint				
06	14 x 10 x 6cm	Shale: hummocky bedded or soft-sediment deformation				
07	17 x 11 x 6cm	Burrowed shale comprising 3 units				
08	18.5 x 9 x 5cm	Shale-siltstone comprising 6 laminated layers displaying soft-sediment folds				
09	17 x 9.5 x 6cm	Shale-siltstone comprising 4 laminated layers displaying soft-sediment folds				
10	17 x13 x 4cm	Shale comprising 2 laminated layers; gentle folds and burrow				
11	16 x12 x 5cm	Shale-siltstone comprising 3 fairly distinct laminated layers; burrow				
12	20 x 14 x 6cm	Shale-siltstone comprising 5 fairly distinct laminated layers; soft-sediment folds; 2 bivalve imprints				
13	20 x 10 x 6cm	Shale comprising 2 laminated zones; upper zone truncates lower zone; soft-sediment folds; bivalve imprint and burrow				
14	13 x 9 x 5cm	Shale comprising 2 laminated zones; upper zone truncates lower zone				
15	25 x 15 x 10cm	5.5 cm thick basalt flow breccia (burrowed), overlain by silty shale				
16	13 x 8 x 5cm	Shale with siltstone interlayers				
17	20 x 15 x 5cm	Laminated siltstone overlying laminated shale				
18	14 x 14 x 7cm	Shale comprising 3 laminated zones				
19	18.5 x 14 x 8cm	Shale-siltstone interlayers comprising 3 laminated zones				
20	29 x 20 x 6cm	Shale comprising 4 laminated zones; soft sediment folds				
21	30 x 17 x 8cm	Shale-siltstone interlayers comprising 10 laminated zones; soft sediment folds				
22	12 x 6 x 4cm	Shale comprising 5 laminated zones				
23	9 x 5 x 4cm	Shale; soft sediment deformation; 2 bivalve imprints				

Station	Date	Dredge	Time (UTC)	Latitude	Longitude	Depth
DL2	28/05/2005	On bottom	22:27	35° 18' 53 S	33° 14' 45 E	4077 m
		Off bottom	23:28	35° 17' 53 S	33° 14'16 E	3526 m

	29/05/2005	On bottom	01:39	35° 18' 37 S	33° 14' 23 E	3932 m
		Off bottom	03:37	35° 17' 06 S	33° 13' 62 E	3508 m
Sample	**Size**	**Description**				
24	10 x 9 x 3cm	Feldspathic arkose				
25	10 x 7.5 x 3.5cm	Leached and altered sedimentary protolith covered by 1.5cm Mn oxide crust				
26	11 x 10 x 9cm	Angular block of altered dolerite encrusted by 1-3cm Mn oxide precipitate				
27	11.5 x 11 x 6cm	Altered dolerite covered by manganese oxide precipitate.				
28	11 x 9.5 x 1.5cm	Thin (1-5mm) altered and leached igneous protolith(?) covered by Mn oxide				
29	28 x 10 x 7cm	Dolerite slab surrounded by manganese oxide precipitate				
30	30 x 20 x 16cm	Spherulitic dolerite covered by manganese oxide precipitate				

Station	**Date**	**Dredge**	**Time (UTC)**	**Latitude**	**Longitude**	**Depth**
DL3	02/06/2005	On bottom	08:05	33° 41 16 S	34° 36 14 E	1898 m
		Off bottom	09:13	33° 40 52 S	34° 36 51 E	1804 m
Sample	**Size**	**Description**				
31	31 x 22 x 8cm	Mn oxide shale and precipitate				
32	33 x 24 x 10cm	Mn oxide encrusted (outer 1cm) laminated shale with 7 distinct layers; burrow and shell trace fossil				
33	29 x 26 x 8cm	Interlayered shale-siltstone with Mn oxide crust				
34	35 x 24 x 9cm	Highly weathered clay-rich beige core surrounded by 4 Mn oxide shale layers; burrows				
35	28 x 22 x 16cm	Mn oxide				
36	27 x 19 x 12cm	Mn oxide precipitate; porous Fe-stained core				
37	24 x 19 x 12cm	Mn oxide precipitate surrounding core possibly of sandstone				
38	40 x 28 x 13cm	Mn silt; bioturbated and burrowed				
39	25 x 21 x 17cm	Mn encrusted laminated silty shale, 5 distinct layers				
40	17 x 15 x 14cm	Mn oxide precipitate with porous Fe-stained chalk-like core				
41	20 x 18 x 11cm	Mn encrusted laminated silty shale, 6 distinct layers				
42	18 x 13 x 15cm	Mn oxide precipitate with porous Fe-stained chalk-like core; 2 bone-like fragments in core				
43	18 x 10 x 8cm	Mn oxide precipitate with silt interlayers				
44	15 x 10 x 10cm	Mn oxide precipitate nodule with $CaCO_3$ core				
45	12 x 11 x 10cm	Mn oxide precipitate with silty interlayers and imprint of bivalve (5cm x 3.5cm)				
46	14 x 11 x 6cm	Mn oxide encrusted shale				
47	13 x 11 x 5cm	1.5cm Mn oxide encrusted shale				
48	18 x 14 x 11cm	Mn oxide surrounding porous Fe-stained partly chalk core				
49	11 x 7 x 4.5cm	1.2cm Mn oxide crust covering Mn shale (burrowed)				
50	14 x 8 x 5cm	Mn shale consisting of 5 folded layers				
51	10.5 x 9.5 x 4.5cm	Mn oxide encrusted shale				
52	12 x 8.5 x 10cm	Nodular Mn oxide precipitate exhibiting concentric growth with Fe-stained layers and chalk cores				
53	11 x 8.5 x 7cm	Mn oxide precipitate surrounding chalk core containing rounded quartz granule				
54	9.5 x 7 x 5cm	1cm Mn oxide crust surrounding highly porous Fe-stained core with burrows				
55	9 x 7 x 5cm	Mn oxide crust surrounding highly porous Fe-stained and Fe-nodule chalk core with bone fragment				
56	10 x 7 x 4cm	Mn oxide shale				

57	11.5 x 8 x 4cm	Mn oxide layers above less Mn rich shale; 5 layers in total
58	9 x 7 x 5cm	Mn oxide crust surrounding pitted core
59	8 x 5.5 x 6cm	Mn oxide crust (3cm) surrounding 3cm contorted silty shale
60	10 x 8 x 7cm	Mn encrusted shale
61	7 x 5 x 9cm	Mn encrusted shale
62	7 x 5 x 7cm	Mn encrusted shale
63	16 x 10 x 7.5cm	Mn encrusted contorted shale

Station	**Date**	**Dredge**	**Time (UTC)**	**Latitude**	**Longitude**	**Depth**
DL4	16/06/05	On bottom	11:22	21° 56' 48 S	39° 28' 71 E	1111 m
		Off bottom	13:03	21° 56' 46 S	39° 28' 57 E	984 m
		On bottom	14:05	21° 56 47 S	39° 28 67 E	1097 m
		Off bottom	15:52	21° 56 23 S	39° 28 32 E	756 m
Sample	**Size**	**Description**				
64	29 x 18 x 6.5cm	Pyroxene-phenocryst basalt with brecciated top				
65	25 x 15 x 9cm	Basalt with felsic layers and immiscibility droplets				
66	12 x 11 x 10cm	Pyroxene-phenocryst basalt				
67	15 x 14 x 9cm	Altered basaltic or felsic dyke cutting brecciated pyroxene basalt				
68	19 x 16 x 6.5cm	Olivine basalt with lapilli tuff				
69	18 x 12 x 10cm	Pyroxene-phenocryst basalt				
70	23 x 12 x 7cm	Pyroxene-phenocryst basalt				
71	14 x 9 x 7cm	Altered and veined basalt				
72	12 x 11 x 5.5cm	Olivine basalt				
73	15 x 11.5 x 5cm	Pyroxene-phenocryst basalt				
74	11 x 8 x 5.5cm	Pyroxene-phenocryst basalt				
75	11 x 6 x 6cm	Altered basalt				
76	17 x 12 x 4cm	Altered and brecciated basalt				
77	13 x 7.5 x 2cm	Mn oxide shale				
78	72 x 36 x 18cm	Altered basalt				
79	24 x 28 x 15cm	Pyroxene-phenocryst basalt				

Station	**Date**	**Dredge**	**Time (UTC)**	**Latitude**	**Longitude**	**Depth**
DL5	05/07/05	On bottom	10:53	30° 33' 43 S	36° 52' 26 E	2945 m
		Off bottom	11:46	30° 32' 67 S	36° 51' 84 E	2621 m
		On bottom	13:19	30° 33' 63 S	36° 52' 31 E	2925 m
		Off bottom	15:01	30° 32' 91 S	36° 51' 90 E	2660 m
Sample	**Size**	**Description**				
80	16 x15 x 6cm	Mn oxide shale with burrows				
81	19 x 17.5 x 12cm	Mn oxide shale				
82	11 x 8 x 5.5cm	Mn oxde shale				
83	9 x 7 x 5cm	Mn oxide shale with angular pebbles of actinolite schist				
84	21 x 16 x 10.5cm	Mn oxide shale with subangular and angular grit and pebble-sized clasts of tremolite schist and quartz				
85	54 x 22 x 16cm	Mn oxide shale with quartz breccia containing angular clasts of diorite gneiss				

Appendix 9 List of Parasound profiles during SO183 cruise

YYMMDD	##	Profil	Description	UTC	Lon(Deg)	Lat(Deg)
050520	0	CTD	CTD	16:35:00	19.0465972	-34.7596011
050521						
050522						
050523	1	DK1-S	Startpunkt Drehkreis	14:32:00	33.6203255	-34.4988142
	2	DK2-E	Endpunkt Drehkreis	15:26:00	33.6203699	-34.5017034
	3	CTD	CTD	15:26:30	33.6196562	-34.5020415
	4	Pr.1	Profil - 1 - Richtung: Sued	15:33:00	33.6058319	-34.4964134
050524						
050525	5	Pr.2	Profil - 2 - Richtung: -Ost	00:10:00	30.0028729	-37.9996789
	6	Pr.3	Profil - 3 - Richtung: Nord	01:04:20	30.1955116	-37.9989891
050526	7	Pr.4	Profil - 4 - zu Dredge Punkt 1	03:15:55	33.8153138	-34.4825140
	8	DP-1	Dredge Punkt 1	06:26:35	33.2821594	-34.8107421
	9	Pr.5	Profil - 5 - Richtung: Sued	16:09:00	34.0067742	-34.4912088
050527	10	Pr.6	Profil - 6 - Richtung: Ost	19:00:00	30.3985321	-38.0010962
	11	Pr.7	Profil - 7 - Richtung: Nord	20:03:00	30.6031407	-38.0010996
050528	12	Pr.8	Profil - 8 - zu Dredge Punkt	16:52:00	33.5023306	-35.1929868
	13	CTD	CTD	18:56:45	33.2369299	-35.3043804
	14	DP-2	Dredge Punkt 2	22:44:55	33.2389312	-35.3049917
050529	15	DK2-S	Startpunkt Drehkreis	06:44:00	33.4711030	-35.2209155
	16	DK2-E	Endpunkt Drehkreis	07:50:00	33.4835339	-35.2097105
	17	Pr.9	Profil - 9 - Richtung: Nord	08:03:00	33.5043762	-35.1905860
	18	Pr.10	Profil -10 - Abwettern	17:47:00	34.2679504	-34.4353515
050530	19	Pr.11	Profil - 11 - Richtung: West	09:54:00	34.2692618	-34.4333639
	20	Pr.12	Profil - 12 - Abwettern -> Richtung: KRZ-Profil1	22:14:00	33.6002516	-34.4986537
050531	21	Pr.13	Profil - 13 - Richtung: Nord	04:48:00	33.5983118	-34.5006618
	22	Pr.14	Profil - 14 - Richtung:Ost	15:54:10	35.0987985	-33.0012679
	23	Pr.15	Profil - 15 - Richtung:Sued	16:51:10	35.2988377	-33.0018690
050601	24	Pr.16	Profil - 16 - Richtung: Ost	03:33:20	33.7839700	-34.5064265
	25	Pr.17	Profil - 17 - Richtung: Nord	04:33:25	34.0075733	-34.5059893
	26	Pr.18	Profil - 18 - Richtung: Ost	15:41:00	35.5001609	-32.9999736
	27	Pr.19	Profil - 19 - Richtung: Sued	16:38:25	35.6991482	-33.0020910
050602	28	Pr.20	Profil - 20 - Richtung: Nord (KRZ Profil-14)	03:03:00	34.2819250	-34.4211823
	29	DP-3	Dredge Punkt 3	07:04:20	34.5868793	-33.7156886
	30	Pr.21	Profil - 21 - Richtung: Nord	14:06:00	35.0997684	-33.0000180
050603	31	Pr.22	Profil - 22 - Richtung: Ost	06:13:30	35.1005334	-30.0029515
	32	Pr.23	Profil - 23 - Richtung: Sued	07:10:25	35.3000056	-30.0016708
050604	33	Pr.24	Profil - 24 - Richtung: Ost (KRZ.Profil (20/21))	00:30:30	35.2848495	-33.0143785
	34	Pr.25	Profil - 25 - Richtung: Nord (KRZ Profil 24)	01:44:00	35.5147400	-33.0142419
	35	Pr.26	Profil -26 - zu Dredge Punkt 4	14:39:00	35.5050069	-30.8358316
	36	DP-4	Dredge Punkt 4	15:04:30	35.5495227	-30.8581595
	37	DK3-S	Startpunkt Drehkreis	22:30:00	35.5048840	-30.8333727
	38	DK3-E	Endpunkt Drehkreis	23:26:00	35.5047747	-30.8341855
	39	Pr.27	Profil - 27 - Richtung: Nord	23:27:00	35.5047269	-30.8324028
050605	40	Pr.28	Profil - 28 - Richtung: Nord-Ost	04:21:00	35.4999492	-30.0008205

	41	Pr.29	Profil - 29 - Richtung: Nord	16:51:45	36.5003499	-27.9984702
050606	42	Pr.30	Profil - 30 - Richtung: West	04:12:00	36.4998377	-26.0000337
	43	Pr.31	Profil - 31 - Richtung: Sued	05:14:05	36.2995629	-26.0008756
	44	Pr.32	Profil - 32 - Richtung: West	16:50:45	36.2998941	-27.9996109
	45	Pr.33	Profil - 33 - Richtung:Nord	17:51:50	36.0993120	-27.9987178
050607	46	Pr.34	Profil - 34 - Richtung: Ost	10:42:00	36.0994861	-25.0052662
	47	Pr.35	Profil - 35 - Richtung: Sued	11:48:00	36.2995629	-25.0050511
	48	Pr.36	Profil - 36 - Richtung: West (KRZ Profil (29/31))	17:30:00	36.2833958	-26.0171092
	49	Pr.37	Profil - 37 - Richtung: Nord	18:44:00	36.5157930	-26.0140817
050608	50	Pr.38	Profil - 38 - Richtung: Ost (Dredge Punkt Suche (keine Durchführung))	00:41:00	36.5015452	-24.9816679
	51	Pr.39	CTD - Profil - 39 - Richtung: Nord	14:10:40	37.9850794	-25.8144729
050609	52	Pr.40	Profil - 40 - Richtung: Ost	17:15:00	37.5997713	-21.0013837
	53	Pr.41	Profil - 41 - Richtung:Sued	18:48:20	37.9019423	-21.0027258
050610						
050611	54	Pr.42	Profil - 42 - Richtung: Ost	07:45:55	38.4300047	-27.3371150
	55	Pr.43	Profil - 43 - Richtung: Nord	09:20:00	38.7322030	-27.3311727
050612	56	Pr.44	Profil - 44 - Richtung: Ost	18:10:30	38.2493770	-21.6028194
	57	Pr.45	Profil - 45 - Richtung: Sued	19:38:45	38.5482080	-21.6023516
050613						
050614	55	Pr.46	Profil - 46 - Richtung: Ost	02:04:25	38.9997040	-26.9985408
	56	Pr.47	Profil - 47 - Richtung: Nord	04:59:55	39.6002859	-26.9986894
050615	60	Pr.48	Profil - 48 - Richtung: Ost	17:51:50	39.0584402	-20.5009050
	61	Pr.49	Profil - 49 - Richtung: Sued	19:28:10	39.3642107	-20.5022710
050616	62	Pr.50	Profil - 50 - Richtung: Drehkreis und Dredge Punkt	05:08:15	39.5001246	-22.1766765
	63	DP-5	Dredge Punkt 5	12:40:30	39.4690233	-21.9402735
	64	Pr.51	Profil - 51 - Richtung: (Fortsetzung des Suedprofils)	20:00:40	39.5001861	-22.1768507
050617	65	Pr.52	Profil - 52 - Richtung:Ost	23:51:35	39.8992877	-26.9957063
050618	66	Pr.53	Profil - 53 - Richtung: Nord	01:24:40	40.1993003	-26.9970279
050619	67	Pr.54	Profil - 54 - Richtung: Ost (Atoll)	08:19:15	39.7469847	-21.5605525
	68	Pr.55	Profil - 55 - Richtung: Nord (Atoll)	08:54:45	39.8530200	-21.5566678
	69	Pr.56	Profil - 56 - Richtung: West (Atoll)	10:10:00	39.8320616	-21.3362713
	70	Pr.57	Profil - 57 - Richtung: Nord (Wiederaufnahme Nordprofil)	10:45:15	39.7265146	-21.3283995
	71	Pr.58	Profil - 58 - Richtung: Ost	12:36:50	39.7000477	-21.0034550
	72	Pr.59	Profil - 59 - Richtung: Sued	14:16:55	39.9997529	-21.0026524
050620						
050621	73	Pr.60	Profil - 60 - Richtung: Ost	02:51:50	40.5433199	-27.4990058
	74	Pr.61	Profil - 61 - Richtung: Nord	04:22:05	40.8451938	-27.4986729
050622	75	Pr.62	Profil - 62 - Richtung: Ost (Atoll L'Europe)	08:56:20	40.4182728	-22.4382216
	76	Pr.63	Profil - 63 - Richtung: Nord (Atoll L'Europe)	09:16:45	40.4716780	-22.4310635
	77	Pr.64	Profil - 64 - Richtung: West (Atoll L'Europe)	10:03:55	40.4522325	-22.2659898
	78	Pr.65	Profil - 65 - Richtung: Nord (Wiederaufnahme Nordprofil)	10:19:00	40.4010095	-22.2588471
	79	Pr.66	Profil - 66 - Richtung: Ost	17:17:40	40.2999910	-21.0005197
	80	Pr.67	Profil - 67 - Richtung: Sued	18:51:05	40.5989654	-21.0020292

050623						
050624	81	Pr.68	Profil - 68 - Richtung: Ost	07:43:15	41.0993690	-26.9961707
	82	Pr.69	Profil - 69 - Richtung: Nord	09:18:35	41.4005462	-26.9950352
050625	83	Pr.70	Profil - 70 - Richtung: Ost	20:35:35	40.9001631	-21.0023826
	84	Pr.71	Profil - 71 - Richtung: Sued	22:18:00	41.1992366	-21.0034823
050626						
050627	85	Pr.72	Profil - 72 - Richtung: Ost	09:58:15	41.6993158	-26.9968794
	86	Pr.73	Profil - 73 - Richtung: Nord	11:34:20	41.9995538	-26.9972858
050628	87	Pr.74	Profil - 74 - Richtung: Ost	22:59:35	41.5001338	-21.0034293
050629	88	Pr.75	Profil - 75 - Richtung: Sued	00:42:55	41.8001089	-21.0035898
050630		DK	Startpunkt Drehkreis	15:42:45	42.3003417	-27.0021779
		Pr.76	Endpunkt Drehkreis Profil - 76 - Richtung: West	16:46:20	42.3195755	-26.9984623
050701		Pr.77	Profil - 77 - Richtung: Nord	09:16:20	39.3013251	-27.0075259
050702		Pr.78	Profil - 78 - Richtung: West	16:38:10	38.8568642	-21.7048795
050703		Pr.79	Profil - 79 - Richtung: Sued	01:01:55	37.3511934	-21.7095121
050704			Ende des Messprofils	17:29:00	37.8000666	-28.0013014
			Profil - 80 - zu Dredge Punkt Richtung Sued	17:29:00	37.8000666	-28.0013014
050705		DP-6	Dredge Punkt 6	10:00:00	36.8746682	-30.5590416
050706						
050707						

Appendix 10 Parasound correction table

***.PS3-Files**			**Software SENT**				
Directory: YYMMDD	**Start**	**End**	**Error description**	**Error in PS3-File: MMDDhhmm.PS3**	**Time of error within PS3-Files: hh:mm:ss**	**Additional information**	**State of processing**
050521	07:56	17:59					
			0 Kbyte, can not read file	05210841.PS3			
			0 Kbyte, can not read file	05211759.PS3			
			Konstante Lon u. Lat: 09:33 - 13:48	05210928.PS3			korrigiert
			Konstante Lon u. Lat: 09:33 - 13:48	05210934.PS3			korrigiert
			Konstante Lon u. Lat: 09:33 - 13:48	05210941.PS3			korrigiert
			Konstante Lon u. Lat: 09:33 - 13:48	05210947.PS3			korrigiert
			Konstante Lon u. Lat: 09:33 - 13:48	05210953.PS3			korrigiert
			Konstante Lon u. Lat: 09:33 - 13:48	05211000.PS3			korrigiert
			Konstante Lon u. Lat: 09:33 - 13:48	05211006.PS3			korrigiert
			Konstante Lon u. Lat: 09:33 - 13:48	05211013.PS3			korrigiert
			Konstante Lon u. Lat: 09:33 - 13:48	05211019.PS3			korrigiert
			Konstante Lon u. Lat: 09:33 - 13:48	05211026.PS3			korrigiert
			Konstante Lon u. Lat: 09:33 - 13:48	05211032.PS3			korrigiert

			Konstante Lon u. Lat: 09:33 - 13:48	05211039.PS3			korrigiert
			Konstante Lon u. Lat: 09:33 - 13:48	05211045.PS3			korrigiert
			Konstante Lon u. Lat: 09:33 - 13:48	05211051.PS3			korrigiert
			Konstante Lon u. Lat: 09:33 - 13:48	05211058.PS3			korrigiert
			Konstante Lon u. Lat: 09:33 - 13:48	05211104.PS3			korrigiert
			Konstante Lon u. Lat: 09:33 - 13:48	05211111.PS3			korrigiert
			Konstante Lon u. Lat: 09:33 - 13:48	05211117.PS3			korrigiert
			Konstante Lon u. Lat: 09:33 - 13:48	05211124.PS3			korrigiert
			Konstante Lon u. Lat: 09:33 - 13:48	05211130.PS3			korrigiert
			Konstante Lon u. Lat: 09:33 - 13:48	05211137.PS3			korrigiert
			Konstante Lon u. Lat: 09:33 - 13:48	05211143.PS3			korrigiert
			Konstante Lon u. Lat: 09:33 - 13:48	05211149.PS3			korrigiert
			Konstante Lon u. Lat: 09:33 - 13:48	05211156.PS3			korrigiert
			Konstante Lon u. Lat: 09:33 - 13:48	05211202.PS3			korrigiert
			Konstante Lon u. Lat: 09:33 - 13:48	05211209.PS3			korrigiert
			Konstante Lon u. Lat: 09:33 - 13:48	05211215.PS3			korrigiert
			Konstante Lon u. Lat: 09:33 - 13:48	05211222.PS3			korrigiert
			Konstante Lon u. Lat: 09:33 - 13:48	05211228.PS3			korrigiert
			Konstante Lon u. Lat: 09:33 - 13:48	05211235.PS3			korrigiert
			Konstante Lon u. Lat: 09:33 - 13:48	05211241.PS3			korrigiert
			Konstante Lon u. Lat: 09:33 - 13:48	05211251.PS3			korrigiert
			Konstante Lon u. Lat: 09:33 - 13:48	05211301.PS3			korrigiert
			Konstante Lon u. Lat: 09:33 - 13:48	05211311.PS3			korrigiert
			Konstante Lon u. Lat: 09:33 - 13:48	05211321.PS3			korrigiert
050522			Keine Messungen!				
050523	16:19	23:59					
050524	00:00	23:59					
			Konstante Lon und Lat: 71 s	05241220.PS3	12:23:44		korrigiert
050525	00:00	23:59					
			UTC Fehler	05250000.PS3	23:59:59	falscher Zeitwert am Anfang der Datei	korrigiert
050526	00:00	23:59					
050527	00:00	23:59					
			Lon- u. Lat-Werte = 0	05271103.PS3	11:05:12		korrigiert
			Lon- u. Lat-Werte = 0	05271337.PS3	13:40:04		korrigiert
050528	00:00	19:12					
			Lon- u. Lat-Werte = 0	05280110.PS3	13:17:17		korrigiert
			Lon- u. Lat-Werte = 0	05281321.PS3	13:29:37		korrigiert
050529	04:47	18:52					
			Lon- u. Lat-Werte = 0	05291427.PS3	14:35:40		korrigiert
050530	06:41	23:59					
			Lon- u. Lat-Werte = 0	05301632.PS3	16:36:32		korrigiert
			Lon- u. Lat-Werte = 0	05301833.PS3	18:34:16		korrigiert
			Lon- u. Lat-Werte = 0	05301933.PS3	19:36:27		korrigiert
			Lon- u. Lat-Werte = 0	05301933.PS3	19:36:41		korrigiert
			Lon- u. Lat-Werte = 0	05302013.PS3	20:17:55		korrigiert
			Lon- u. Lat-Werte = 0	05302033.PS3	20:38:38		korrigiert
			Lon- u. Lat-Werte = 0	05302053.PS3	20:59:22		korrigiert
			Lon- u. Lat-Werte = 0	05302113.PS3	21:20:06		korrigiert
			Lon- u. Lat-Werte = 0	05302233.PS3	22:42:46		korrigiert

			Lon- u. Lat-Werte = 0	05302253.PS3	23:03:30		korrigiert
050531	00:00	23:59					
			Lon- u. Lat-Werte = 0	05310050.PS3	00:52:09		korrigiert
			Lon- u. Lat-Werte = 0	05311842.PS3	18:42:39		korrigiert
			Lon- u. Lat-Werte = 0	05311922.PS3	19:24:48		korrigiert
050601	00:00	23:59					
050602	00:00	23:59					
			Lon- u. Lat-Werte = 0	06022220.PS3	22:27:22		korrigiert
050603	00:00	23:59					
050604	00:00	15:50					
	22:45	23:59					
			Lon- u. Lat-Werte = 0	06042245.PS3	22:47:32		korrigiert
050605	00:00	23:59					
			Lon- u. Lat-Werte = 0	06050220.PS3	02:25:02		korrigiert
			Lon- u. Lat-Werte = 0	06050240.PS3	02:45:43		korrigiert
			Lon- u. Lat-Werte = 0	06050510.PS3	05:15:52		korrigiert
			Lon- u. Lat-Werte = 0	06050530.PS3	05:36:36		korrigiert
			Lon- u. Lat-Werte = 0	06050611.PS3	06:12:48		korrigiert
			Lon- u. Lat-Werte = 0	06050741.PS3	07:45:59		korrigiert
			Lon- u. Lat-Werte = 0	06050801.PS3	08:06:42		korrigiert
			Lon- u. Lat-Werte = 0	06050901.PS3	09:08:53		korrigiert
			Lon- u. Lat-Werte = 0	06050921.PS3	09:24:23		korrigiert
			Lon- u. Lat-Werte = 0	06051448.PS3	14:58:03		korrigiert
050606	00:00	23:59					
050607	00:00	23:59					
			Lon- u. Lat-Werte = 0	06071336.PS3	13:43:18		korrigiert
050608	00:00	23:59					
			Lon- u. Lat-Werte = 0	06081635.PS3	16:37:50		korrigiert
			Lon- u. Lat-Werte = 0	06081702.PS3	17:03:49		korrigiert
			Lon- u. Lat-Werte = 0	06081847.PS3	18:47:27		korrigiert
			Lon- u. Lat-Werte = 0	06081907.PS3	19:08:11		korrigiert
			Lon- u. Lat-Werte = 0	06082057.PS3	21:07:17		korrigiert
			Lon- u. Lat-Werte = 0	06082137.PS3	21:43:31		korrigiert
050609	00:00	23:59					
			Lon- u. Lat-Werte = 0	06091752.PS3	17:53:53		korrigiert
			Lon- u. Lat-Werte = 0	06091852.PS3	19:01:18		korrigiert
050610	00:00	23:59					
			Lon- u. Lat-Werte = 0	06100446.PS3	04:48:20		korrigiert
			Lon- u. Lat-Werte = 0	06100707.PS3	07:08:10		korrigiert
			Lon- u. Lat-Werte = 0	06101057.PS3	11:01:23		korrigiert
			Lon- u. Lat-Werte = 0	06101107.PS3	11:16:53		korrigiert
			Lon- u. Lat-Werte = 0	06101417.PS3	14:23:25		korrigiert
			Lon- u. Lat-Werte = 0	06101448.PS3	14:49:23		korrigiert
			Lon- u. Lat-Werte = 0	06101548.PS3	15:57:03		korrigiert
			Lon- u. Lat-Werte = 0	06101708.PS3	17:14:17		korrigiert
			Lon- u. Lat-Werte = 0	06101948.PS3	19:54:53		korrigiert
			Lon- u. Lat-Werte = 0	06102104.PS3	21:07:17		korrigiert
			Lon- u. Lat-Werte = 0	06102157.PS3	21:59:00		korrigiert
			Lon- u. Lat-Werte = 0	06102233.PS3	22:40:27		korrigiert
			Lon- u. Lat-Werte = 0	06102259.PS3	23:01:11		korrigiert
050611	00:00	23:59					

			UTC-Fehler	06110000.PS3	23:59:59	falscher Zeitwert am Anfang der Datei	korrigiert
			Lon- u. Lat-Werte = 0	06110017.PS3	00:23:54		korrigiert
			Lon- u. Lat-Werte = 0	06110232.PS3	02:38:18		korrigiert
			Lon- u. Lat-Werte = 0	06110320.PS3	03:24:57		korrigiert
050612	00:00	23:59					
			Lon- u. Lat-Werte = 0	06121722.PS3	17:32:15		korrigiert
050613	00:00	23:59					
			Lon- u. Lat-Werte = 0	06131001.PS3	10:07:38		korrigiert
			Lon- u. Lat-Werte = 0	06131021.PS3	10:28:23		korrigiert
			Lon- u. Lat-Werte = 0	06131101.PS3	11:04:36		korrigiert
			Lon- u. Lat-Werte = 0	06131101.PS3	11:05:29		korrigiert
			Lon- u. Lat-Werte = 0	06131101.PS3	11:06:09		korrigiert
050614	00:00	23:59					
			UTC-Fehler	06140000.PS3	23:59:59	falscher Zeitwert am Anfang der Datei	korrigiert
050615	00:00	23:59					
			Lon- u. Lat-Werte = 0	06151612.PS3	16:14:04		korrigiert
			Lon- u. Lat-Werte = 0	06151622.PS3	16:30:02		korrigiert
			Lon- u. Lat-Werte = 0	06151632.PS3	16:40:02		korrigiert
			Lon- u. Lat-Werte = 0	06151652.PS3	16:55:34		korrigiert
			Lon- u. Lat-Werte = 0	06151702.PS3	17:11:16		korrigiert
			Lon- u. Lat-Werte = 0	06151712.PS3	17:21:30		korrigiert
050616	00:00	23:59					
			Lon- u. Lat-Werte = 0	06162045.PS3	20:49:30		korrigiert
			Lon- u. Lat-Werte = 0	06162055.PS3	21:02:02		korrigiert
			Lon- u. Lat-Werte = 0	06162225.PS3	22:35:13		korrigiert
050617	00:00	23:59					
			Lon- u. Lat-Werte = 0	06170110.PS3	01:10:33		korrigiert
			Lon- u. Lat-Werte = 0	06170230.PS3	02:38:28		korrigiert
			Lon- u. Lat-Werte = 0	06170310.PS3	03:19:56		korrigiert
			Lon- u. Lat-Werte = 0	06170500.PS3	05:03:22		korrigiert
050618	00:00	23:59					
			UTC Fehler	06180000.PS3	23:59:59	falscher Zeitwert am Anfang der Datei	korrigiert
050619	00:00	23:59					
050620	00:00	23:59					
			GPS Sprung: Longitude	06200651.PS3	06:58:50		
			UTC-Fehler	06202357.PS3	00:00:00	falscher Zeitwert am Ende der Datei	korrigiert
050621	00:00	23:59					
			Lon- u. Lat-Werte = 0	06211429.PS3	14:31:15		korrigiert
050622	00:00	23:59					
			keine Messwerte von 6:11 - 6:38				
050623	00:00	23:59					
050624	00:00	23:59					

050625	00:00	23:59					
			Lon- u. Lat-Werte = 0	06250948.PS3	09:51:45		korrigiert
050626	00:00	23:59					
			GPS Sprung	06260000.PS3	00:00:00		korrigiert
050627	00:00	23:59					
			keine Messwerte von 10:00 -10:32				
050628	00:00	23:59					
050629	00:00	23:59					
050630	00:00	23:59					
050701	00:00	23:59					
050702	00:00	23:59					
				07021201.PS3	12 11 13		korrigiert
			keine Messwerte von 16:43 - 17:12				
				07022053.PS3	20 54 02		korrigiert
050703	00:00	23:59					
050704	00:00	23:59					
			Profilende: 17:41:52				
050705							
050706							
050707							

Abkürzungen / Abbreviation

z.W	zu Wasser
a.D.	an Deck
SL (max.)	(maximale)Seillänge
LT	Lottiefe nach Hydrosweep
W x	eingesetzte Winde
SM	Simrad - Multibeam - Lot
PS	Parasound
rwk:	Rechtweisender Kurs
d:	Distanz
v:	Geschwindigkeit in Knoten
SL:	Seillänge
KL:	Kabellänge

Eingesetzte Geräte

KD	Kettensackdredge
CTD	CTD / C-Sonde
KAL	Kalibrierungsdrehkreise
Magn	Magnetometerprofil
VekMg	Vektor-Magnetometer
Gvm	Gravimeter
Vermess.	EM 120 - Vermessungsprofile

Geräteverluste: **Keine**

Einsätze

11		
6		
6	Zeit: 6,1 Std. Länge: 44 nm	
12	Profilzeit: 913 Std. Profillänge 9214 nm	
20.05.-04.07.2005	Zeit:1090 Std. Länge:10570 nm	
20.05.-07.07.2005	Zeit:1154,5 Std. Länge 11088 nm	
20.05.-07.07.2005	Zeit: 1146 Std. Länge 11038 nm	

Winde	D/M	Typ	RF-Nr	SO 183 Einsatz	Gesamt Einsatz	SO 183 S`länge	Gesamt S`länge	Zust.	SO 183 gefierte max. L	jemals gefierte max. Länge
W 1	18,2	LWL	812001	0 h	472 h	0 m	240495	3-4	0 m	8022 m
W 2	18.2	LWL	120301500	0 h	0 h	0 m	0 m	1	0 m	0 m
W 4	11	NSW	818045	10 h	285 h	14600 m	246373 m	3	3900 m	8081 m
W 5	11	NSW	818237	0 h	3 h	0 m	4000 m	2	0 m	4000 m
W 6	18.2	Koax	815286	27,3 h	33,5 h	33391 m	38891 m	2	4744 m	4744 m

Station	Datum	UTC	PositionLat	PositionLon	Tiefe [m]	Windstärke [m/s]	Kurs [°]	v [kn]	Gerät	Gerätekürzel	Aktion	Bemerkung
Transit	20.05.05	07:30	33° 53,10´ S	18° 26,10´ E		S 2	350	11.8	Gravimeter / Vektor-Magn	Gvm/VekMg	Beginn Messungen	Laufen ab jetzt stets mit
Transit	20.05.05	10:00	34° 14,50´ S	18° 14,20´ E		S 2	176	12.5	SIMRAD	SM	Beginn Messungen	Läuft ab jetzt stets mit
SO183/001-1	20.05.05	14:39	34° 44,23' S	19° 0,00' E	156	ESE 1	58	0.2	CTD	CTD	Beginn Station	Kalibrierung SIMRAD
SO183/001-1	20.05.05	14:40	34° 44,23' S	19° 0,01' E	155	SSE 2	217	0.2	CTD	CTD	zu Wasser	W 4, 2x CTD bei 20 m
SO183/001-1	20.05.05	14:49	34° 44,21' S	19° 0,01' E	155	SSW 1	83	0.5	CTD	CTD	auf Tiefe	Lmax= 150 m
SO183/001-1	20.05.05	15:00	34° 44,17' S	18° 59,98' E	155	S 1	344	0.4	CTD	CTD	an Deck	
SO183/001-2	20.05.05	15:15	34° 44,69' S	19° 0,91' E	150	SSW 4	73	7.4	Kalibrierung	KAL	Beginn Drehkreis	Kalibrierung Vektor-Magnetometer
SO183/001-2	20.05.05	16:21	34° 44,26' S	19° 0,00' E	154	ENE 5	181	8.1	Kalibrierung	KAL	Ende Drehkreis	d= 10 sm
SO183/001-2	20.05.05	16:21	34° 44,26' S	19° 0,00' E	154	ENE 5	181	8.1	Kalibrierung	KAL	Ende Station	
Transit	21.05.05	06:30	35° 04,00´ S	11° 14,40´ E	115	N 3	79	11.7	Parasound	PS	Beginn Messungen	Läuft ab jetzt stets mit
SO183/002-1	22.05.05	07:56	34° 46,86' S	27° 48,98' E	4137	NNW 14	16	5.9	Magnetometer	MAGN	Beginn Station	rwK: 035 ; v: 4kn; Test Magn
SO183/002-1	22.05.05	08:04	34° 46,45' S	27° 49,29' E	4133	NNE 13	26	3.2	Magnetometer	MAGN	Magnetometer zu Wasse	L=200m; d= 1sm
SO183/002-1	22.05.05	08:05	34° 46,39' S	27° 49,34' E	4131	NNE 14	26	3.9	Magnetometer	MAGN	Beginn Profil	
SO183/002-1	22.05.05	08:06	34° 46,33' S	27° 49,39' E	4130	NNE 13	35	3.8	Magnetometer	MAGN	Kursänderung	rwK: 087 ; v= 6kn
SO183/002-1	22.05.05	09:04	34° 46,18' S	27° 55,77' E	4169	N 13	90	5.1	Magnetometer	MAGN	Ende Profil	d: 5 sm
SO183/002-1	22.05.05	09:10	34° 46,22' S	27° 56,22' E	4171	N 13	99	5.8	Magnetometer	MAGN	Magnetometer an Deck	
SO183/002-1	22.05.05	09:12	34° 46,23' S	27° 56,37' E	4171	N 13	80	4.3	Magnetometer	MAGN	Ende Station	Anf.AG
SO183/003-1	22.05.05	11:58	34° 45,13' S	28° 29,74' E	4246	N 14	78	4.9	Magnetometer	MAGN	Beginn Station	Teststat.
SO183/003-1	22.05.05	11:59	34° 45,12' S	28° 29,82' E	4245	NNE 13	96	5.1	Magnetometer	MAGN	Magnetometer zu Wasse	FdW 4 kn, stecken 200 m aus

Station	Datum	UTC	PositionLat	PositionLon	Tiefe [m]	Windstärke [m/s]	Kurs [°]	v [kn]	Gerät	Gerätekürzel	Aktion	Bemerkung
SO183/003-1	22.05.05	12:05	34° 45,08' S	28° 30,22' E	4263	N 13	64	5.6	Magnetometer	MAGN	Beginn Profil	rwK 087°, L 200 m, FüG ca. 10 kn
SO183/003-1	22.05.05	12:52	34° 44,58' S	28° 39,11' E	4281	NNE 15	84	10.2	Magnetometer	MAGN	Ende Profil	reduzieren auf 4 kn, Beginn Einholen Mag.
SO183/003-1	22.05.05	13:00	34° 44,55' S	28° 39,89' E	4273.9	NNE 12	86	2.8	Magnetometer	MAGN	Magnetometer an Deck	d: 8 sm
SO183/003-1	22.05.05	13:00	34° 44,55' S	28° 39,89' E	4273.9	NNE 12	86	2.8	Magnetometer	MAGN	Ende Station	Fortsetzung Anf. AG, VV
SO183/004-1	23.05.05	12:37	34° 30,04' S	33° 36,01' E	2303	W 11	284	1.8	CTD	CTD	Beginn Station	
SO183/004-1	23.05.05	12:42	34° 30,04' S	33° 36,01' E	2303.6	NNW 10	93	0.8	CTD	CTD	zu Wasser	W4
SO183/004-1	23.05.05	13:23	34° 30,04' S	33° 36,18' E	2306.7	NW 8	152	1.1	CTD	CTD	auf Tiefe	SLmax 2000m
SO183/004-1	23.05.05	14:07	34° 30,18' S	33° 36,43' E	2316.5	NNW 8	56	1.1	CTD	CTD	an Deck	
SO183/004-2	23.05.05	14:13	34° 30,09' S	33° 36,39' E	2320	NW 9	328	3.5	Magnetometer	MAGN	Magnetometer zu Wasse	d: 1 sm
SO183/004-3	23.05.05	14:32	34° 29,93' S	33° 37,22' E	2333.1	N 4	173	8.3	Kalibrierung	KAL	Beginn Drehkreis	v: 7,5 kn
SO183/004-3	23.05.05	15:24	34° 29,88' S	33° 37,24' E	2333.6	NW 9	198	7.3	Kalibrierung	KAL	Ende Drehkreis	d: 7 sm
SO183/004-2	23.05.05	15:35	34° 29,99' S	33° 36,07' E	2320.3	NNW 9	228	10	Magnetometer	MAGN	Beginn Profil	Nr. 01, rwk: 220°, d: 273 sm
SO183/004-2	25.05.05	00:10	37° 59,98' S	30° 0,17' E	4091.5	W 14	172	5.8	Magnetometer	MAGN	Kursänderung	rwk: 090°, d: 9 sm
SO183/004-2	25.05.05	01:05	37° 59,88' S	30° 11,86' E	4150.8	WSW 5	53	11.3	Magnetometer	MAGN	Kursänderung	rwk: 040°, d: 273 sm
SO183/004-2	26.05.05	03:00	34° 30,04' S	33° 47,95' E	2128.9	NNW 7	44	10.7	Magnetometer	MAGN	Ende Profil	hieven MAGN
SO183/004-2	26.05.05	03:11	34° 29,24' S	33° 48,70' E	2188	NNW 6	28	3.8	Magnetometer	MAGN	Magnetometer an Deck	
SO183/004-2	26.05.05	03:11	34° 29,24' S	33° 48,70' E	2188	NNW 6	28	3.8	Magnetometer	MAGN	Ende Station	
SO183/005-1	26.05.05	06:47	34° 48,55' S	33° 17,28' E	2756	NE 7	244	1.5	Kettensackdredge	KD	Stationsbeginn	
SO183/005-1	26.05.05	06:49	34° 48,54' S	33° 17,26' E	2711	NNE 4	182	0.6	Kettensackdredge	KD	z.W.	W 6
SO183/005-1	26.05.05	07:26	34° 48,52' S	33° 17,27' E	2699	NNE 9	71	1.4	Kettensackdredge	KD	Boko	SL: 2742m
SO183/005-1	26.05.05	08:02	34° 48,26' S	33° 17,57' E	2478	NNE 6	132	1.9	Kettensackdredge	KD	Beginn dredgen	SLmax: 3120m; d: 1 sm
SO183/005-1	26.05.05	08:20	34° 48,15' S	33° 17,62' E	2461	NNE 7	3	5	Kettensackdredge	KD	frei vom Grund	SL: 2570 m
SO183/005-1	26.05.05	08:53	34° 48,18' S	33° 17,74' E	2470	N 8	168	0.8	Kettensackdredge	KD	a.D.	
SO183/005-2	26.05.05	09:33	34° 48,52' S	33° 17,25' E	2704	ENE 8	214	2.9	Kettensackdredge	KD	z.W.	W 6
SO183/005-2	26.05.05	10:02	34° 48,58' S	33° 17,21' E	2725	NNE 9	322	0.2	Kettensackdredge	KD	Boko	SL: 2751 m
SO183/005-2	26.05.05	11:02	34° 48,10' S	33° 17,74' E	2442	NE 8	145	0.4	Kettensackdredge	KD	Beginn dredgen	SLmax: 4744 m
SO183/005-2	26.05.05	12:00	34° 48,04' S	33° 17,78' E	2439	NE 7	330	2.6	Kettensackdredge	KD	frei vom Grund	SL: 2683 m
SO183/005-2	26.05.05	12:41	34° 48,18' S	33° 17,74' E	2468	NE 9	158	0.8	Kettensackdredge	KD	a.D.	ohne Probe
SO183/005-2	26.05.05	12:41	34° 48,18' S	33° 17,74' E	2468	NE 9	158	0.8	Kettensackdredge	KD	Stationsende	KÄ 063°, d 39 sm, Anf. Profil
SO183/006-1	26.05.05	16:09	34° 29,47' S	34° 0,41' E	2350	ESE 11	181	4.6	Magnetometer	MAGN	Beginn Station	setzen MAGN aus
SO183/006-1	26.05.05	16:13	34° 29,72' S	34° 0,24' E	2345	NNE 5	210	3.6	Magnetometer	MAGN	Magnetometer zu Wasse	SL: 200 m
SO183/006-1	26.05.05	16:16	34° 29,93' S	34° 0,09' E	2343	NNE 4	204	6.7	Magnetometer	MAGN	Beginn Profil	# 02, rwk: 220°, d: 273 sm
SO183/006-1	27.05.05	18:58	37° 59,83' S	30° 24,14' E	4189	SSE 17	218	8.9	Magnetometer	MAGN	Kursänderung	rwk: 090°, d: 10 sm
SO183/006-1	27.05.05	20:01	38° 0,09' S	30° 35,81' E	4167	SSE 22	73	9.4	Magnetometer	MAGN	Kursänderung	rwk: 040°, d: 102 sm
SO183/006-1	28.05.05	16:52	35° 11,58' S	33° 30,14' E	3184	SE 14	44	11.3	Magnetometer	MAGN	Ende Profil	hieven MAGN
SO183/006-1	28.05.05	17:06	35° 11,68' S	33° 31,08' E	3267	SE 12	117	2.2	Magnetometer	MAGN	Magnetometer an Deck	
SO183/006-1	28.05.05	17:06	35° 11,68' S	33° 31,08' E	3267	SE 12	117	2.2	Magnetometer	MAGN	Ende Station	

Station	Datum	UTC	PositionLat	PositionLon	Tiefe [m]	Windstärke [m/s]	Kurs [°]	v [kn]	Gerät	Gerätekürzel	Aktion	Bemerkung
SO183/007-1	28.05.05	18:53	35° 18,38´ S	33° 14,30' E	3958	E 11	274	1.5	CTD	CTD	Beginn Station	
SO183/007-1	28.05.05	18:53	35° 18,38' S	33° 14,30' E	3958	E 11	274	1.5	CTD	CTD	zu Wasser	W 4
SO183/007-1	28.05.05	20:02	35° 17,06' S	33° 13,55' E	3497	ESE 14	4	2.2	CTD	CTD	auf Tiefe	sl = 3500m
SO183/007-1	28.05.05	21:10	35° 16,23' S	33° 13,29' E	3330	ESE 12	297	1.9	CTD	CTD	an Deck	
SO183/007-2	28.05.05	21:42	35° 18,38' S	33° 14,31' E	3997	ESE 13	134	1.2	Kettensackdredge	KD	z.W.	W 6
SO183/007-2	28.05.05	22:27	35° 18,53' S	33° 14,45' E	4077	E 13	70	1.1	Kettensackdredge	KD	Boko	SL: 4009 m
SO183/007-2	28.05.05	22:35	35° 18,53' S	33° 14,47' E	4090	E 13	5	1.8	Kettensackdredge	KD	Beginn dredgen	SL: 4009 m
SO183/007-2	28.05.05	23:28	35° 17,53' S	33° 14,16' E	3526	ESE 14	319	0.2	Kettensackdredge	KD	frei vom Grund	SL: 3520 m
SO183/007-2	29.05.05	00:20	35° 17,49' S	33° 14,12' E	3516	ESE 13	247	0.6	Kettensackdredge	KD	a.D.	ohne Probe
SO183/007-3	29.05.05	00:39	35° 18,43' S	33° 14,29' E	3972	E 15	15	1.3	Kettensackdredge	KD	z.W.	W 6
SO183/007-3	29.05.05	01:39	35° 18,37' S	33° 14,23' E	3932	ESE 13	234	1.5	Kettensackdredge	KD	Boko	SL: 4188 m
SO183/007-3	29.05.05	01:50	35° 18,22' S	33° 14,18' E	3897	E 14	2	0.2	Kettensackdredge	KD	Beginn dredgen	SL: 4494 m
SO183/007-3	29.05.05	03:09	35° 17,20' S	33° 13,74' E	3499	E 14	343	2.1	Kettensackdredge	KD	hieven	
SO183/007-3	29.05.05	03:37	35° 17,06' S	33° 13,62' E	3509	E 16	23	1.6	Kettensackdredge	KD	frei vom Grund	Sl: 3500 m
SO183/007-3	29.05.05	04:25	35° 16,87' S	33° 13,35' E	3509	E 14	290	1.3	Kettensackdredge	KD	a.D.	1/4 voll
SO183/007-3	29.05.05	04:43	35° 16,65' S	33° 13,36' E	3448	ENE 16	38	1.1	Kettensackdredge	KD	Stationsende	
SO183/008-1	29.05.05	06:06	35° 14,02' S	33° 23,78' E	3199	ENE 18	358	4.1	Magnetometer	MAGN	Beginn Station	
SO183/008-1	29.05.05	06:08	35° 13,99' S	33° 23,82' E	3201	E 18	119	0.8	Magnetometer	MAGN	Magnetometer zu Wasse	L: 200m
SO183/008-2	29.05.05	06:47	35° 13,19' S	33° 28,61' E	3350	ENE 19	60	7.6	Kalibrierung	KAL	Beginn Drehkreis	
SO183/008-2	29.05.05	07:49	35° 12,67' S	33° 28,96' E	3316	E 19	18	5.5	Kalibrierung	KAL	Ende Drehkreis	
SO183/008-1	29.05.05	07:56	35° 12,13' S	33° 29,59' E	3326	E 21	48	6.5	Magnetometer	MAGN	Beginn Profil	rwk: 40°, d: 60 sm
SO183/008-1	29.05.05	18:18	34° 24,46' S	34° 17,83' E	5530	NE 22	342	2.1	Magnetometer	MAGN	Ende Profil	Abruch wegen Schlechtwetter
SO183/008-1	29.05.05	18:32	34° 24,07' S	34° 18,39' E	2872	NE 21	20	5	Magnetometer	MAGN	Magnetometer an Deck	
SO183/008-1	29.05.05	18:35	34° 23,99' S	34° 18,51' E	2591	NE 22	39	5.4	Magnetometer	MAGN	Ende Station	
SO183/009-1	30.05.05	09:43	34° 26,48' S	34° 16,40' E	2671	NW 18	285	3.5	Magnetometer	MAGN	Beginn Station	ff. Profil # 02
SO183/009-1	30.05.05	09:44	34° 26,48' S	34° 16,33' E	2670	NW 17	266	2.9	Magnetometer	MAGN	Magnetometer zu Wasser	
SO183/009-1	30.05.05	09:45	34° 26,47' S	34° 16,26' E	2677	NW 18	260	3.6	Magnetometer	MAGN	Beginn Profil	rwk: 262°, d: 32 sm
SO183/009-1	30.05.05	18:00	34° 26,98' S	33° 52,74' E	2385	WSW 14	238	4.3	Magnetometer	MAGN	Kursänderung	
SO183/009-1	30.05.05	22:00	34° 29,75' S	33° 37,13' E	2344	WSW 13	246	4.2	Magnetometer	MAGN	Ende Profil	
SO183/009-1	30.05.05	22:07	34° 29,84' S	33° 36,56' E	2328	WSW 12	260	4.7	Magnetometer	MAGN	Magnetometer an Deck	
SO183/009-1	30.05.05	22:12	34° 29,90' S	33° 36,16' E	2356	WSW 12	271	4.8	Magnetometer	MAGN	Ende Station	Stby., wettern ab
SO183/010-1	31.05.05	04:33	34° 30,70' S	33° 34,24' E	2372	WSW 6	109	3.9	Magnetometer	MAGN	Beginn Station	setzen MAGN aus
SO183/010-1	31.05.05	04:38	34° 30,79' S	33° 34,60' E	2360	W 4	74	3.9	Magnetometer	MAGN	Magnetometer zu Wasser	
SO183/010-1	31.05.05	04:45	34° 30,42' S	33° 35,49' E	2339	WSW 3	47	11.3	Magnetometer	MAGN	Beginn Profil	# 03, rwk: 40°, d: 118 sm
SO183/010-1	31.05.05	15:54	33° 0,10' S	35° 5,91' E	1566	NNE 10	42	11.4	Magnetometer	MAGN	Kursänderung	rwk: 90°, d: 10 sm
SO183/010-1	31.05.05	16:50	32° 59,99' S	35° 17,83' E	1340	NNW 6	90	10.6	Magnetometer	MAGN	Kursänderung	rwk: 220°, d: 118 sm
SO183/010-1	01.06.05	03:33	34° 30,34' S	33° 47,07' E	2160	N 6	219	10.9	Magnetometer	MAGN	Kursänderung	rwk: 90°, d: 11 sm

Station	Datum	UTC	PositionLat	PositionLon	Tiefe [m]	Windstärke [m/s]	Kurs [°]	v [kn]	Gerät	Gerätekürzel	Aktion	Bemerkung
SO183/010-1	01.06.05	04:33	34° 30,39' S	34° 0,38' E	2335	NNW 11	69	11.2	Magnetometer	MAGN	Kursänderung	rwk: 40°, d: 117 sm
SO183/010-1	01.06.05	15:41	33° 0,00' S	35° 30,01' E	1389	NW 9	77	10	Magnetometer	MAGN	Kursänderung	rwk: 90°, d: 10 sm
SO183/010-1	01.06.05	16:37	32° 59,99' S	35° 41,85' E	1546	NW 6	90	10.5	Magnetometer	MAGN	Kursänderung	rwk: 220°, d: 111 sm
SO183/010-1	02.06.05	03:02	34° 25,16' S	34° 17,06' E	2664	N 4	216	9.3	Magnetometer	MAGN	Ende Profil	hieven MAGN
SO183/010-1	02.06.05	03:12	34° 24,65' S	34° 17,07' E	2680	NNE 9	32	4.7	Magnetometer	MAGN	Magnetometer an Deck	
SO183/010-1	02.06.05	03:12	34° 24,65' S	34° 17,07' E	2680	NNE 9	32	4.7	Magnetometer	MAGN	Ende Station	
SO183/011-1	02.06.05	07:39	33° 41,18' S	34° 35,85' E	1900	NNW 7	31	2.1	Kettensackdredge	KD	Beginn Station	
SO183/011-1	02.06.05	07:39	33° 41,18' S	34° 35,85' E	1900	NNW 7	31	2.1	Kettensackdredge	KD	z.W.	W 6
SO183/011-1	02.06.05	08:05	33° 41,16' S	34° 36,14' E	1898	NNE 7	330	0.9	Kettensackdredge	KD	Boko	SL: 1906m
SO183/011-1	02.06.05	09:03	33° 40,49' S	34° 36,42' E	1772	NE 7	48	1.1	Kettensackdredge	KD	hieven	SL: 2104 m
SO183/011-1	02.06.05	09:13	33° 40,52' S	34° 36,51' E	1804	NNE 6	227	0.8	Kettensackdredge	KD	frei vom Grund	SL=1806m
SO183/011-1	02.06.05	09:34	33° 40,58' S	34° 36,65' E	1850	NNE 6	97	0.6	Kettensackdredge	KD	a.D.	
SO183/011-1	02.06.05	09:42	33° 40,57' S	34° 36,69' E	1861	NNE 6	202	1.4	Kettensackdredge	KD	Stationsende	
SO183/012-1	02.06.05	13:52	33° 1,32' S	35° 5,04' E	1560	NNE 6	16	3.6	Magnetometer	MAGN	Beginn Station	setzen MAGN aus
SO183/012-1	02.06.05	13:57	33° 1,08' S	35° 5,21' E	1555	NE 4	38	3.7	Magnetometer	MAGN	Magnetometer zu Wasse	200 m ausgesteckt, FüG ca. 10 kn
SO183/012-1	02.06.05	14:06	33° 0,00' S	35° 5,99' E	1568	NNE 7	23	11.2	Magnetometer	MAGN	Beginn Profil	# 04, rwk: 360°, d: 180 sm
SO183/012-1	03.06.05	06:12	30° 0,43' S	35° 6,02' E	2117	NNE 14	1	10	Magnetometer	MAGN	Kursänderung	rwk: 090°, d: 10 sm
SO183/012-1	03.06.05	07:11	30° 0,20' S	35° 18,01' E	2182	ENE 11	183	10.3	Magnetometer	MAGN	Kursänderung	rwk: 180°, d: 181 sm
SO183/012-1	04.06.05	00:31	33° 0,94' S	35° 17,12' E	1375	SSW 9	132	9.6	Magnetometer	MAGN	Kursänderung	rwk: 090°, d: 12 sm
SO183/012-1	04.06.05	01:43	33° 0,96' S	35° 30,76' E	1409	S 6	63	9.8	Magnetometer	MAGN	Kursänderung	rwk: 360°, d: 131 sm
SO183/012-1	04.06.05	14:35	30° 50,58' S	35° 30,26' E	1916	NNE 14	5	8.6	Magnetometer	MAGN	Ende Profil	
SO183/012-1	04.06.05	14:46	30° 49,68' S	35° 30,41' E	1884	NNE 12	30	4.7	Magnetometer	MAGN	Magnetometer an Deck	
SO183/012-1	04.06.05	14:46	30° 49,68' S	35° 30,41' E	1884	NNE 12	30	4.7	Magnetometer	MAGN	Ende Station	
SO183/013-1	04.06.05	15:22	30° 53,02' S	35° 35,06' E	2284	NNE 8	233	1	CTD	CTD	Beginn Station	
SO183/013-1	04.06.05	15:25	30° 53,04' S	35° 35,07' E	2288	N 8	113	0.5	CTD	CTD	zu Wasser	W4, 2 x CTD (20 m, 300 m)
SO183/013-1	04.06.05	16:08	30° 53,40' S	35° 35,31' E	2290	NNE 9	197	0.5	CTD	CTD	auf Tiefe	Slmax= 2250 m
SO183/013-1	04.06.05	17:07	30° 53,84' S	35° 35,71' E	2345	N 10	124	0.5	CTD	CTD	an Deck	
SO183/013-1	04.06.05	17:07	30° 53,84' S	35° 35,71' E	2345	N 10	124	0.5	CTD	CTD	Ende Station	
SO183/014-1	04.06.05	17:33	30° 52,97' S	35° 33,10' E	2214	N 11	23	1.6	Kettensackdredge	KD	Stationsbeginn	
SO183/014-1	04.06.05	17:35	30° 52,96' S	35° 33,10' E	2194	N 11	88	0.7	Kettensackdredge	KD	z.W.	W6
SO183/014-1	04.06.05	18:12	30° 53,04' S	35° 33,26' E	2264	N 11	359	1.9	Kettensackdredge	KD	Boko	Sl= 2320 m
SO183/014-1	04.06.05	18:34	30° 52,47' S	35° 33,26' E	1919	NNW 10	24	0.6	Kettensackdredge	KD	Beginn dredgen	Slmax= 2515 m
SO183/014-1	04.06.05	18:49	30° 52,47' S	35° 33,27' E	1921	N 8	339	0.4	Kettensackdredge	KD	frei vom Grund	Sl=2006 m
SO183/014-1	04.06.05	19:13	30° 52,46' S	35° 33,25' E	1921	N 9	24	0.8	Kettensackdredge	KD	a.D.	
SO183/014-2	04.06.05	19:33	30° 53,33' S	35° 33,45' E	2349	N 10	2	1	Kettensackdredge	KD	z.W.	
SO183/014-2	04.06.05	20:07	30° 53,32' S	35° 33,43' E	2346	N 9	339	1	Kettensackdredge	KD	Boko	Sl= 2383 m
SO183/014-2	04.06.05	20:51	30° 52,15' S	35° 33,49' E	1889	NNW 9	280	0.5	Kettensackdredge	KD	Beginn dredgen	Slmax= 2753 m

Station	Datum	UTC	PositionLat	PositionLon	Tiefe [m]	Windstärke [m/s]	Kurs [°]	v [kn]	Gerät	Gerätekürzel	Aktion	Bemerkung
SO183/014-2	04.06.05	21:15	30° 52,16' S	35° 33,45' E	1885	NNW 9	107	0.3	Kettensackdredge	KD	frei vom Grund	SI= 1950 m
SO183/014-2	04.06.05	21:41	30° 52,08' S	35° 33,50' E	1880	N 9	311	0.6	Kettensackdredge	KD	a.D.	
SO183/014-2	04.06.05	21:41	30° 52,08' S	35° 33,50' E	1880	N 9	311	0.6	Kettensackdredge	KD	Stationsende	
SO183/015-1	04.06.05	22:10	30° 51,73' S	35° 30,29' E	1928	NNW 10	6	3.2	Magnetometer	MAGN	Beginn Station	Beginn Aussetzen Mag., rwK 360°, FdW 4 kn
SO183/015-1	04.06.05	22:15	30° 51,45' S	35° 30,40' E	1926	NNW 9	358	4	Magnetometer	MAGN	Magnetometer zu Wasse	MAGN 200 m ausgesteckt
SO183/015-2	04.06.05	22:29	30° 50,10' S	35° 30,32' E	1896	NNW 11	356	6.3	Kalibrierung	KAL	Beginn Drehkreis	
SO183/015-2	04.06.05	23:26	30° 50,05' S	35° 30,29' E	1893	N 11	351	6.9	Kalibrierung	KAL	Ende Drehkreis	gehen auf FüG ca. 10 kn
SO183/015-1	04.06.05	23:26	30° 50,05' S	35° 30,29' E	1893	N 11	351	6.9	Magnetometer	MAGN	Beginn Profil	# 5, rwk: 360°, d: 50 sm
SO183/015-1	05.06.05	04:21	30° 0,05' S	35° 30,00' E	2268	NNW 13	4	10.8	Magnetometer	MAGN	Kursänderung	rwk: 24°, d: 131 sm
SO183/015-1	05.06.05	16:51	28° 0,04' S	36° 29,98' E	1843	SSW 4	22	11.3	Magnetometer	MAGN	Kursänderung	rwk: 360°, d: 120 sm
SO183/015-1	06.06.05	04:12	26° 0,00' S	36° 29,99' E	2274	S 4	342	10.3	Magnetometer	MAGN	Kursänderung	rwk: 270°, d: 11 sm
SO183/015-1	06.06.05	05:13	26° 0,00' S	36° 18,15' E	2103	S 11	270	11.6	Magnetometer	MAGN	Kursänderung	rwk: 180°, d: 120 sm
SO183/015-1	06.06.05	16:51	28° 0,01' S	36° 17,97' E	1903	SW 9	216	8.3	Magnetometer	MAGN	Kursänderung	rwk: 270°, d: 11 sm
SO183/015-1	06.06.05	17:51	28° 0,01' S	36° 6,05' E	1799	SSW 6	280	10.3	Magnetometer	MAGN	Kursänderung	rwk: 360°, d: 180 sm
SO183/015-1	07.06.05	10:42	25° 0,32' S	36° 5,97' E	1921	NE 13	12	10.1	Magnetometer	MAGN	Kursänderung	rwk: 090°, d: 11 sm
SO183/015-1	07.06.05	11:46	25° 0,02' S	36° 17,79' E	2034	NNE 12	113	9.9	Magnetometer	MAGN	Kursänderung	rwk: 181°, d: 61 sm
SO183/015-1	07.06.05	17:30	26° 1,03' S	36° 17,00' E	2092	NNE 8	152	9.7	Magnetometer	MAGN	Kursänderung	rwk: 090°, d: 13 sm
SO183/015-1	07.06.05	18:44	26° 0,84' S	36° 30,95' E	2245	N 14	18	8.5	Magnetometer	MAGN	Kursänderung	rwK: 359°, d: 61 sm
SO183/015-1	08.06.05	00:26	25° 0,16' S	36° 29,99' E	1719	NNE 15	4	9.8	Magnetometer	MAGN	Ende Profil	Einholen MAGN, reduzieren auf FdW 4 kn
SO183/015-1	08.06.05	00:37	24° 59,16' S	36° 30,06' E	1724	NNE 10	6	3.6	Magnetometer	MAGN	Magnetometer an Deck	
SO183/015-1	08.06.05	00:38	24° 59,10' S	36° 30,07' E	1724	NNE 10	14	4.1	Magnetometer	MAGN	Ende Station	KÄ 149°, Anf. # 16, d: 106 sm
SO183/016-1	08.06.05	10:17	26° 1,05' S	38° 0,02' E	4054	NNW 11	282	1.3	CTD	CTD	Beginn Station	
SO183/016-1	08.06.05	10:17	26° 1,05' S	38° 0,02' E	4054	NNW 11	282	1.3	CTD	CTD	zu Wasser	W 4
SO183/016-1	08.06.05	11:33	26° 0,76' S	37° 59,92' E	4060	N 7	242	0.2	CTD	CTD	auf Tiefe	hieven, SLmax: 3900 m
SO183/016-1	08.06.05	12:53	26° 0,58' S	37° 59,72' E	4051	N 8	257	0.4	CTD	CTD	an Deck	
SO183/016-1	08.06.05	12:53	26° 0,58' S	37° 59,72' E	4051	N 8	257	0.4	CTD	CTD	Ende Station	KÄ 024°, Anf. Profil, d: 1 sm
SO183/017-1	08.06.05	12:58	26° 0,59' S	37° 59,69' E	4054	NNE 7	279	0.3	Magnetometer	MAGN	Beginn Station	
SO183/017-1	08.06.05	13:05	26° 0,25' S	37° 59,84' E	4029	N 9	14	4.1	Magnetometer	MAGN	Magnetometer zu Wasse	L: 200 m
SO183/017-1	08.06.05	13:07	26° 0,08' S	37° 59,93' E	4043	N 10	27	7.6	Magnetometer	MAGN	Beginn Profil	# 06, rwk: 356°, d: 301 sm
SO183/017-1	09.06.05	17:15	21° 0,09' S	37° 35,99' E	2893	ENE 7	355	10.2	Magnetometer	MAGN	Kursänderung	rwk: 090°, d: 17 sm
SO183/017-1	09.06.05	18:47	21° 0,00' S	37° 53,95' E	2850	NE 8	101	11.5	Magnetometer	MAGN	Kursänderung	rwk: 176°, d: 381sm
SO183/017-1	11.06.05	07:46	27° 20,24' S	38° 25,81' E	4744	E 7	155	10.7	Magnetometer	MAGN	Kursänderung	rwk: 090°, d: 16 sm
SO183/017-1	11.06.05	09:20	27° 19,87' S	38° 43,93' E	4607	ENE 8	356	8.7	Magnetometer	MAGN	Kursänderung	rwk: 356°, d: 345 sm
SO183/017-1	12.06.05	18:01	21° 36,26' S	38° 14,97' E	3140	ESE 6	352	11.4	Magnetometer	MAGN	Kursänderung	rwk: 090°, d: 17 sm
SO183/017-1	12.06.05	19:38	21° 36,04' S	38° 32,82' E	3116	SSE 9	121	10.4	Magnetometer	MAGN	Kursänderung	rwk: 176°, d: 325 sm
SO183/017-1	14.06.05	02:05	26° 59,98' S	39° 0,03' E	4621	N 0	115	8.7	Magnetometer	MAGN	Kursänderung	rwk: 090°, d: 32 sm
SO183/017-1	14.06.05	04:59	27° 0,00' S	39° 35,95' E	4600	NNW 9	68	11	Magnetometer	MAGN	Kursänderung	rwk: 356°, d: 391 sm

Station	Datum	UTC	PositionLat	PositionLon	Tiefe [m]	Windstärke [m/s]	Kurs [°]	v [kn]	Gerät	Gerätekürzel	Aktion	Bemerkung
SO183/017-1	15.06.05	17:52	20° 30,03' S	39° 3,51' E	2755	E 6	12	10.3	Magnetometer	MAGN	Kursänderung	rwk: 090°, d: 17 sm
SO183/017-1	15.06.05	19:28	20° 30,11' S	39° 21,85' E	2875	SE 9	165	8.7	Magnetometer	MAGN	Kursänderung	rwk: 176°, d: 100 sm
SO183/017-1	16.06.05	05:04	22° 10,01' S	39° 29,93' E	2904	S 12	176	8.5	Magnetometer	MAGN	Ende Profil	
SO183/017-2	16.06.05	05:19	22° 10,53' S	39° 31,09' E	2920	SSE 8	62	9.2	Kalibrierung	KAL	Beginn Drehkreis	v ~ 7 - 8 kn
SO183/017-2	16.06.05	06:32	22° 10,24' S	39° 30,35' E	2914	SSE 10	223	7.1	Kalibrierung	KAL	Ende Drehkreis	d: 9 sm
SO183/017-1	16.06.05	06:42	22° 10,87' S	39° 29,91' E	2917	SE 9	221	3.9	Magnetometer	MAGN	Magnetometer an Deck	
SO183/017-1	16.06.05	06:43	22° 10,93' S	39° 29,87' E	2919	SE 9	204	4.4	Magnetometer	MAGN	Ende Station	
SO183/018-1	16.06.05	07:41	22° 3,06' S	39° 24,10' E	2399	SSE 0	356	11	Vermessung	EM / PS	Beginn Profil	rwk: 033°, d: 6sm
SO183/018-1	16.06.05	08:13	21° 57,66' S	39° 27,87' E	154	SSE 7	18	11.2	Vermessung	EM / PS	Kursänderung	rwk: 355°, d: 11sm
SO183/018-1	16.06.05	09:06	21° 46,67' S	39° 26,85' E	803	SE 4	342	9.4	Vermessung	EM / PS	Kursänderung	rwk: 270 , d: 1sm
SO183/018-1	16.06.05	09:14	21° 46,78' S	39° 25,58' E	1135	ENE 6	163	9.4	Vermessung	EM / PS	Kursänderung	rwk: 174 , d: 11sm
SO183/018-1	16.06.05	10:10	21° 57,58' S	39° 27,00' E	206	SSE 10	157	11.3	Vermessung	EM / PS	Kursänderung	rwK: 088°, d: 2 sm
SO183/018-1	16.06.05	10:20	21° 57,64' S	39° 28,74' E	580	SSE 9	80	7.5	Vermessung	EM / PS	Ende Profil	
SO183/019-1	16.06.05	11:05	21° 56,44' S	39° 28,68' E	1106	SSE 5	105	1.1	Kettensackdredge	KD	Stationsbeginn	
SO183/019-1	16.06.05	11:06	21° 56,45' S	39° 28,69' E	1110	S 5	102	1.1	Kettensackdredge	KD	z.W.	W 6
SO183/019-1	16.06.05	11:22	21° 56,48' S	39° 28,71' E	1111	ESE 4	273	0.2	Kettensackdredge	KD	Boko	SL: 1117 m
SO183/019-1	16.06.05	11:23	21° 56,48' S	39° 28,70' E	1114	SE 4	87	0.2	Kettensackdredge	KD	Beginn dredgen	driften rwK 284°
SO183/019-1	16.06.05	12:10	21° 56,28' S	39° 27,98' E	566	ESE 3	230	1	Kettensackdredge	KD	hieven	Slmax: 1507m
SO183/019-1	16.06.05	12:15	21° 56,27' S	39° 27,97' E	556	ESE 4	198	0.1	Kettensackdredge	KD	KD hakt	
SO183/019-1	16.06.05	13:03	21° 56,46' S	39° 28,57' E	984	SE 3	41	1.2	Kettensackdredge	KD	frei vom Grund	SL: 965 m
SO183/019-1	16.06.05	13:21	21° 56,38' S	39° 28,50' E	950	ESE 5	262	0.2	Kettensackdredge	KD	a.D.	mit Probe
SO183/019-2	16.06.05	13:48	21° 56,45' S	39° 28,74' E	1139	SSE 6	57	1.4	Kettensackdredge	KD	z.W.	W 6
SO183/019-2	16.06.05	14:05	21° 56,47' S	39° 28,67' E	1097	SE 5	155	0.4	Kettensackdredge	KD	Boko	Sl: 1073 m
SO183/019-2	16.06.05	14:05	21° 56,47' S	39° 28,67' E	1097	SE 5	155	0.4	Kettensackdredge	KD	Auslegen	driften rwK: 284
SO183/019-2	16.06.05	14:20	21° 56,48' S	39° 28,56' E	935	SE 5	301	0.7	Kettensackdredge	KD	Beginn dredgen	Sl: 1319 m, rwK: 284°
SO183/019-2	16.06.05	14:53	21° 56,34' S	39° 28,22' E	743	SE 7	342	1.7	Kettensackdredge	KD	KD hakt	Sl: 1320 m
SO183/019-2	16.06.05	15:00	21° 56,29' S	39° 28,18' E	702	SE 6	16	1.5	Kettensackdredge	KD	hieven	Slmax: 1386 m
SO183/019-2	16.06.05	15:52	21° 56,23' S	39° 28,34' E	756	SSE 5	110	1.4	Kettensackdredge	KD	frei vom Grund	Sl: 780 m
SO183/019-2	16.06.05	16:11	21° 56,31' S	39° 28,32' E	759	SE 5	231	1.2	Kettensackdredge	KD	a.D.	
SO183/019-2	16.06.05	16:20	21° 56,37' S	39° 28,37' E	821	SE 4	207	2.7	Kettensackdredge	KD	Stationsende	
SO183/020-1	16.06.05	17:33	22° 8,82' S	39° 29,78' E	2878	SE 5	192	1	CTD	CTD	Beginn Station	W 4
SO183/020-1	16.06.05	17:35	22° 8,82' S	39° 29,79' E	2878	SE 5	177	0.7	CTD	CTD	zu Wasser	1. CTD: 20 m, 2.CTD: 1000 m
SO183/020-1	16.06.05	18:32	22° 8,92' S	39° 29,91' E	2879	SSE 6	178	0.8	CTD	CTD	auf Tiefe	Slmax: 2800m
SO183/020-1	16.06.05	19:31	22° 8,96' S	39° 29,89' E	2880	SSE 5	86	1.6	CTD	CTD	an Deck	
SO183/020-1	16.06.05	19:33	22° 8,98' S	39° 29,89' E	2880	S 6	178	0.7	CTD	CTD	Ende Station	
SO183/021-1	16.06.05	19:39	22° 9,01' S	39° 29,85' E	2882	S 6	168	0.8	Magnetometer	MAGN	Beginn Station	
SO183/021-1	16.06.05	19:42	22° 9,09' S	39° 29,83' E	2883	SSE 6	194	3.5	Magnetometer	MAGN	Magnetometer zu Wasser	

Station	Datum	UTC	PositionLat	PositionLon	Tiefe [m]	Windstärke [m/s]	Kurs [°]	v [kn]	Gerät	Gerätekürzel	Aktion	Bemerkung
SO183/021-1	16.06.05	20:00	22° 10,53' S	39° 30,00' E	2913	S 8	169	6.9	Magnetometer	MAGN	Beginn Profil	# 07, rwk: 176°, d: 290 sm
SO183/021-1	17.06.05	23:52	26° 59,80' S	39° 53,99' E	4556	SE 8	153	9.2	Magnetometer	MAGN	Kursänderung	rwk: 090°, d: 16 sm
SO183/021-1	18.06.05	01:23	27° 0,01' S	40° 11,75' E	4523	SSE 9	76	9.9	Magnetometer	MAGN	Kursänderung	rwk: 356°, d: 328 sm
SO183/021-1	19.06.05	08:19	21° 33,68' S	39° 44,82' E	1477	SSE 3	357	11.1	Magnetometer	MAGN	Kursänderung	Bassas da India, rwk: 090°, d: 5 sm
SO183/021-1	19.06.05	08:54	21° 33,49' S	39° 51,12' E	2141	S 10	51	9.1	Magnetometer	MAGN	Kursänderung	Bassas da India, rwk: 356°, d: 13 sm
SO183/021-1	19.06.05	10:10	21° 20,18' S	39° 49,92' E	3038	SE 3	336	9.9	Magnetometer	MAGN	Kursänderung	Bassas da India, rwk: 270°, d: 6 sm
SO183/021-1	19.06.05	10:43	21° 19,94' S	39° 43,84' E	2863	SSE 7	276	10.4	Magnetometer	MAGN	Kursänderung	Bassas da India, rwk: 356°, d: 20 sm
SO183/021-1	19.06.05	12:37	21° 0,18' S	39° 42,01' E	3079	SSE 2	15	10.9	Magnetometer	MAGN	Kursänderung	rwk: 090°, d: 17 sm
SO183/021-1	19.06.05	14:15	21° 0,01' S	39° 59,71' E	3088	S 8	86	9.9	Magnetometer	MAGN	Kursänderung	rwk: 176°, d: 391 sm
SO183/021-1	21.06.05	02:52	27° 29,97' S	40° 32,61' E	4554	E 9	156	10.6	Magnetometer	MAGN	Kursänderung	rwk: 090°, d: 16 sm
SO183/021-1	21.06.05	04:21	27° 30,01' S	40° 50,58' E	4517	SSE 7	92	11.3	Magnetometer	MAGN	Kursänderung	rwk: 356°, d: 305 sm
SO183/021-1	22.06.05	08:55	22° 26,52' S	40° 25,10' E	1752	SE 7	358	10.9	Magnetometer	MAGN	Kursänderung	rwk: 090°, d: 3 sm
SO183/021-1	22.06.05	09:16	22° 25,99' S	40° 28,27' E	2371	ESE 15	34	10.5	Magnetometer	MAGN	Kursänderung	rwk: 356°, d: 10 sm
SO183/021-1	22.06.05	10:03	22° 16,15' S	40° 27,17' E	2774	SE 6	354	12.8	Magnetometer	MAGN	Kursänderung	rwk: 270°, d: 3 sm
SO183/021-1	22.06.05	10:19	22° 15,53' S	40° 24,06' E	2524	S 8	336	10.1	Magnetometer	MAGN	Kursänderung	rwk: 356°, d: 76 sm
SO183/021-1	22.06.05	17:18	20° 59,99' S	40° 18,03' E	3087	SE 6	42	8.6	Magnetometer	MAGN	Kursänderung	rwk: 090°, d: 17 sm
SO183/021-1	22.06.05	18:51	21° 0,11' S	40° 35,93' E	3003	SSW 16	160	5.9	Magnetometer	MAGN	Kursänderung	rwk: 176°, d: 361 sm
SO183/021-1	24.06.05	07:44	26° 59,88' S	41° 6,03' E	4402	E 12	143	9.6	Magnetometer	MAGN	Kursänderung	rwk: 090°, d: 16 sm
SO183/021-1	24.06.05	09:19	26° 59,63' S	41° 24,03' E	4378	E 11	354	10.6	Magnetometer	MAGN	Kursänderung	rwk: 356°, d: 361 sm
SO183/021-1	25.06.05	20:37	20° 59,97' S	40° 54,16' E	2931	SW 0	59	9.6	Magnetometer	MAGN	Kursänderung	rwk: 090°, d: 17 sm
SO183/021-1	25.06.05	22:17	21° 0,08' S	41° 11,87' E	2969	SSW 6	131	9.3	Magnetometer	MAGN	Kursänderung	rwk: 176°, d: 361 sm
SO183/021-1	27.06.05	09:59	26° 59,91' S	41° 42,01' E	4354	SSE 7	138	7.8	Magnetometer	MAGN	Kursänderung	rwk: 090°, d: 16 sm
SO183/021-1	27.06.05	11:33	27° 0,00' S	41° 59,85' E	4458	S 6	55	9.5	Magnetometer	MAGN	Kursänderung	rwk: 356°, d: 361 sm
SO183/021-1	28.06.05	23:00	21° 0,15' S	41° 30,03' E	2905	S 2	27	9.3	Magnetometer	MAGN	Kursänderung	rwk: 090°, d: 17 sm
SO183/021-1	29.06.05	00:41	21° 0,02' S	41° 47,78' E	2846	S 13	107	8.7	Magnetometer	MAGN	Kursänderung	rwk: 176°, d: 361 sm
SO183/021-1	30.06.05	15:41	26° 59,85' S	42° 18,00' E	4342	NNE 4	172	10.9	Magnetometer	MAGN	Ende Profil	
SO183/021-1	30.06.05	15:42	27° 0,01' S	42° 18,01' E	4342	ENE 5	177	8.8	Magnetometer	MAGN	Ende Station	
SO183/022-1	30.06.05	15:53	27° 0,06' S	42° 19,20' E	4339	NNE 6	26	7.5	Kalibrierung	KAL	Beginn Station	v ~ 7-8 kn
SO183/022-1	30.06.05	15:53	27° 0,06' S	42° 19,20' E	4339	NNE 6	26	7.5	Kalibrierung	KAL	Beginn Drehkreis	
SO183/022-1	30.06.05	16:45	27° 0,02' S	42° 19,23' E	4337	NE 6	1	6.9	Kalibrierung	KAL	Ende Drehkreis	d: 7 sm
SO183/022-1	30.06.05	16:45	27° 0,02' S	42° 19,23' E	4337	NE 6	1	6.9	Kalibrierung	KAL	Ende Station	
SO183/023-1	30.06.05	16:53	27° 0,00' S	42° 18,06' E	4344	NNE 5	275	9.1	Magnetometer	MAGN	Beginn Station	
SO183/023-1	30.06.05	16:53	27° 0,00' S	42° 18,06' E	4344	NNE 5	275	9.1	Magnetometer	MAGN	Beginn Profil	# 08, rwk: 270°, d: 161 sm
SO183/023-1	01.07.05	09:00	26° 59,02' S	39° 18,30' E	4607	SSW 10	272	10.3	Magnetometer	MAGN	Kursänderung	KÃ Bb, d: 3 sm, rwk: 356°, d: 318 sm
SO183/023-1	02.07.05	16:38	21° 42,32' S	38° 51,42' E	3184	SSE 2	354	10.3	Magnetometer	MAGN	Kursänderung	rwk: 270°, d: 84 sm
SO183/023-1	03.07.05	01:01	21° 42,43' S	37° 21,15' E	3057	SE 13	219	9.6	Magnetometer	MAGN	Kursänderung	rwk: 176°, d: 379 sm
SO183/023-1	04.07.05	17:29	28° 0,08' S	37° 48,00' E	4667	ESE 11	174	8.1	Magnetometer	MAGN	Ende Profil	

Station	Datum	UTC	PositionLat	PositionLon	Tiefe [m]	Windstärke [m/s]	Kurs [°]	v [kn]	Gerät	Gerätekürzel	Aktion	Bemerkung
SO183/023-1	04.07.05	17:37	28° 0,62' S	37° 47,80' E	4668.5	ESE 11	225	2.8	Magnetometer	MAGN	Magnetometer an Deck	
SO183/023-1	04.07.05	17:37	28° 0,62' S	37° 47,80' E	4669	ESE 11	225	2.8	Magnetometer	MAGN	Ende Station	
Transit	04.07.05	17:37	28° 0,62' S	37° 47,80' E	4669	ESE 11	225	2.8	Vektor-Magnetometer	VekMg	Ende Messung	
SO183/024-1	05.07.05	09:55	30° 33,56' S	36° 52,42' E	3040	E 12	64	2.3	Kettensackdredge	KD	Stationsbeginn	
SO183/024-1	05.07.05	09:58	30° 33,55' S	36° 52,47' E	3100	E 11	60	0.5	Kettensackdredge	KD	z.W.	W 6
SO183/024-1	05.07.05	10:53	30° 33,43' S	36° 52,26' E	2946	E 8	316	1.4	Kettensackdredge	KD	Boko	SL: 3170 m; driften mit FüG 1- 2 kn, 330°
SO183/024-1	05.07.05	10:58	30° 33,32' S	36° 52,21' E	2914	E 10	321	2.2	Kettensackdredge	KD	Beginn dredgen	SL: 3296 m
SO183/024-1	05.07.05	11:25	30° 32,76' S	36° 51,85' E	2605	ENE 11	347	2	Kettensackdredge	KD	hieven	SLmax: 3346 m, d 1 sm
SO183/024-1	05.07.05	11:46	30° 32,67' S	36° 51,84' E	2621	ENE 9	345	0.5	Kettensackdredge	KD	frei vom Grund	SL: 2600 m
SO183/024-1	05.07.05	12:21	30° 32,62' S	36° 51,83' E	2616	ENE 10	263	1	Kettensackdredge	KD	a.D.	mit Probe; Anf. # 24-2
SO183/024-2	05.07.05	12:40	30° 33,52' S	36° 52,29' E	2892	ENE 12	328	1.1	Kettensackdredge	KD	z.W.	W 6
SO183/024-2	05.07.05	13:19	30° 33,63' S	36° 52,31' E	2926	E 10	218	0.8	Kettensackdredge	KD	Boko	SL: 2938 m; driften mit FüG 1 - 2 kn, 330°
SO183/024-2	05.07.05	13:20	30° 33,64' S	36° 52,31' E	2951	ENE 10	176	0.5	Kettensackdredge	KD	Auslegen	rwK: 330
SO183/024-2	05.07.05	13:38	30° 33,32' S	36° 52,19' E	2902	E 10	334	1.6	Kettensackdredge	KD	Beginn dredgen	SL: 3295m
SO183/024-2	05.07.05	14:15	30° 32,64' S	36° 51,74' E	2519	E 10	348	1.1	Kettensackdredge	KD	KD hakt	SL:3396m
SO183/024-2	05.07.05	14:33	30° 32,64' S	36° 51,80' E	2584	ENE 11	205	0.8	Kettensackdredge	KD	hieven	Slmax: 3413m
SO183/024-2	05.07.05	15:01	30° 32,91' S	36° 51,90' E	2660	ENE 10	197	0.5	Kettensackdredge	KD	frei vom Grund	Sl: 2644m
SO183/024-2	05.07.05	15:36	30° 32,86' S	36° 52,03' E	2808	E 11	351	1.3	Kettensackdredge	KD	a.D.	mit Probe
SO183/024-2	05.07.05	15:45	30° 32,84' S	36° 52,09' E	2852	E 10	47	0.7	Kettensackdredge	KD	Stationsende	
Transit	07.07.05	04:00	29° 54,28' S	31° 20,93' E	420	NNE 6	286	9	SIMRAD	Vermess.	Ende Messung	
Durban	07.07.05	10:00	29° 52,88' S	31° 01,98' E		NE 3	76	0	Gravimeter	Gvm	Ende Messung	

Appendix 12 List of scientists

Name	**First Name**	**Nationality**	
Brayshaw	Matthew	South African	Durban University
Jokat	Wilfried	German	AWI
Kitada	Kazuya	Japanese	Kobe University
Kopsch	Konrad	German	AWI, Potsdam
Krocker	Ralf	German	AWI
Labrenz	Alexander	German	AWI
Niebling	Roland	German	AWI
Riedel	Sven	German	AWI
Tauchnitz	Michael	German	AWI
Thackeray	Zane	South African	Durban University
Watkeys	Michael	British	Durban Univerisity

Appendix 13 Crew list

CREW LIST SO 183

R/V SONNE	**Flag: German**	**Port of Arrival:**	**Durban**
Owner: RF, Bremen	**Callsign: DFCG**	**Date of Arrival:**	**07.07.2005**

No.	Name	Given Name	Rank
1	Meyer	Oliver	Master
2	Korte	Detlef	Chief Offc.
3	Kowitz	Torsten	1st Offc.
4	Linnenbecker	Matthias	2nd Offc.
5	Guzman-Navarrete	Werner	Ch. Eng.
6	Rex	Andreas	2nd Eng.
7	Klinder	Klaus Dieter	2nd Eng.
8	Rieper	Uwe	Electr.
9	Bräutigam	Tim-Oliver	Doc.
10	Angermann	Rudolf	Ch. El. Eng.
11	Grossmann	Matthias	Sys.-Man.
12	Rosemeyer	Rainer	Fitter
13	Golabowski	Daniel	Motorman
14	Sebastian	Frank	Motorman
15	Wieden	Wilhelm	Cook
16	Jastrzebski	Seweryn	2nd Cook
17	Gruebe	Gerlinde	Steward
18	Majka	Tomasz	2nd Stwd.
19	Mucke	Hans-Peter	Bosun
20	Schrapel	Andreas	A.B.
21	Vor	Hans-Jürgen	A.B.
22	Dehne	Dirk	A.B.
23	Müller	Gerhard	A.B.
24	Tessnow	Norman	A.B.
25	Tauscher	Jan	A.B.
26	Fricke	Ingo	A.B.
27	Förster	Tino	Trainee